

24TH ANNUAL GASEOUS ELECTRONICS CONFERENCE

THIRD ARC SYMPOSIUM

OCTOBER 5-8, 1971
AT THE UNIVERSITY OF FLORIDA
GAINESVILLE, FLORIDA

A topical conference of: *The American Physical Society*

Sponsoring departments of the University of Florida: Aerospace Engineering, Chemistry, Electrical Engineering, Nuclear Engineering, and Physics.

Supported by the U. S. Army Research Office – Durham

PROGRAM

TWENTY-FOURTH ANNUAL
GASEOUS ELECTRONICS CONFERENCE
AND
THIRD ARC SYMPOSIUM

OCTOBER 5-8, 1971

PROGRAM
THIRD ARC SYMPOSIUM

Registration

Second Floor East Lobby of the J. Wayne Reitz Union

Monday, October 4: 7:00 p.m. - 10:00 p.m.

Tuesday, October 5: 8:00 a.m. - 10:00 p.m.

Wednesday, October 6: 8:00 a.m. - 5:00 p.m.

(See GEC Program for remainder of schedule)

Tuesday, October 5

8:30 a.m. - 9:45 a.m.: Reitz Auditorium

Chairman: W. Braun
Aerospace Research
Laboratories, WPAFB

SESSION A. ARC PROPERTIES

- A1. TEMPERATURE PROFILE DETERMINATION IN AN ABSORBING PLASMA
J. L. Usher and H. D. Campbell
- A2. PLASMA PROPERTIES OF A D. C. URANIUM ARC
J. M. Mack, Jr., J. L. Usher, H. D. Campbell, and R. T. Schneider
- A3. ELECTRICAL AND OPTICAL MEASUREMENTS IN 1000 ATM ARCS
D. Bartelheimer and U. H. Bauder
- A4. ELECTRICAL CONDUCTIVITY FROM ARC MEASUREMENTS
R. S. Devoto and D. Mukherjee
- A5. EQUILIBRIUM COMPOSITION AND TRANSPORT PROPERTIES OF SF₆
R. W. Liebermann

9:45 a.m. - 11:00 a.m.: Reitz Auditorium

**SESSION B. RADIATIVE AND EQUILIBRIUM
PROPERTIES OF ARCS**

Chairman: R. S. Tankin
Northwestern University

- B1. A WALL-STABILIZED ARC AS A STANDARD LIGHT SOURCE BELOW 1100 Å
G. L. Weissler and S. K. Srivastava
- B2. A NEW RADIATION STANDARD FOR THE VACUUM ULTRAVIOLET
W. R. Ott

Sessions B, C, D

- B3. MEASUREMENTS OF THE GROUND STATE RECOMBINATION CROSS SECTION OF ARGON 700 to 800 ANGSTROMS
J. C. Morris
- B4. A STUDY OF EQUILIBRIUM IN ARGON ARCS
J. B. Shumaker and C. H. Popenoe
- B5. TRANSITION PROBABILITIES OF THE 4108, 4916 AND 10139 Hg LINES
J. C. Morris and P. L. Patterson

11:20 a.m. - 12:20 p.m.: Reitz Auditorium

SESSION C. MAGNETIC AND FLOW EFFECTS IN ARCS. 1. Chairman: C. J. Michels
NASA Lewis Research
Center

- C1. A CONFINED-DISCHARGE PLASMA GENERATOR WITH LOCAL RADIAL GAS INJECTION
J. R. Mahan
- C2. HEAT FLUX AND CURRENT DENSITY TO A TUBE IMMERSSED IN AN ARC PLASMA
T. Meyer
- C3. STABLE CONFIGURATION OF ELECTRIC ARCS IN TRANSVERSE MAGNETIC FIELDS
H. O. Schrade
- C4. MAGNETICALLY BALANCED CROSS FLOW-ARCS
V. R. Malghan and D. M. Benenson

2:00 p.m. - 3:30 p.m.: Reitz Auditorium

SESSION D. MAGNETIC AND FLOW EFFECTS IN ARCS II. Chairman: E. Pfender
University of
Minnesota

- D1. PRODUCTION OF EQUILIBRIUM PLASMA INSIDE A HOLLOW MAGNETICALLY CONFINED ARC
C. M. Fitts and C. E. Nielsen
- D2. STABILITY CHARACTERISTICS OF A DENSE HIGHLY-IONIZED MAGNETIZED ARC COLUMN
D. L. Jassby, M. Marhic, and D. R. Regan
- D3. THE INCLUSION OF AN ARC PLASMA AT ATMOSPHERIC PRESSURE IN TOROIDAL GEOMETRIES
A. Wynands and G. Schmitz

- D4. ENDOTHERMIC REACTIONS IN ARC DISCHARGES
C. H. Leigh
- D5. UNSTEADY PHENOMENA IN A CIRCUIT BREAKER NOZZLE
J. M. Novak and R. L. Phillips
- D6. FLOW CHARACTERISTICS IN THE EXHAUST OF A PULSED
MEGAWATT GAS-FED ARC
C. J. Michels, and T. M. York

3:50 - 4:50 p.m.: Reitz Auditorium

SESSION E. TIME VARYING ARCS. I.

Chairman: P. W. Schreiber
Aerospace Research
Laboratories, WPAFB

- E1. MODULATED SPECTRA OF AC ARC LAMPS
P. L. Patterson
- E2. SPECTROSCOPIC ANALYSIS OF A HIGH CURRENT, FREE BURNING
ARC IN ARGON AT ATMOSPHERIC PRESSURE
E. Schultz-Gulde and P. G. Slade
- E3. SPECTROSCOPIC MEASUREMENTS OF THE ELECTRON DENSITY IN
MANOSECOND DISCHARGES IN HYDROGEN-DOPED ARGON
L. L. Wiese and J. A. Augis
- E4. TIME RESOLVED RADIAL PROFILES OF WALL STABILIZED ARC
DISCHARGES IN XENON, KRYPTON AND CESIUM
S. Levy

4:50 p.m. - 5:50 p.m.: Reitz Auditorium

SESSION F. TIME VARYING ARCS. II.

Chairman: L. P. Harris
General Electric

- F1. MEASUREMENT OF TEMPERATURE IN DECAYING SF₆ ARC PLASMA
H. C. Ludwig
- F2. DECAY OF CONDUCTIVITY OF HIGH PRESSURE CYLINDRICAL PLASMAS
J. J. Lowke, R. E. Voshall and H. C. Ludwig
- F3. THE ROLE OF GAS HEATING IN THE CONSTRICTION OF A HIGH-PRESSURE
GLOW DISCHARGE COLUMN
G. L. Rogoff
- F4. ENHANCEMENT OF ELECTRON DENSITY IN A CONVERGENT HIGH CURRENT
PULSE DISCHARGE
D. C. Schubert and H. Goldie

7:30 p.m. - 10:00 p.m.: Arredondo Room, Reitz Union

GEC AND ARC MIXER

Wednesday, October 6

8:30 a.m. - 10:15 a.m.: Ballroom A

SESSION G. VACUUM ARCS AND ELECTRODE PHENOMENA

Chairman: C. J. Cremers
University
of Kentucky

- G1. THE PLASMA POTENTIAL ADJACENT TO THE VACUUM ARC CATHODE
G. W. McClure
- G2. ENERGY DISTRIBUTIONS OF IONS FROM THE ANODE PLASMA OF A
PULSED VACUUM ARC
J. T. Grissom
- G3. VACUUM ARC ANODE TEMPERATURE MEASUREMENTS
J. C. Newton and J. T. Grissom
- G4. PLASMA ELECTRON TEMPERATURE MEASUREMENT NEAR AN ANODE
SPOT OF A PULSED VACUUM ARC
F. M. Bacon
- G5. CHOPPING, INSTABILITY AND SPOT MULTIPLICITY OF THE
VACUUM ARC
G. H. Ecker
- G6. ANODE CURRENT DENSITY IN HIGH CURRENT PULSED ARCS
K. T. Shih
- G7. ARC CONSTRICTION AND SPOT FORMATION AT THE ANODE OF
A HIGH INTENSITY ARC
E. Pfender and T. S. Chou
- G8. ANODE HEAT TRANSFER IN A HIGH-INTENSITY ARC WITH SUPERIMPOSED
AXIAL FLOW
R. Paulson and E. Pfender

10:35 a.m. - 11:35 a.m.: Ballroom A

SESSION H. RF ARCS

Chairman: J. A. Sprouse
ARO, Incorporated

- H1. MULTIPHASIC EXPERIMENTAL STUDY OF AN ARGON RF PLASMA
AND SONIC AFTERGLOW
L. N. Medgyesi-Mitschang and R. A. Hefferlin
- H2. ANALYSIS OF OPTICALLY THICK COUPLED R. F. - D. C. ARC DISCHARGES
P. W. Schreiber, A. M. Hunter, P. Taylor, and K. R. Benedetto
- H3. EXPERIMENTS WITH BLUFF-BODY AND VORTEX STABILIZED
ELECTRODELESS ARCS
D. R. Keefer and P. J. Gross
- H4. ANALYSIS OF THERMAL INDUCTION PLASMAS BETWEEN COAXIAL
CYLINDERS
H. U. Eckert

11:35 a.m. - 12:00 noon: Ballroom A

ARC SYMPOSIUM BUSINESS MEETING

Free afternoon and excursion to Rainbow Springs

1:00 p.m. - 5:00 p.m.

Thursday, October 7

PLENARY SESSION

Chairman: Prof. W. P. Allis, M.I.T.
11:15 a.m. - 12:00 noon
Ballroom A

RECEPTION

7:00 p.m.

Pool Deck, Flagler Inn (Cash Bar)

BANQUET

8:00 p.m.

Grand Hall, Flagler Inn

Chairman: Dr. Gordon H. Dunn, JILA

1. Opening remarks and announcements
2. A tribute to Leonard Loeb on the occasion of his eightieth birthday.
3. Principal Speaker: Dr. James R. Cade, Chief of Renal Medicine, College of Medicine, University of Florida.

"Sweat, Urine, and Apple Pie"

PROGRAM
TWENTY-FOURTH ANNUAL
GASEOUS ELECTRONICS CONFERENCE

Registration

Second Floor, East Lobby of the J. Wayne Reitz Union

Monday, October 4	7:00 p.m. - 10:00 p.m.
Tuesday, October 5	8:00 a.m. - 10:00 p.m.
Wednesday, October 6	8:00 a.m. - 5:00 p.m.
Thursday, October 7	8:00 a.m. - 5:00 p.m.
Friday, October 8	8:00 a.m. - 2:00 p.m.

Tuesday, October 5

10:30 a.m. - 12:00 noon: Ballroom A

SESSION I. AFTERGLOWS IN RARE GAS-MERCURY MIXTURES

Chairman: J. Ingold
 Lightning Research
 Laboratories

11. ELECTRON-TEMPERATURE DECAY IN Hg-RARE GAS AFTERGLOWS
 P. C. Drop and J. Polman
12. QUENCHING OF AFTERGLOW RADIATION BY ELECTRON HEATING
 AT PLASMA RESONANCES
 S. C. Bloch and J. L. Auel
13. INITIAL AFTERGLOW OF THE SELF-ABSORBED Hg 2537 Å RADIATION
 IN Hg - Ar DISCHARGES
 T. J. Hammond and C. F. Gallo
14. STATISTICAL TIME LAGS IN HELIUM-MERCURY AFTERGLOWS
 B. M. Lancaster, Jr. and K. J. Nygaard
15. PLASMA DIAGNOSTICS USING SLOW POSITRONS
 W. M. Schikorr, G. H. Lohnert, R. T. Schneider

2:00 p.m. - 3:30 p.m.: Ballroom A

SESSION J. BREAKDOWN

Chairman: A. A. Dougal
University of
Texas at Austin

- J1. DETERMINATION OF SPATIAL AND TEMPORAL ELECTRON DENSITY AND TEMPORAL ELECTRON TEMPERATURE IN LASER-PRODUCED GASEOUS DEUTERIUM PLASMAS
W. K. Pendleton and A. H. Guenther
- J2. LASER INDUCED BREAKDOWN IN HIGH PRESSURE NOBLE GASES
G. W. Haynes, O. M. Friedrich, Jr. and A. A. Dougal
- J3. VACUUM BREAKDOWN VOLTAGE AS A FUNCTION OF CROSSED MAGNETIC FIELD STRENGTH
Alan Watson
- J4. PULSED MICROWAVE BREAKDOWN OF AIR FROM 1 TO 1000 TORR
S. J. Tetenbaum, A. D. MacDonald, and H. W. Bandel
- J5. INTERACTION OF TRICHEL PULSES FROM ADJACENT NEGATIVE NEEDLE CORONAS
W. L. Lama and C. F. Gallo
- J6. SYSTEMATIC EXPERIMENTAL STUDY OF THE ELECTRICAL CHARACTERISTICS OF THE "TRICHEL" CURRENT PULSES FROM NEGATIVE NEEDLE-TO-PLANE CORONAS
W. L. Lama and C. F. Gallo
- J7. THEORETICAL ANALYSIS OF TRICHEL CURRENT PULSES FROM NEGATIVE NEEDLE-TO-PLANE CORONAS
W. L. Lama and C. F. Gallo
- J8. KINETIC ION-ELECTRON EMISSION FROM CLEAN AND CONTAMINATED METAL SURFACES
J. T. Breunig

4:00 p.m. - 5:30 p.m.: Ballroom A

SESSION K. TRANSPORT PROPERTIES AND DISTRIBUTIONS

Chairman: A. V. Phelps
JILA

- K1. TWO-FLUID THEORY OF THE POSITIVE COLUMN
J. H. Ingold
- K2. DETERMINATION OF CROSS SECTIONS FROM RATE CONSTANTS MEASURED IN DRIFT TUBES
S. B. Woo, J. H. Whealton, C. Russ, and S. F. Wong

- K3. DETERMINATION OF ELECTRON TRANSPORT COEFFICIENTS NEAR THERMAL ENERGIES IN OXYGEN
D. R. Nelson and F. J. Davis
- K4. MOMENTUM TRANSFER CROSS SECTIONS FOR ELECTRONS IN A WEAKLY IONIZED CESIUM PLASMA
F. Murray, D. M. Cox, H. H. Brown, Jr. and B. Bederson
- K5. IONIZATION AND ATTACHMENT IN BORON TRIFLUORIDE
D. Kenneth Davies

GEC/AS MIXER

7:30 p.m. - 10:00 p.m.
Arredondo Room
Reitz Union

Wednesday, October 6

8:30 a.m. - 10:00 a.m.: Reitz Auditorium

SESSION L. CLUSTERING (PANEL)

Chairman: F. E. Niles,
Aberdeen Research
and Development Laboratory

- L1. MOLECULAR CLUSTERING ABOUT GASEOUS METAL IONS
A. W. Castleman, Jr. and I. N. Tang
- L2. CLUSTERING OF N_2 TO Li^+
G. E. Keller and L. M. Romano
- L3. ION INDUCED LARGE CLUSTER FORMATION
Peter Coffey and V. A. Mohnen
- L4. LABORATORY PRODUCTION OF POSITIVE WATER CLUSTER IONS
P. Mahadevan and H. C. Carpenter
- L5. NEGATIVE ION MOLECULE REACTIONS OF ATMOSPHERIC INTEREST
V. A. Mohnen and Peter Coffey
- L6. THE REACTION OF NO^+ WITH H_2O , H_2S , AND METHANOL
Larry I. Bone
- L7. CO_2 AND CO CLUSTERING TO NO^+
J. M. Heimerl and J. A. Vanderhoff
- L8. PARTIAL CHARGE-TRANSFER AND CLUSTER REACTIONS OF Mg^+ , Ca^{++} , AND Ba^{++} .
K. G. Spears, F. C. Fehsenfeld, M. McFarland, and E. E. Ferguson

10:30 a.m. - 12:00 noon: Reitz Auditorium

SESSION M. NEUTRAL-NAUTRAL COLLISIONS AND
EXCITATION TRANSFER (PANEL)

Chairman: R. M. St. John
University of
Oklahoma

- M1. DYNAMICAL COUPLING POTENTIAL IN SIMPLE EXCHANGE COLLISIONS:
TWO STATE COUPLED CHANNEL CALCULATIONS OF ATOMIC EXCHANGE
CROSS SECTIONS FOR $H+H_2$, $D+H_2$, AND $H+D_2$.
Paul McGuire and David Micha
- M2. AN EXTENSION OF THE UNIFORM SEMICLASSICAL APPROXIMATION
FOR DIFFERENTIAL ELASTIC SCATTERING
J. M. Mullen
- M3. DISTRIBUTION OF EXCITATION TRANSFER IN HELIUM
J. D. Jobe and R. M. St. John
- M4. EXCITATION TRANSFER REACTIONS INVOLVING THE $He_2(2p^3)$
MOLECULE
C. B. Collins, B. W. Johnson and J. J. Shaw
- M5. CROSS SECTIONS FOR VIBRATIONAL ENERGY TRANSFER, CO_2-N_2
T. A. Dillon and E. W. Smith

Free afternoon and excursion to Rainbow Springs

1:00 p.m. - 5:00 p.m.

8:00 p.m. - 9:35 p.m.: Ballroom A

SESSION N. LASERS I

Chariman: A. Garscadden
Aerospace Research
Laboratory, WPAFB

- N1. ELECTRON DENSITY AND TEMPERATURE MEASUREMENT IN A CO LASER
PLASMA
D. Cohn, B. O'Brien, W. B. Lacina and M. L. Bhaumik
- N2. COMPARISON OF CW AND PULSED OPERATION OF CARBON MONOXIDE
LASER (CO, N_2 , Xe, He Mix)
W. J. Graham and J. C. Kershenstein
- N3. $CO-N_2-He$ DIRECT DISCHARGE LASER MODEL
Edward R. Fisher, George Abraham and Alexander Glass
- N4. ELECTRON KINETIC PROCESSES IN CO LASERS
W. L. Nighan

- N5. RATE COEFFICIENTS FOR PROCESSES IN CO LASERS
G. Hancock, C. Morely, B. A. Ridley and I. W. M. Smith
- N6. VIBRATION-TO-VIBRATION ENERGY TRANSFER IN COLLISIONS BETWEEN DIATOMIC MOLECULES
J. Daniel Kelley
- N7. V-V TRANSFER PROCESSES IN CO LASERS
W. Q. Jeffers and J. Daniel Kelley

8:00 p.m. - 9:30 p.m.: Bless Auditorium

SESSION P. IONIZATION

Chairman: C. Opal
JILA

- P1. SIMULTANEOUS PHOTOIONIZATION-EXCITATION OF HELIUM: OPTICAL MEASUREMENTS
D. H. Tracy and F. L. Roesler
- P2. ALKALI ATOM PHOTOIONIZATION CROSS SECTIONS: SPIN-ORBIT AND CORE POLARIZATION EFFECTS
J. C. Weisheit
- P3. PHOTOIONIZATION OF PHOTOEXCITED CESIUM
R. E. Hebner, Jr. and Kaare J. Nygaard
- P4. PRODUCTION OF EXCITED IONS BY ELECTRON COLLISIONS WITH CESIUM ATOMS
Yu Bong Hahn and Kaare J. Nygaard
- P5. ELECTRON IMPACT ON ARGON
L. R. Peterson and J. E. Allen, Jr.
- P6. SECONDARY ELECTRON DISTRIBUTIONS
A. E. S. Green., T. Sawada and A. J. Yezzi
- P7. IONIZATION OF RARE GASES IN THE BORN APPROXIMATION
R. A. Berg and A. E. S. Green

9:50 p.m. - 11:15 p.m.: Ballroom A

SESSION O. AFTERGLOWS IN MOLECULAR GASES

Chairman: M. Biondi
University of
Pittsburgh

- O1. COLLISIONAL DEACTIVATION OF METASTABLE $\text{Ar}(^3\text{P}_{0,2})$ ATOMS AND $\text{N}_2(\text{A}^3\Sigma_u^+)$ MOLECULES
R. A. Gutcheck and E. C. Zipf

- O2. DETECTION OF VIBRATIONALLY EXCITED NITROGEN BY RAMAN SPECTROSCOPY
L. Y. Nelson, A. W. Saunders, Jr., A. B. Harvey and G. O. Neely
- O3. TWO-BODY RECOMBINATION OF O_2^+ AND O_2^- IN LOW PRESSURE OXYGEN
M. N. Hirsh and P. N. Eisner
- O4. ION-ION RECOMBINATION, IONIC MOBILITIES, AND ION-NEUTRAL COLLISION FREQUENCIES IN THERMAL $N_2:O_2$ PLASMAS AT 300°K
P. N. Eisner and M. N. Hirsh
- O5. CALCULATED DENSITIES IN IONIZED AIR AT PRESSURES OF 2, 5, AND 10 TORR
F. E. Niles and E. L. Lortie
- O6. TIME-RESOLVED SPECTROSCOPY OF PLASMA INSTABILITIES
W. G. Braun, R. F. Paulson and R. D. Franklin

9:45 p.m. - 11:15 p.m.: Bless Auditorium

SESSION Q. EXCITATION BY ELECTRONS (PANEL)

Chairman: C. C. Lin
University of
Wisconsin

- Q1. ELECTRON EXCITATION OF POTASSIUM AND CESIUM
Jerry E. Solomon, Dale F. Korff and Chun C. Lin
- Q2. ELECTRON IMPACT EXCITATION OF ATOMIC NITROGEN
E. C. Zipf and E. J. Stone
- Q3. ELECTRON IMPACT EXCITATION OF THE WERNER BANDS OF H_2
E. J. Stone and E. C. Zipf
- Q4. EXCITATION OF THE METASTABLE $A^3\Sigma_u^+$ STATE OF N_2 BY ELECTRON IMPACT
Walter L. Borst
- Q5. TRANSLATIONAL SPECTROSCOPY OF FAST METASTABLES PRODUCED BY ELECTRON IMPACT DISSOCIATION OF ATMOSPHERIC GASES
W. C. Wells, W. L. Borst and E. C. Zipf
- Q6. HYDROGEN BALMER CROSS-SECTIONS FROM ELECTRON-MOLECULE COLLISIONS
R. A. Mickish and R. M. St. John

Thursday, October 7

8:30 a.m. - 10:00 a.m.: Ballroom A

SESSION R. LASERS II

Chairman: D. R. Keefer
University of
Florida

- R1. OPERATING PARAMETERS OF SEALED-OFF CO₂ AND CO₂-He LASERS
W. T. Whitney
- R2. THE INFLUENCE OF PLASMA-GENERATED IMPURITIES ON MOLECULAR
GAS DISCHARGES
W. J. Wiegand
- R3. INFLUENCE OF CONTAMINANTS ON THE CO₂ LASER
P. Bletzinger, M. Hughes, P. D. Tannen and A. Garscadden
- R4. EXPERIMENTAL STUDIES ON EFFECTS OF Na VAPOR MIXED
WITH ACTIVE N₂
R. E. Walker and J. C. Pirkle
- R5. MEASUREMENT OF THE VIBRATIONAL POPULATION DISTRIBUTION
IN DISCHARGED N₂
S. J. Young and K. P. Horn
- R6. LASER EXCITED VIBRATIONAL ENERGY TRANSFER STUDIES OF
HYDROGEN FLUORIDE
W. H. Green and J. K. Hancock

8:30 a.m. - 9:50 a.m.: Reitz Auditorium

SESSION V. ION-MOLECULE REACTIONS AND
CHARGE TRANSFER

Chairman: R. C. Isler
University of
Florida

- V1. ION-MOLECULE EXPERIMENTS INVOLVING NEGATIVE IONS
OF TUNGSTEN AND RHENIUM OXIDES
R. E. Center
- V2. REACTIONS OF H⁻ AND D⁻ WITH D₂, H₂, AND HD
J. F. Paulson
- V3. CHARGE TRANSFER AND IONIZATION IN COLLISIONS BETWEEN
ATOMIC IONS AND RARE GAS ATOMS-FOR PRIMARY ION ENERGIES
BELOW 100 eV.
W. B. Maier II
- V4. ELECTRON TRANSFER IN COLLISIONS OF DOUBLY CHARGED RARE
GAS IONS AND RARE GAS ATOMS FOR PRIMARY ION ENERGIES
BELOW 100 eV
W. B. Maier II and Bruce Stewart

PLENARY SESSION

11:15 - 12:00 noon, Thursday, October 7

Ballroom A, Reitz Union

Chairman: Prof. W. P. Allis

Invited Speaker: Prof. R. Wieniecke, Technical Institute for
Plasma Physics, Stuttgart

Topic: ELECTRICAL GAS DISCHARGES IN STRONG MAGNETIC FIELDS

- V5. DRIFT TUBE MEASUREMENTS OF THE REACTIONS $U^+ + O_2$ AND $U^+ + N_2$ FROM THERMAL ENERGY TO ~ 11 eV
R. Johnson, and Manfred A. Biondi
- V6. TOTAL COLLISION CROSS SECTIONS FOR ION-POLAR MOLECULE COLLISIONS
J. V. Dugan, Jr. and J. L. Magee

10:20 a.m. - 11:05 a.m.: Ballroom A

SESSION S. LASERS III

Chairman: D. R. Keefer
University of
Florida

- S1. GAS PUMPING BY STRIATIONS IN DC DISCHARGES
C. C. Leiby, Jr.
- S2. LASER EMISSION FROM THE WERNER BAND OF HYDROGEN
R. W. Waynant
- S3. EXCITATIONS AND HEATING PROCESSES IN A PULSED ARGON ION LASER PLASMA
B. G. Bricks, John D. Litke, Donald E. Kerr

10:10 a.m. - 11:10 a.m.: Reitz Auditorium

SESSION W. ELECTRON SCATTERING

Chairman: P. D. Burrow
Yale University

- W1. CROSSED BEAM EXPERIMENTS ON LOW ENERGY $e-O_2$ COLLISION PROCESSES
F. Linder and H. Schmidt
- W2. ELECTRON TRANSMISSION SPECTRA OF NO AND O_2
L. Sanche and G. J. Schulz
- W3. LOW ENERGY ELECTRON SCATTERING BY POLAR MOLECULES
W. R. Garrett
- W4. MEASUREMENTS OF LARGE ANGLE INELASTIC SCATTERING CROSS SECTIONS IN HELIUM
C. B. Opal and E. C. Beaty

PLENARY SESSION

Chairman: Prof. W. P. Allis, M.I.T.
11:15 a.m. - 12:00 noon
Ballroom A

G. E. C. BUSINESS MEETING

Chairman: G. H. Dunn
12:00 noon - 12:30 p.m.
Ballroom A

2:30 p.m. - 4:00 p.m.: Ballroom A

SESSION T. LASERS IV

Chairman: W. Graham
Naval Research
Laboratory

- T1. A STABLE, SCALABLE, HIGH PRESSURE GAS DISCHARGE AS APPLIED TO THE CO₂ LASER
J. D. Daugherty, E. R. Pugh, D. H. Douglas-Hamilton
- T2. CHARACTERISTICS OF AN ELECTRON BEAM CONTROLLED PLASMA DISCHARGE
Charles A. Fenstermacher, Murlin J. Nutter, Wallace T. Leland and Keith Boyer
- T3. A COLD GLOW DISCHARGE LASER ENERGY SOURCE
Carroll B. Mills
- T4. CURRENT IN THE COLD LASER PLASMA
Carroll B. Mills and Jay Todd, Jr.
- T5. THE KINETICS OF ELECTRON BEAM CONTROLLED CO₂ LASER SYSTEMS
Andrew M. Lockett III
- T6. THE TRANSIENT GLOW DISCHARGE IN A PULSED ATMOSPHERIC CO₂ LASER
Jean Rocca Serra

2:30 p.m. - 4:00 p.m.: Reitz Auditorium

SESSION X. CHEMI-IONIZATION (PANEL)

Chairman: C. B. Collins
University of
Texas at Dallas

- X1. EXCITATION TRANSFER BETWEEN HELIUM METASTABLES AND CO
W. B. Hurt and W. C. Grable
- X2. PENNING IONIZATION OF ATOMIC HYDROGEN
J. S. Cohen and Neal F. Lane
- X3. ROTATIONAL EXCITATION IN PENNING EXCITATION OF MOLECULES
W. K. McGregor and J. M. Lents
- X4. COHERENT EXCITATION OF IONS BY PENNING COLLISIONS
L. D. Schearer
- X5. MEASUREMENT OF REACTION TIMES IN THE NANO-SECOND RANGE
C. B. Collins, B. W. Johnson and M. J. Shaw

4:30 p.m. - 6:00 p.m.: Ballroom A

SESSION U. LASERS V

Chairman: W. L. Nighan
United Aircraft
Research Laboratories

- U1. BEHAVIOR OF A LARGE VOLUME GLOW DISCHARGE IN A HIGH PRESSURE
CONVECTIVE FLOW GAS LASER
O. Judd
- U2. AFTERGLOW GAIN CHARACTERISTICS OF UNIFORM GLOW HIGH PRESSURE
DISCHARGES IN CO₂-N₂-He MIXTURES
L. J. Denes
- U3. THE GENERATION OF INFRARED RADIATION AND THE TRANSITION
FROM GLOW TO ARC IN DISCHARGES THROUGH CO₂:N₂ NEAR
ATMOSPHERIC PRESSURE
T. V. George and E. W. Sufov
- U4. EXCITATION AND IONIZATION OF A CO₂ LASER PLASMA BY
NUCLEAR REACTION PRODUCTS
H. S. Rhoads and R. T. Schneider
- U5. COMBINED RF AND DC EXCITATION OF A CO₂ LASER
J. C. Swingle and D. R. Keefer
- U6. FAST PULSE RATE ELECTRICAL DISCHARGES IN A SUPERSONIC
CO₂-N₂-He GAS
W. M. Brandenburg

4:30 p.m. - 6:00 p.m.: Reitz Auditorium

SESSION Y. ELECTRON-ION RECOMBINATION

Chairman: D. E. Kerr
The Johns Hopkins
University

- Y1. RECOMBINATION OF ELECTRONS WITH POSITIVE IONS OF THE H_3O^+ -
(H_2O)_n SERIES
M. T. Leu, M. A. Biondi and R. Johnsen
- Y2. RECOMBINATION OF ELECTRONS WITH MOLECULAR HELIUM IONS
A. Wayne Johnson and J. B. Gerardo
- Y3. MEASUREMENTS OF THE SPECTRAL LIGHT EMISSION FROM DECAYING
HIGH PRESSURE HELIUM PLASMAS
J. Stevefelt, J. Johansson, and F. Robben
- Y4. THE EFFECT OF ROTATIONAL STATES ON THE COLLISIONALLY
STABILIZED RECOMBINATION OF MOLECULAR IONS WITH ELECTRONS
C. B. Collins
- Y5. DIRECT MEASUREMENT OF THE RATE COEFFICIENT FOR THE
RECOMBINATION OF He^+ WITH ELECTRONS IN A HIGH PRESSURE
AFTERGLOW
C. B. Collins, H. S. Hicks, and W. E. Wells
- Y6. DIRECT MEASUREMENT OF THE RATE COEFFICIENTS FOR RECOMBINATION
OF He^+ AND He_2^+ WITH ELECTRONS AT AN ASYMPTOTICALLY LOW
NEUTRAL GAS PRESSURE
R. Burton, C. B. Collins, and H. S. Hicks

RECEPTION

7:00 p.m.
Pool Deck, Flagler Inn (Cash Bar)

BANQUET

8:00 p.m.
Grand Hall, Flagler Inn

Chairman: Dr. Gordon H. Dunn, JILA

1. Opening remarks and announcements
2. A tribute to Leonard Loeb on the occasion of his eightieth birthday.
3. Principal Speaker: Dr. James R. Cade, Chief of Renal Medicine,
College of Medicine, University of Florida.
"Sweat, Urine, and Apple Pie"

Friday, October 8

8:30 a.m. - 10:00 a.m.: Reitz Auditorium

SESSION Z. EXCITATION BY IONS (PANEL)

Chairman: L. D. Doverspike
College of William
and Mary

- Z1. STUDY OF LIGHT PRODUCED BY COLLISIONS OF LOW-ENERGY He^+ WITH N_2
Redus F. Holland and William B. Maier II
- Z2. POLARIZATION OF THE H_α LINE PRODUCED IN $\text{He}^+ + \text{H}_2$ COLLISIONS
R. C. Isler and R. D. Nathan
- Z3. CROSS SECTIONS FOR EXCITATION OF PURE VIBRATIONAL TRANSITIONS
IN H_2 BY PROTON IMPACT
F. A. Herrero and J. P. Doering
- Z4. ADIABATIC POTENTIAL CURVES FOR $\text{Li}^+ + \text{Li}$ COLLISIONS
H. H. Michels
- Z5. CURVE CROSSING IN THE $\text{Ne} - \text{He}^+$ SYSTEM
S. M. Bobbio, L. D. Doverspike, W. A. Rich, and R. L. Champion
- Z6. ABSOLUTE DIFFERENTIAL CROSS SECTIONS FOR EXCITATION OF THE
 $\text{He}(1s2s) + \text{Ne}^+(2p^5)$ STATE IN $\text{He}^+ - \text{Ne}$ COLLISIONS
Preben Loftager, Donald C. Lorents, and James R. Peterson

8:30 a.m. - 9:50 a.m.: Ballroom A

SESSION BB. ATTACHMENT

Chairman: R. Celotta
NBS, Washington

- BB1. FINAL-STATE EFFECTS IN THE DISSOCIATIVE ATTACHMENT
OF ELECTRONS TO H_2 , HD AND D_2
George V. Nazarov
- BB2. ELECTRON ATTACHMENT IN SF_4
C. L. Chen and Peter J. Chantry
- BB3. DISSOCIATIVE ATTACHMENT IN OZONE
P. J. Chantry
- BB4. DISSOCIATIVE ATTACHMENT FROM THE $a^1\Delta_g$ STATE OF O_2
P. D. Burrow
- BB5. THREE-BODY ATTACHMENT IN O_2 USING ELECTRON BEAMS
D. Spence and G. J. Schulz
- BB6. LOW TEMPERATURE THERMAL ELECTRON ATTACHMENT IN O_2
F. K. Truby

10:15 a.m. - 11:20 a.m.: Reitz Auditorium

SESSION AA. RADIATIVE LIFETIMES

Chairman: D. A. Micha
University of
Florida

- AA1. EXCITED STATE LIFETIME MEASUREMENTS IN ATOMIC HELIUM
R. G. Fowler and R. T. Thompson
- AA2. RADIATIVE LIFETIME OF THE $A^2\Sigma^+$ STATE OF OH
R. Anderson and R. Sutherland
- AA3. RADIATIVE LIFETIME OF THE $v = 1$ LEVEL OF THE $A^1\Pi$ STATE OF
CARBON MONOXIDE
R. L. Burnham and R. C. Isler
- AA4. EMISSION FROM LONG-LIVED STATES OF NO^+
Redus F. Holland and William B. Maier II
- AA5. STUDY OF THE $A \rightarrow X$ TRANSITIONS IN CO^+ AND N_2^+
William B. Maier II and Redus F. Holland

10:15 a.m. - 11:15 a.m.: Ballroom A

SESSION CC. DETACHMENT

Chairman: C. L. Chen
Westinghouse
Research Labs.

- CC1. ELECTRON AVALANCHES IN OXYGEN: A FAST ELECTRON
DETACHMENT PROCESS
D. Goodson, L. Frommhold and R. Corbin
- CC2. ELECTRON AVALANCHES IN OXYGEN: A SLOW ELECTRON
DETACHMENT PROCESS
L. Frommhold, D. Goodson, and R. Corbin
- CC3. PHYSICS OF ASSOCIATIVE DETACHMENT
J. L. Mauer and G. J. Schulz
- CC4. COLLISIONAL DETACHMENT STUDIES OF NO^+
M. McFarland, D. B. Dunkin, F. C. Fehsenfeld, A. L. Schmeltekopf
and E. E. Ferguson

Gaseous Electronics Conference Executive Committee

G. H. Dunn, Chairman
JILA

C. C. Lin
University of Wisconsin

W. P. Allis, Honorary Chairman
Massachusetts Institute of Technology

J. W. McGowan
University of Western Ontario

R. H. Bullis, DEAP Representative
United Aircraft Research Laboratories

J. C. Morris
AVCO

D. M. Benenson
SUNY at Buffalo

H. J. Oskam
University of Minnesota

F. C. Fehsenfeld
ESSA Research Laboratories

G. J. Schulz
Yale University

T. L. Bailey, Secretary-Treasurer
University of Florida

Local Arrangements Committee

S. O. Colgate

D. A. Micha

A.E.S. Green

E. E. Muschlitz, Jr.

R. C. Isler

R. T. Schneider

D. R. Keefer

ABSTRACTS

Third Arc Symposium

5-6 October, 1971

J. Wayne Reitz Union
University of Florida
Gainesville, Florida

SESSION A

Tuesday Morning, 5 October

8:30 a.m.

ARC PROPERTIES

Chairman: W. Braun, Aerospace Research Laboratories, WPAFB

A1. Temperature Profile Determination in an Absorbing Plasma. J. L. USHER AND H. D. CAMPBELL, University of Florida - A method for the determination of the temperature profile of an absorbing, cylindrically-symmetric plasma is described. The technique is an extension of the brightness emissivity method to the nonhomogeneous case. Knowledge of the atomic constants of the plasma constituents is not required. A sample temperature profile is found using an argon arc, and the method is shown to be viable. A sensitivity analysis shows the new technique to be more accurate than those previously developed.

A2. Plasma Properties of a D.C. Uranium Arc. J. M. MACK, JR., J. L. USHER, H. D. CAMPBELL, and R. T. SCHNEIDER, University of Florida - Measurements of the intensity in the near ultra-violet and visible region of a uranium arc plasma are reported. In addition, the boiling point of the anode material (Uranium) is also determined from current-voltage characteristics. Spatial unfolding is used to determine the emission coefficient in the spectral range 2000 angstroms to 6000 angstroms. The uranium partial pressure is estimated to range between .01 and .1 atmospheres, and the corresponding temperature range is 8000 - 12000 degrees Kelvin.

A3. Electrical and Optical Measurements in 1000 atm Arcs. D. BARTELHEIMER, Systems Research Lab. and U.H. BAUDER, Aerospace Research Lab - Arc discharges in argon are operated steady state in the pressure range from 1-1000atm. The electrode consist of water cooled tungsten rods. Above 200 atm a free burning arc configuration may be used for spectroscopic measurements at currents, $I \leq 60$ amp. Higher arc currents lead to corkscrew instabilities. Vortex and straight flow stabilization schemes are used for the high pressure/high current regime. The field strength of the cylindrical part of the column is determined by varying the arc length (0-15mm), values of $E = 160V/cm$ result at $I = 50$ amp and 950 atm. The radiative diameter, d , of the arc column is $d \leq 5mm$. as determined from spectroscopic measurements of the absolute intensity in different wavelength regions. Estimates of the plasma temperature are performed from the optical measurements (assuming the plasma to have an optical depth $\tau \gg 1$). The resulting temperatures in the 6000-9000^o K range are compared to estimates based on Ohm's law using theoretical values of the electrical conductivity and the measured values of E , I , and d .

A4. Electrical Conductivity from Arc Measurements.*
R. S. DEVOTO, D. MUKHERJEE, Stanford University.
A new technique has been developed for the deduction of electrical conductivity σ (as a function of temperature T) from the current-voltage characteristics and radial temperature profiles measured in an electric arc. By using the functional fit $\sigma = aT^{-b}e^{-c/T}$ (a, b, c are undetermined constants) chosen on the basis of knowledge of the temperature dependence of theoretical conductivity values for a typical gas (e.g. argon), the Ohm's law equation for an arc has been solved by an iterative scheme. Arc data for atmospheric nitrogen and argon have been analyzed using this technique and the deduced conductivity values are found to be in good agreement with theory. The agreement is extremely good for argon and removes the discrepancy at low temperatures between theory and previous conductivity deductions from the same data.

*Research sponsored by Aerospace Research Laboratories, USAF.

A5. Equilibrium Composition and Transport Properties of SF₆. R.W. Liebermann, Westinghouse Research Labs.

The equilibrium composition of SF₆ was determined as a function of temperature and pressure by minimizing the Gibbs free energy using geometric programming. Chapman Enskog approximations have been used to calculate the thermal conductivity and the viscosity. The electrical conductivity was calculated by solving the electron mobility integral assuming the electrons have a Maxwellian velocity distribution. Demixing effects have been simulated by using ratios of S:F of 1:3 and 1:12. Resultant changes in thermal and electrical conductivities are less than 15% for temperatures above 5000°K. Of the 9 negative ion species considered only F⁻, S⁻ and SF⁻ have mole fractions > 10⁻⁸ at a pressure of 1 atmosphere. The presence of negative ions has a negligible effect on the thermal conductivity but reduces the electrical conductivity at low temperatures, e.g. by a factor of 3 at 4000°K. The S-S and F-F cross sections based on a Lennard Jones 6-12 potential gives thermal conductivities less consistent with experimental data than an S-S and F-F cross section equal to published values for 0-0.

SESSION B

Tuesday Morning, 5 October

9:45 a.m.

RADIATIVE AND EQUILIBRIUM PROPERTIES OF ARCS

Chairman: R. S. Tankin, Northwestern University

B1. A Wall-Stabilized Arc as a Standard Light Source Below 1100 Å.* G. L. WEISSLER and S. K. SRIVASTAVA, U. of So. Calif.--A method is described for the determination of a standard source for the vacuum uv, using the blackbody properties of the plasma generated in a wall-stabilized high current ($\sim 100A$) arc, operated in either argon or helium at atmospheric pressure. Making use of the conditions of Local Thermodynamic Equilibrium (LTE), emission and absorption are related by Kirchoff's law, with the Planck function $B_{\lambda}(T)$ as the proportionality factor between them. The value of this function has been determined experimentally by using either the carbon¹ or the argon continuum covering the wavelength range from 1100 Å to 900 Å and 750 Å to 550 Å. The continuous character of $B_{\lambda}(T)$ permits interpolation in the region where spectral lines are present. For the 750 Å-550 Å region the arc was operated in helium, and trace argon was flown in its central portion. Questions of argon being in LTE, when immersed in a helium plasma, will be discussed, and experimental proof will be given in terms of temperatures data, which were obtained by using three independent methods.

*Partially supported by ONR.

¹W. Hofman and G. L. Weessler, J. Opt. Soc. Am. 61, 223 (1971).

B2. A New Radiation Standard for the Vacuum Ultraviolet.* W. R. Ott, P. Fieffe-Prevost, and W. L. Wiese, National Bureau of Standards --- A radiation standard offering a nearly continuous spectrum of known intensity is being developed for use in the wavelength region 50nm - 360nm. The light source is a wall-stabilized arc discharge operating in pure hydrogen. It emits a spectrum between 110nm and 360nm, the range of the present investigation, which is continuous and optically thin except for the blackbody-limited Lyman alpha line of hydrogen. The calibration of a spectrometer-detector system is realized by observing along the axis of the discharge where the temperature is nearly uniform. Since the plasma, to a good approximation, is in LTE and since the theoretical emissivity of the hydrogen plasma is very accurately known, a measurement of just one property of the homogeneous plasma, e.g. electron density, is sufficient to determine the absolute emission intensity. The response of our system has been measured in this way and compared both in the near UV with tungsten strip lamp calibrations and in the VUV with calibrations using the blackbody ceilings of resonance lines of additive gases. Consistent results have been obtained which appear to be within the expected 10-20% uncertainty limits.

*Work supported in part by NASA.

B3. Measurements of the Ground State Recombination Cross Section of Argon 700 to 800 Angstroms.*

J. C. MORRIS** - AVCO, Wilmington, Mass. - The recombination cross section for the ground state continuum of the argon atom has been measured in the wavelength region of 700 to 800 angstroms using the emission spectra of argon heated in a mechanically constructed neon arc. The temperature of the neon arc was determined from the absolute intensities of various neon lines and through electron number density measurements using $H\alpha$, hydrogen being added in trace amounts. The amount of argon added to the neon arc was determined through composition calculations and through the absolute intensities of atomic argon lines in the visible portion of the spectra. The ground state emission of argon was put on an absolute basis by comparing it to the black body emission of a neon arc with hydrogen and/or nitrogen added in sufficient quantities to make it optically thick. The measured cross sections for argon were 30 to 35 mb which agree with the data of Samson⁽¹⁾ to within $\pm 15\%$.

1. J. A. R. Samson, JOSA 54, 420 (1964)

* Work supported by Aerospace Research Laboratories,
Wright Patterson Airforce Base under Contract
AF33(613)2976

** Presently at GTE Sylvania Inc., Danvers, Mass.

B4. A Study of Equilibrium in Argon Arcs, J. B. Shumaker and C. H. Popenoe, NBS, Wash. D.C. -- Measurements were made of the intensities of the 7147 \AA Ar I line and the 4806 \AA Ar II line in a wall-stabilized arc at pressures from 0.2 to 5 atm. and over a temperature range from 10 000 K to 20 000 K. The results are presented in a log-log plot in order to demonstrate departures from local thermodynamic equilibrium (LTE) at electron densities below $5 \times 10^{16} \text{ cm}^{-3}$ and the apparent existence of LTE at higher electron densities. In this approach no a priori transition probability values are needed. The departures from LTE are interpreted as ground state overpopulations of both neutral and ionic species. Transition probabilities obtained from the data at high electron densities are $5.57 \times 10^5 \text{ sec}^{-1}$ for 7147 \AA Ar I and $7.86 \times 10^7 \text{ sec}^{-1}$ for 4806 \AA Ar II. The agreement with lifetime measurements is poor for the Ar I line but good for the Ar II line.

B5. Transition Probabilities of the 4108, 4916 and 10139 Hg Lines. J. C. MORRIS and P. L. PATTERSON, GTE Sylvania Inc. - The relative transition probabilities for the 4108, 4916 and 10139 angstrom $n^1S_0-6^1P_1$ singlet mercury atomic lines have been measured using a 2 atmosphere pressure mercury arc as an emission source. The standard procedures for Abel inverting the measured intensity to obtain emission versus radius, and of making double pass transmission measurements to insure optical thin conditions were followed. The resulting A values have been compared with a theoretical calculation using the coulomb approximation method of Bates and Damgaard⁽¹⁾ and using a scaled Thomas-Fermi-Dirac wave functions approach by Warner.⁽²⁾ The experimental data agree on a relative scale to within $\pm 15\%$ with both theoretical calculations. Using Kenty's⁽³⁾ relationship for estimating the pressure in the discharge tube, the absolute A values were found to agree with theory to within an uncertainty of $\pm 30\%$.

1. D. R. Bates, A. Damgaard, Phil. Trans. Roy. Soc. London, Ser. A, 242 (1949)
2. B. Warner, Mon. Not. R. Astr. Soc. 140, 539 (1967)
3. C. Kenty, Phy. Rev. 61, 543 (1942)

SESSION C

Tuesday Morning, 5 October

11:20 a.m.

MAGNETIC AND FLOW EFFECTS IN ARCS. I.

Chairman: C. J. Michels, NASA Lewis Research Center

C1. A Confined-Discharge Plasma Generator with Local Radial Gas Injection.* J. R. MAHAN, Virginia Polytechnic Institute and State University, and C. J. CREMERS, University of Kentucky -- The energy conversion efficiency and the mean plasma enthalpy of conventional confined-discharge plasma generators are inversely related, so that one can be increased only at the expense of the other. This undesirable behavior is a consequence of the manner in which the cold working fluid is introduced into the arc colume. A new technique for introducing the working fluid is described which results in significant increases in both the energy conversion efficiency and the mean plasma enthalpy. A portion of the gas is injected radially through one or more circumferential slits in the wall of the confining duct, thus constricting the arc colume in the vicinity of each injection station. This causes local increases in energy density and plasma temperature concomitant with local decreases in wall heat flux. Experimental results are presented which document and explain the observed improvement in performance.

* Supported by NSF grant GK1243.

C2. Heat Flux and Current Density to a Tube Immersed in an Arc Plasma. T. Meyer, Westinghouse Corp., Pittsburgh and E. Pfender, University of Minnesota.-- A water-cooled copper tube is immersed in an atmospheric pressure free-burning argon arc. Velocities of 500 m/sec and temperatures of 16,000°K are typical centerline conditions of the free stream near the tube. Over the tube's circumference, average local heat fluxes and current densities are determined, and the dependence of the heat flux on the current density is established. A tube coated with a 20 micron layer of pyrex glass is found to absorb identical heat fluxes as the locally floating copper surface and an analytical argument for the equivalence is given. For both pyrex and copper surfaces, local floating heat fluxes can be accurately repeated (within 3%).--Measured ion saturation current densities, together with an analysis of the region near the wall dominated by ambipolar diffusion and thermal conduction, indicate this region, plus the viscous layer, to be of frozen chemistry. A simple heat transfer model describes the heat flux-current density characteristics.

C3. Stable Configuration of Electric Arcs in Transverse Magnetic Fields. H. O. Schrade, Aerospace Research Laboratories, WPAFB, Ohio. Deviations from rotational symmetry of arc columns exposed to transverse magnetic fields cause convection and a momentum transport between the column and its surrounding gas. As a consequence the arc moves and changes its geometry until it reaches a stable configuration. Based on the momentum transport equation, the arc behavior is discussed under various operating conditions and stable arc configurations are determined.

C4. Magnetically Balanced Cross-Flow Arcs^{*}, V. R. MALGHAN and D. M. BENENSON, State Univ. of N.Y. at Buffalo--By specifying two of the arc variables (current (I), voltage gradient (E), velocity (U_{∞}), magnetic field (B), and characteristic length in cross-section (L)) and through force balance, heat balance, and Ohm's law (incorporating details of temperature field within arc), both absolute magnitude and (implicit) power law dependence of three variables were obtained in terms of the two independent variables. Phenomenological solid body relations for drag and heat transfer coefficients were employed. Determination of B, E, and L as functions of U_{∞} and I were within 10-40 percent of experimental results of Roman and Meyers over the range of currents and velocities (I:200-400A; U_{∞} :5-15 m/s). Predicted values of B as functions of U_{∞} (I=const.) were about two times greater than Winograd and Klein's experiments (I=20A); and about an order of magnitude greater than obtained in low current experiments (I=4A) by Thiene. This difference in low current case may be due to flow through arc, with consequent reductions in drag and required B. For Reynolds numbers corresponding to those of Thiene's experiments, such behavior was predicted in the analysis of Malghan and Benenson.

*Research supported by NSF Grants GK-1174 and GK-2886 and USAFOSR Grant 70-1928.

SESSION D

Tuesday Afternoon, 5 October

2:00 p.m.

MAGNETIC AND FLOW EFFECTS IN ARCS II.

Chairman: E. Pfender, University of Minnesota

D1. PRODUCTION OF EQUILIBRIUM PLASMA INSIDE A HOLLOW MAGNETICALLY CONFINED ARC -- C. M. Fitts and C.E. Nielsen
The Ohio State University, Columbus, Ohio

Magnetically confined arcs between solid cylindrical electrodes and also between electrodes of annular cross section have previously been used to obtain temperatures $\sim 10^5$ °K. With solid electrodes temperature and pressure are maximum on axis, while with hollow electrodes the longitudinal plasma outflow can lead to profiles with axial minima. We are operating a helium arc using an incandescent tungsten cathode having an axial hole, but with longitudinal outflow prevented. This configuration would be expected to yield nearly flat profiles in the current-free core, which is in effect enclosed in a plasma oven consisting of the current-heated hollow cylindrical arc. This core may be closer to a static equilibrium plasma than found in either solid or open ended arcs, lacking the strong radial gradients of the first and the strong flow pattern of the second. In a 1000 amp arc with ambient $p \sim 1$ Torr, $B \sim 1500$ gauss, cathode 12 mm diam. and hole 6 mm we estimate core $T \sim 4 \times 10^4$ °K. Profiles in He^+ light indicate that T is lower in the core near the cathode and fairly uniform across the core near the center of a 16 cm arc.

D2. Stability Characteristics of a Dense Highly-Ionized Magnetized Arc Column.* D. L. JASSBY, M. MARHIC, D. R. REGAN, UCLA.--A steady-state argon arc is operated between cooled tungsten electrodes (10 to 15 cm separation) at plasma densities up to 10^{16} cm⁻³, in an axial magnetic field up to 10 kG. Neutral pressure is 0.7 to 5 torr, so the dominant collisions are electron-ion. At smaller arc current, J , smaller magnetic field, B (but $B > 1.8$ kG), and larger pressure, P , the plasma fluctuation level is about 0.1%, as observed on water-cooled probes and the arc current. An intense coherent instability, 25 to 40 decibels above the background noise, is observed when either a) J is raised above a critical value, or b) B is raised above a critical value, or c) P is lowered below a critical value. The instability is azimuthally propagating, and its frequency lies between 15 kHz and 60 kHz. The observed properties of this instability are compared with macroscopic fluid theory.

*Work supported by the U. S. Atomic Energy Commission.

D3. THE INCLUSION OF AN ARC PLASMA AT ATMOSPHERIC PRESSURE IN TOROIDAL GEOMETRIES

A. WYNANDS and G. SCHMITZ, I. Phys. Inst. TH, Aachen, Germany. The inclusion of a plasma in a toroidal geometry is intensively investigated in the last years, essentially for experiments of nuclear fusion. Contrary to cylindrically symmetric arcs there occur asymmetries caused by the curvature of the tube, which complicate a theoretical determination of thermal and magnetogasdynamic quantities. In this paper the influence of a curved geometry on a d. c. -plasma at high density is discussed. Results for a N_2 - and H_2 -plasma are communicated and discussed as functions of the total electric current and the curvature of the discharge tube. In particular results-gained by a computer simulation- are presented for the distribution of temperature and pressure, the magnetic field, the balance of power, the thermal load capacity of the wall, the Lorentz forces and a rotation of the plasma in form of a double whirl caused thereby. A comparison of the toroidal arc with a cylindrical one shows furthermore its advantages and disadvantages.

D4. Endothermic Reactions in Arc Discharges.

C.H. LEIGH, Hydro-Quebec Institute of Research, Varennes, Quebec, Canada.--The present paper describes the studies made to determine the energy absorbed by an endothermic reaction initiated by a high energy electrical discharge. The research is directed towards the utilization of endothermic reactions to absorb the discharge energy of an electric arc, leading to arc extinction.

We have investigated the efficiency of the reaction $2CH_4 \rightarrow C_2H_2 + 3H_2$, $-\Delta H = 90$ k.cals. using discharge currents of 25 kiloamperes and discharge times of up to 0.8 milliseconds.

Experimental techniques, data reduction techniques and analytical results are presented.

D5. Unsteady Phenomena in a Circuit Breaker Nozzle*. J. M. NOVAK and R. L. PHILLIPS, U. of Michigan. An efficient numerical model of a gas-blast circuit breaker has been developed to study the effects of nozzle geometry and "arc-like" heat addition on the flow in a DeLaval nozzle. An explicit, second-order, predictor-corrector technique is used to solve the unsteady quasi-one-dimensional conservation equations of gasdynamics. Numerical instabilities are successfully avoided without the introduction of artificial diffusion terms into the equations. The results detail the approach to the steady or quasi-steady state (from an initially isentropic flow) for DC and AC arc heat inputs, respectively. Several transient phenomena important to the circuit-breaking potential of a supersonic nozzle, such as (1) reverse flow in the subsonic portion of the nozzle (i. e. "clogging"), (2) the density and static temperature distributions after current zero, and (3) the variation of the voltage drop across the nozzle are readily interpreted by means of a computer-generated film which will be presented.

* Submitted by R. S. B. Ong

D6. Flow Characteristics in the Exhaust of a Pulsed Megawatt Gas-Fed Arc. C. J. Michels, NASA-Lewis Research Center and T. M. York, Penn State University. --The transient flow generated by a pulsed, megawatt-level gas-fed arc has been examined with a new design piezoelectric pressure transducer. Sensor thermal conduction and accelerations have been identified and accounted for in the 500 μ sec plasma flow period. Existence of a large magnitude cold gas pressure front of 20 μ sec duration has been reconfirmed and its relationship to the following plasma flow of about 200 μ sec duration has been clarified. At a point 30 cm from the arc source, initially near vacuum conditions, typically with 11.2 kiloamp current and 1 tesla diverging applied magnetic field, a pressure pulse magnitude of 10^4 N/m² with apparently unionized gas is followed by plasma flows with nearly constant impact pressure of 10^3 N/m². Pressure in this plasma region is seen to decrease with applied magnetic field strength. With electron density derived from Thomson scattering measurements (10^{20} m⁻³) plasma flow velocities on the order of 5×10^4 m/sec are indicated.

SESSION E

Tuesday Afternoon, 5 October

3:50 p.m.

TIME VARYING ARCS. I.

Chairman: P. W. Schreiber, Aerospace Research Laboratories, WPAFB

E1. Modulated Spectra of AC Arc Lamps.

P. L. PATTERSON, GTE Sylvania Inc. - Light emanating from AC arcs operating on 60 Hz power exhibits a 120 Hz modulation of intensity. Although time averaged spectra of such arcs are usually reported, the instantaneous light spectrum and its dependence on the oscillating plasma temperature is a more valuable source of spectroscopic information. An experimental technique is described for scanning the light spectrum of an AC discharge at any fixed phase in the arc operating cycle. Spectra were recorded at phases corresponding to maximum and minimum light output for a pure Hg arc; a Hg-Na, Sc, Th metal iodide arc; and a Hg-SnI₂ arc. All these arcs had operating pressures of about 2-4 atmospheres and core temperatures of about 3000-6000°K. Intensity ratios I_{\max}/I_{\min} of spectral lines were generally found to increase with increasing upper state energy. Many of the dominant lines also exhibited sizeable changes in line profile with variations of phase. In the Hg-Na, Sc, Th metal iodide arc, it was possible to use the intensity variations of optically thin lines to obtain rough estimates of upper state energies and relative gA values of some Sc and Th lines for which these quantities were previously unknown.

E2. Spectroscopic Analysis of a High Current, Free Burning Arc in Argon at Atmospheric Pressure, E. SCHULZ-GULDE and P. G. SLADE, Westinghouse Research Laboratories--A technique has been developed to take short-time exposure photographic spectroscopy on ac arcs. In these experiments a free burning argon arc was formed between Cu electrodes (0.96 cm spacing) and spectra perpendicular to the axis of the arc were taken at ± 500 μ sec around current maximum (1100 A peak) of an ac half cycle. Spectra were taken for five axial positions between cathode and anode. The diameter of the arc varied from 1.7 cm, 1.25 mm from the cathode to 1.6 cm at mid gap to 1 cm, 1.25 mm from the anode. The maximum temperature of the arc was found to be 15,800 \pm 600°K. The assumption of LTE is discussed in terms of these results and the introduction of a small percentage of metal vapor into the arc is briefly discussed.

E3. Spectroscopic Measurements of the Electron Density in Nanosecond Discharges in Hydrogen-doped Argon. L. L. WIESE and J. A. AUGIS, Bell Telephone Laboratories, Columbus, Ohio.--Spectrographic measurements of the Stark broadening of the Balmer line H_{β} have been used to determine the electron density in short duration discharges in a mixture of 90% Argon + 10% H_2 at a pressure of 760 torr. The discharges were produced in an impedance-matched coaxial system of the type used by Augis and Gray.¹ Measurements were made as a function of axial position in the gap for discharge currents of 6 and 15 amperes and for discharge durations of 20, 80, and 250 nanoseconds. In all cases the breakdown voltage and gap were held approximately constant. The electron densities obtained ranged around $1 \times 10^{16} \text{ cm}^{-3}$.

¹ E. W. Gray, J. A. Augis, and F. J. Gibson, *Int. J. Electronics*, 30, 4 (1971).

E4. Time Resolved Radial Profiles of Wall Stabilized Arc Discharges in Xenon, Krypton and Cesium by S. Levy, Electronic Technology & Devices Laboratory (ECOM) Fort Monmouth, N. J. - The time dependence of the emission coefficients, absorption coefficients, and electron temperature distributions were determined for pulsed wall stabilized arcs. Measurements were made in narrow bore high pressure Xe, Kr, and Cs discharges. The particular spectral regions studied were those that correspond to the pumping bands of Nd:YAG lasers and the IR out to 4.2 micrometers. Square wave excitation, 100 to 500 microseconds in duration and over an energy range of from 1 to 30 joules were used. Side-on absolute intensities were recorded using a modification of Braun's¹ scanning apparatus. Time resolution was achieved with a boxcar integrator. The side-on profiles were converted to radial profiles by a computer program wherein self-absorption is taken into account. The results are prepared in the form of temporal growth and decay of radial distributions. A comparison of the results with Buhler's² model for non-steady thermal characteristics of Cs arcs has been made.

1 W. G. Braun, *Rev Sci Inst* 36, 802-5 (1965)

2 R. D. Buhler, *Bull Amer Phys Soc Series* 11, 15, 415 (1970)

SESSION F

Tuesday Afternoon, 5 October

4:50 p.m.

TIME VARYING ARCS. II.

Chairman: L. P. Harris, General Electric

F1. Measurement of Temperature in Decaying SF₆ Arc Plasma, H. C. LUDWIG, Westinghouse Research Laboratories --A spectroscopic method for the measurement of temperature in a decaying blown SF₆ arc plasma was developed. This method called a combination--single spectral line technique provides an internal emission coefficient standard of absolute intensities. Two representative spectral lines were chosen whose calculated absolute emission coefficient curves intersect or cross-over at a temperature occurring in the decaying plasma. Streak photography was used in acquiring the plasma spatial dependence necessary in computing the temperatures of the decaying plasma. The laboratory apparatus was designed to produce a blown SF₆ arc plasma with critical pressure flow conditions in a convergent-divergent nozzle. The decay of the plasma was observed in a time period after the initiation of a current crowbar from 400 amps. The current decreased at the rate of 11 amps/μsec. At the onset of crowbarring, the nozzle throat temperature was 15,900°K and 13,400°K at the nozzle exit. The emission from electronic excitation of the vibration states of the molecule S₂ was observed in the late stage of plasma decay.

F2. Decay of Conductivity of High Pressure Cylindrical Plasmas. J. J. LOWKE, R. E. VOSHALL and H. C. LUDWIG, Westinghouse Research Labs, -- Calculations assuming thermal equilibrium have been made of the properties of cylindrical arc plasmas which decay after the removal of the electric field. Account is taken of energy losses due to thermal conduction, radial convection and radiation. Self absorption effects are included in the treatment of radiation. Results of the total electrical conductivity as a function of time agree well with experimental results for N₂, Ar and SF₆ in 0.5 cm channels provided that the central plasma temperature is > 7500°K. When central plasma temperatures are < 7500°K experimental values of conductivity for N₂, Ar and air become greater than theoretical values. For SF₆, however, the experimental values become markedly less than the theoretical values. The theoretical curves indicate that radiation losses are dominant at a pressure of 8 atmospheres whereas at 1 atmosphere for currents of 100 A and less, conduction and radial convection are the dominant losses. Theoretical results are also given of examples of decaying temperature profiles and radial velocities of the contracting plasma.

F3. The Role of Gas Heating in the Constriction of a High-Pressure Glow Discharge Column. GERALD L. ROGOFF, Westinghouse Res. Labs.--Numerical simulation is used to examine the role of gas heating and radial expansion in initiating the constriction of a high-pressure positive column. The discharge model consists of an ionized column contained in a background of perfect gas which is initially of uniform density and temperature. The electron current density is expressed in terms of the gas density N , a constant axial electric field E , and an initial diffuse radial profile. The gas dynamics are described by time-dependent fluid equations for the conservation of mass, momentum, and energy written as explicit finite-difference equations. Radial profiles of gas properties and current density are calculated as functions of time for a 500 Torr hydrogen discharge similar to that examined in an experimental study¹ of the glow-to-arc transition. At ~ 60 nsec, when rapid changes in measured discharge properties appear, the axial gas temperature is calculated to be sufficiently high for significant dissociation to begin, and, due to the decrease in N and the resultant increase in E/N , the axial current density is twice its initial value.

¹M.C. Cavenor & J. Meyer, Aust. J. Phys. 22, 155 (1969).

F4. Enhancement of Electron Density in a Convergent High Current Pulse Discharge* D. C. SCHUBERT and H. GOLDIE, Westinghouse Electric Corp., Baltimore, MD.-- Electron densities and electron temperatures have been measured by means of spherical Langmuir probes at two points in a convergent conical gas discharge. This discharge is produced by passing a pulsed current (5-100 A) through 0.4 torr of H_2 surrounded by a conical metal electrode with a base diameter of 1 inch and a 20:1 beam area compression ratio. Pulsed operation was essential to prevent probe burnout. Interpretation of the probe V-I curves followed the spherical probe theory of Medicus. Measured electron densities continue the trends established in earlier low current measurements with dc discharges for the same geometry. Even at 100 amperes, the electron density is enhanced by a factor of 10 through beam compression and electron densities greater than 10^{14} electrons/cm³. Dense plasmas are thus generated without resort to converging magnetic fields or high gas pressures. The beam is stable, reproducible, and non-destructive to the electrode surfaces. Comparison is made of density measurements made with the Langmuir probes and with RF techniques.

* Work supported by Wright-Patterson AFB, Dayton, Ohio.

SESSION G

Wednesday Morning, 6 October

8:30 a.m.

VACUUM ARCS AND ELECTRODE PHENOMENA

Chairman: C. J. Cremers, University of Kentucky

G1. The Plasma Potential Adjacent to the Vacuum Arc Cathode.*G. W. McCLURE, Sandia Laboratories, Albuquerque, N. M.--The plasma over the cathode spot in a vacuum arc has been thought by Plyutto and co-workers to attain a potential several tens of volts positive relative to the cathode and the surrounding plasma. Some experimental data are consistent with this view. The cathode potential peak and the resultant kinetic energy of the effluent ions was thought to be due to ambipolar diffusion in which thermal energy of electrons is given to the ions. This process has been further examined in the light of experimental data from which the density, temperature, and size of the plasma zone over the cathode can be deduced. It is found that the escape of fast electrons in the tail of the Maxwell distribution causes a potential maximum whose peak value is several times the cathode fall voltage, and that the plasma continually reheats to sustain the production of energetic ions. The profound implications of this process relative to the mechanism of ionization and the ionic heating of the cathode are discussed.

*Research supported by the U.S. Atomic Energy Commission

¹A. A. Plyutto, V. N. Ryzhkov and A. T. Kapin, Sov. Phys.--JETP 20, 328 (1965)

G2. Energy Distributions of Ions from the Anode Plasma of a Pulsed Vacuum Arc.* J. T. GRISSOM, Sandia Laboratories.--Time- and mass-resolved energy distributions of ions emitted from the anode plasma of a pulsed vacuum arc of 5 μ sec duration have been measured using a spectrometer composed of a cylindrical electrostatic energy analyzer in tandem with a quadrupole mass filter. The energy resolution of the spectrometer is 1% and the mass resolution is better than 100. The arc current was 60 A with an anode current density of 2×10^4 A/cm². Ion species observed in the arc plasma include Al and O ions from the alumina ceramic insulator surrounding the anode, V ions from the arc initiation film between the anode and cathode, and Fe, Co, and Ni ions from the kovar anode. Multiply-charged ion species were observed. The energy distributions display low energy cut-offs corresponding to the plasma potential in the region of extraction. The mass-resolved energy distributions are in general agreement with those reported previously¹ for the same type of vacuum arc.

¹J. T. Grissom and G. W. McClure, Bull. Am. Phys. Soc. 16, 196 (1971)

*Research supported by the U.S. Atomic Energy Commission

G3. Vacuum Arc Anode Temperature Measurements.* J.C. NEWTON and J.T. GRISSOM, Sandia Laboratories, Albuquerque, N.M.--The radiance from vacuum arc anode spots and the average radiance from the total anode surface have been measured using an infrared microscope. Duration of the rectangular shape arc current pulse was varied from 1 to 12 microseconds for various currents ranging from 20 to 150 amperes. The area of the anode electrode exposed to the arc was limited by a ceramic insulator. The diameter of the exposed anode area ranged from 0.4 to 1.0 millimeters. Measurements were made using various metal electrodes and metal hydride films for the anode. Variations in the measured radiance as a function of time indicate that the anode surface radiance, not the plasma radiance, was measured. The spot temperatures, indicated by the measured radiance, range from approximately 900°C for metal hydrides to greater than 3000°C for metal electrodes. The observed change from a rapidly increasing to a quasi-steady state temperature in less than a microsecond indicates a significant reduction in anode spot current density during this time period.

* Research supported by the U.S. Atomic Energy Commission

G4. Plasma Electron Temperature Measurement Near an Anode Spot of a Pulsed Vacuum Arc.* F. M. BACON, Sandia Labs., Albuquerque--The plasma electron temperature near an anode spot of a pulsed vacuum arc between a 0.015 in. O.D. molybdenum cathode and a 0.035 in. O.D. aluminum anode has been measured spectroscopically from ratios of Al III spectral lines. The arc constant-current pulse length is 10 μ sec and the arc current is varied from 50 to 150 A. The time-resolved Al III spectral line intensities are constant or slightly increasing during the period from 2 to 10 μ sec arc duration. The electron temperature during this period is approximately 2 eV. In the 10 to 11 μ sec period when the arc current decreases to zero, the Al III spectral line intensities pass through maximum values that are as much as 10 times the intensity at 10 μ sec arc duration. This peak in intensity is attributed to the plasma electron temperature passing through the norm-temperature for the Al III spectral lines as the anode plasma decays. These data indicate that a portion of the plasma near an anode spot has a higher electron temperature than the 2 eV that is measured from the line ratios.

* Research supported by the U.S. Atomic Energy Commission

G5. Chopping, instability and spot multiplicity of the vacuum arc. G. H. Ecker, Ruhr-Universität Bochum, Germany. - Theoretical analysis requires for the existence of the stationary cathode spot of the vacuum arc a minimum current depending on the cathode material. Similarly the Existence-Diagram of a non-stationary spot moving across the cathode surface with a velocity v demands a minimum current larger than that for the stationary spot and depending on the spot velocity. Above a certain maximum velocity existence is precluded for any current I . If the spot velocity v increases with the spot current I - as is the case for magnetic interactions - then the maximum velocity results also in an upper limit for the spot current I . Chopping and instability are direct consequences of the minimum current requirement. Spot multiplicity follows from the upper current limitation.

G6. Anode Current Density in High Current Pulsed Arcs.*
K. T. Shih, Convair Aerospace Division of General Dynamics, San Diego -- The current density at the anode surface is an important arc parameter. Past determinations of anode current density were limited to indirect methods based on the size of the emission surface - either the size of the anode erosion spot or the arc luminescence area. The validity of such methods has been questioned. In this work, a method has been developed using a split anode to measure the anode current density distribution in high-current pulsed arcs. Rogowski coils were used to detect the current to each half of the split anode as a function of arc position relative to the splitting plane. Transformation equations were derived to obtain local values of current density from the measured lateral distributions. The data were taken using a copper anode in air at one atmosphere with arc current from 750 to 2250 amps. The peak anode current densities were found to be between 3.4×10^4 and 5.5×10^4 amps/cm².

*Work supported by Office of Aerospace Research, Contract No. F33615-67-C-1386.

G7. Arc Constriction and Spot Formation at the Anode of a High Intensity Arc. E. Pfender, University of Minnesota and T. S. Chou, Honeywell, Inc., St. Petersburg, Fla.--A simple analytical model is proposed which describes the region between a plane, cooled non-ablating anode and an arc column normal to the anode. The model takes an initial arc constriction due to the low temperature of the anode ("thermal pinch") into account. The resulting magnetic pinch effect leads to a corresponding entrainment of cold gas which determines the final shape of the arc column according to the adopted model. The conservation equations are solved numerically for the anode region with a relaxation method and results obtained for three different working fluids (argon, nitrogen, and hydrogen) are in qualitative agreement with experimental findings. Extremely high current densities ($> 10^4$ amp/cm²) and plasma temperatures ($> 4 \times 10^4$ K) in the constriction zone suggest that radiation has to be included to improve the present model. Although the length of the constriction zone is in the order of only 1 mm, the voltage drop over this length may be as high as 20 volts.

G8. Anode Heat Transfer in a High-Intensity Arc with Superimposed Axial Flow. R. Paulson, ARL, WPAFB, Ohio and E. Pfender, University of Minnesota.--A.D.C. arc operated in argon at pressures between 100 and 760 mm Hg, axial flow velocities from 0 to 100 m/sec, and currents from 50 to 100 amps utilizes a double-anode configuration which allows a separation of heat transfer due to the electron flow from combined convection and radiation. A correlation between the calorimetrically measured anode heat transfer and the arc parameters is established. - Since the anode arc attachment is appreciably smaller than the available anode surface, a new method using an optical and/or a floating potential probe is employed to measure the size of the near-anode arc column and the associated local heat fluxes on a relative scale. The results reveal that the cross-section of the near-anode column is not circular and the local heat fluxes show a strong dependence on the arc parameters.

SESSION H

Wednesday Morning, 6 October
10:35 a.m.

RF Arcs

Chairman: J. A. Sprouse, ARO, Incorporated

H1. Multiphasic Experimental Study of an Argon rf Plasma and Sonic Afterglow* L. N. MEDGYESI-MITSCHANG, McDonnell Douglas Research Laboratories and R. A. HEFFERLIN, Southern Missionary College. Results on argon from microwave interferometer and radiometer, optical spectrometer, and thermocouple measurements in an rf discharge and sonic afterglow are presented. The effects of discharge pressures (60-650 Torr) and rf power (42-60 kW) on the excitation, gas, and electron temperature, and electron density are examined. Temperatures inferred from minute amounts of seeded nitrogen, using N_2 and N_2^+ lines, are in agreement with thermocouple data and a gas dynamic prediction. Electron densities from optical and microwave methods are higher than equilibrium calculations based on measured Ar I excitation temperatures. Correlation of the various diagnostic methods establishes that the plasma is in a (pressure dependent) two-temperature local thermodynamic equilibrium (LTE) state. All excited levels are shown to be in equilibrium with the free electrons with equality of temperatures and compatibility of population densities.

*The research reported in this paper was sponsored by the Air Force Cambridge Research Laboratories, Air Force Systems Command, under Contract F19628-71-C-0024.

H2. Analysis of Optically Thick Coupled R.F.-D.C. Arc Discharges. P. W. Schreiber, A. M. Hunter, P. Taylor, Aerospace Research Laboratories, and K. R. Benedetto, Systems Research Laboratories - The object of this study is to analytically determine the properties of an arc discharge generated by a combination of r.f. and d.c. electromagnetic fields. R.F. power is supplied to the discharge by a solenoidal coil whose axis of symmetry is aligned with the applied d.c. electric field. A numerical technique is used to simultaneously solve a set of linear differential equations which include Maxwell's field equations, the single fluid energy equation, the momentum balance equation, Ohm's law, and the radiation diffusion equation at different wavelengths. It is necessary to make a number of reasonable assumptions to obtain the final set of equations for programming. These assumptions restrict the calculations to azimuthally symmetric plasmas with axial gradients only in static pressure. In addition, the radiant energy flux is assumed to be isotropic within the plasma. Input data are mass flow rate, d.c. electric field strength, center-line temperature and magnetic field, plasma transport properties, and the specifications of the solenoid. Computer output data are power inputs to the gas, power radiated per unit arc length, total d.c. current, coil current, voltage per unit length, and phase angle, and the radial distributions of temperature, current density and electromagnetic fields.

H3. Experiments with Bluff-Body and Vortex Stabilized Electrodeless Arcs*. D. R. KEEFER and P. J. GROSS, University of Florida, Gainesville, Florida--Experiments were performed to compare the performance of bluff-body and vortex stabilized arcs as gas heaters. Bulk temperature and mass flow rates were determined for both arcs operating in argon at atmospheric pressure over a range of input power from 1.6-3.6 KW. Stable operation with the bluff-body was attained with mass flows 3.8 times greater than that for the vortex. The maximum heating efficiency, based on net power input to the arc, was 18.1% with the bluff-body and 1.75% with the vortex.

*The research reported in this paper was sponsored by Arnold Engineering Development Center, Air Force Systems Command, Arnold Air Force Station, Tennessee, under Contract No. F40600-70-C-0003. Further reproduction is authorized to satisfy the needs of the U. S. Government.

H4. Analysis of Thermal Induction Plasmas Between Coaxial Cylinders. H. U. ECKERT, The Aerospace Corp.-- A previously derived approximate solution of the one dimensional energy balance equation for steady thermal induction plasmas is applied to the case of an annular plasma maintained between coaxial cylinders. It is assumed that heat conduction is the only loss mechanism and that both walls are at zero temperature. Charted material is presented to facilitate determination of heat loads to either wall and calculation of temperature distributions across the gap. Results for an atmospheric pressure argon discharge are compared with both exact numerical calculations and with experimental data. With the former agreement is fair to good; with the latter it is poor. The disagreement is shown to be caused by electron diffusion which leads to overpopulation near the walls and suggests erroneously high temperatures when Saha equilibrium is assumed. The experimental temperature profiles are reproduced with excellent accuracy from a diffusion profile for the electrons which takes into account the nonuniformity of the induced electric field.

ABSTRACTS

Twenty-Fourth Annual
Gaseous Electronics Conference

5-8 October, 1971

J. Wayne Reitz Union
University of Florida
Gainesville, Florida

SESSION I

Tuesday Morning, 5 October

10:30 a.m.

AFTERGLOWS IN RARE GAS-MERCURY MIXTURES

Chairman: J. Ingold, Lightning Research Laboratories, General Electric Co.

I1. Electron-Temperature Decay in Hg-Rare Gas Afterglows* P.C.DROP and J.POLMAN, Philips Research Labs, Eindhoven, Netherlands.-- Numerical calculations have been made on the decay of the electron temperature T_e in Hg-Ne and Hg-Ar afterglows. The T_e -decay time, τ_E , is governed by both elastic e-Ne or e-Ar collisions and inelastic collisions of the 1th and 2nd kind. For 10 Torr Ne+Hg ($p_{Hg}=6$ mTorr, $R=2.6$ cm, current pulse 0.4A) the calculations have shown that τ_E is about 10 times longer than in the case where only elastic losses are considered. This is in good agreement with results from microwave noise measurements giving $\tau_E=60$ μ s in the late afterglow. The Hg(6^3P)-decay times are 60 μ s (6^3P_0) and 25 μ s (6^3P_1 and 6^3P_2), as determined by optical absorption measurements. For 2.5 Torr Ar+Hg ($p_{Hg}=6$ mTorr, $R=1.8$ cm, current pulse 0.4A) both measurements and calculations give $\tau_E=150$ μ s in the late afterglow. In the early afterglow ($t < 2$ μ s) the decay is about two orders of magnitude faster due to inelastic collisions of the 1th kind.

*Submitted by R. Bleekrode

I2. Quenching of Afterglow Radiation by Electron Heating at Plasma Resonances.* S. C. BLOCH and J. L. AUBEL, University of South Florida.-- Afterglow plasmas formed in He and Hg-Ar were monitored spectroscopically while the plasmas were irradiated with low-power microwaves. Studies were carried out in a traveling wave configuration at X-band and in an orthomode cavity at L-band. It was found that when the cylindrical plasmas passed through dipole and Tonks-Dattner plasma resonances the total light and selected spectral lines were quenched, for incident power levels up to 100 mw. This decrease in the afterglow was a strong function of the incident power of the disturbing wave. Measurement of electron density and collision frequency in the TM_{010} cavity mode, while plasma resonance heating was carried out in the TE_{111} mode, indicated that enhanced diffusion and decreased electron impact excitation were more important than decreased recombination, for the range of parameters studied.

* Research supported in part by The Atmospheric Sciences Section, National Science Foundation, Grant GA-10425.

I3. Initial Afterglow of the Self-Absorbed Hg 2537Å Radiation in Hg + Ar Discharges. T. J. HAMMOND and C. F. GALLO, Xerox Research Laboratories. - The initial decay time (τ) of the self-absorbed Hg 2537Å radiation in the afterglow of Hg + Ar discharges has been measured as independent functions of the mercury pressure (.8 to 70 mTorr) and the argon pressure (5 to 200 Torr). The initial decay time (τ) increases with the mercury density but is inversely related to the argon pressure. These measurements of τ are in good agreement with the concept that the initial decay is primarily limited by self-absorption for our range of variables. A detailed theoretical analysis indicates that there are several ways that additional argon reduces the Hg 2537Å self-absorption: (1) The Hg 2537Å line gets broader simply because the additional argon atoms increase the Hg-Ar collision frequency, (2) Adding argon causes the gas temperature to rise and this drives the Hg-Ar collision frequency still higher, (3) The rise in gas temperature also causes an increase in the Hg 2537Å Doppler width. The theoretical calculations were performed from the self-absorption theory of Holstein and Walsh. All these results are consistent with our previous analysis performed on measurements of the Hg 2537Å intensity in these discharges.

I4. Statistical Time Lags in Helium-Mercury Afterglows* BEAUFORT M. LANCASTER, JR. and KAARE J. NYGAARD Univ. of Missouri-Rolla -- Data are given from experiments measuring metastable densities and average cross-sections for energy transfer in collisions of the second kind. A breakdown pulse was used to produce the metastables which were detected in the afterglow by means of measuring the breakdown probability of a sampling pulse. A von Laue plot reveals the statistical time lags which give the metastable densities in the gas. A metastable density of about 100 per cm³ can be measured with this technique.

* Supported in part by the Aerospace Research Laboratories, Wright-Patterson AFB.

15. Plasma Diagnostics Using Slow Positrons. W.M. SCHIKORR, G. H. LOHNERT, R. T. SCHNEIDER, University of Florida - As described recently¹ interactions of positrons with a plasma can be used to determine plasma properties. A parallel beam of low energy positrons which is injected into a plasma will be spread into an angle α due to cumulative scattering effects of small angle scatterings. In measuring α electron density can be found. As reported², these measurements compared well with spectroscopic and probe measurements. The deviation of 10% is thought to be caused by the unknown energy distribution of the positron beam. Therefore a precise determination of this distribution was required. Using a cylindrical electrostatic energy analyzer, the beam was found to be highly monoenergetic for all selected beam energies. For a typical energy of 1000 eV the F.W.H.M. was measured to be 2.75 eV.

1. Bull of the Amer. Pys. Soc. Ser. II, Vol. 15, No. 10, Oct. 1970.

2. G. H. Lohnert, R. T. Schneider, J. Appl. Phys., Oct. 1971.

SESSION J

Tuesday Afternoon, 5 October

2:00 p.m.

BREAKDOWN

Chairman: A. A. Dougal, University of Texas at Austin

J1. Determination of Spatial and Temporal Electron Density and Temporal Electron Temperature in Laser-Produced Gaseous Deuterium Plasmas. WINSTON K. PENDLETON and ARTHUR H. GUENTHER, AF Weapons Laboratory, Kirtland Air Force Base - Pulse interferometric holography has been employed to temporally and spatially determine the electron density distribution at low pressure (100-600 Torr) deuterium plasmas produced by a focused laser beam. Maximum values of electron density corresponding to from 20-30% ionization were typical in this pressure region. In addition, the free electron kinetic temperature was determined during the 4 nanosecond laser radiation and typical values of 4×10^5 K were obtained. The techniques employed were dictated by the high density, low temperature and the highly transient nature of gaseous plasmas produced by pulsed lasers. Such techniques are becoming increasingly useful in the study of other transient gaseous discharges.

J2.

LASER INDUCED BREAKDOWN IN HIGH PRESSURE NOBLE GASES*

G.W. Haynes, O.M. Friedrich, Jr., and Arwin A. Dougal
Department of Electrical Engineering and Electronics
Research Center

The University of Texas at Austin, Austin, Texas 78712

An analysis based on balancing electron production against electron loss is compared with experimental data for ruby laser induced breakdown in helium, neon and argon gases in the pressure range from one atmosphere to 2,000 atmospheres. In the model used inverse bremsstrahlung is the heating process; free electrons are produced by collisional ionization and from photoionization and associative ionization of excited neutrals; they are lost by diffusion. The data taken with a mode-restricted ruby laser indicates a minimum in the plot of threshold electric field versus pressure for helium and argon and a possible minimum beyond 2,000 atmospheres for neon. The agreement between experiment and theory is particularly good at low fields.

*Research supported in part by TAERF and the DoD JSEP.

J3. Vacuum Breakdown Voltage As a Function of Crossed Magnetic Field Strength. ALAN WATSON, University of Western Ontario - Theoretical curves of breakdown voltage variation with increasing transverse magnetic field strength have been calculated from the ionic field enhancement instability model of the mechanism.⁽¹⁾ There is excellent agreement with results from factorial experiments on copper electrodes.⁽²⁾ Preparatory cathode bakeout in hydrogen alters the form of the experimental voltage variation curve consistently with the model of field emission influenced by the Hall effect⁽³⁾ in which gaseous diffusion from the metal dopes the semiconducting oxide layer.

(1) Alan Watson, *Bul.A.P.S.* 14, 253 (1969).

(2) Alan Watson, *Bul.A.P.S.* 13, 200 (1968).

(3) Alan Watson, *Bul.A.P.S.* 15, 424 (1970).

J4. Pulsed Microwave Breakdown of Air from 1 to 1000 Torr. S.J. TETENBAUM, A.D. MAC DONALD, and H.W. BANDEL, Lockheed Palo Alto Research Lab.*, - There have been a number of experimental studies of pulsed microwave breakdown in air¹, but very few measurements have been made utilizing sub-microsecond pulse widths in the pressure range above 100 Torr. We have measured pulsed breakdown electric field strengths in two S-band cavities filled with dry air at a temperature of 40°C in the approximate pressure range from 1 to 1000 Torr. The data were taken at a pulse repetition frequency of 20 Hz and for effective pulse widths of 0.6, 0.2, and 0.1 μ sec. Gould and Roberts² have made measurements over a limited range of pressures and pulse widths. In the present study, data are obtained for a much wider range of experimental parameters, and particular care was taken with the definition of the pulse width effective in causing breakdown. Our results are consistent with those of Gould and Roberts in the range of experimental parameters common to both. Our results are also in reasonable agreement with the 0.1 μ sec breakdown predictions of Felsenthal³ based upon pulsed dc breakdown fields.

*Work supported by Lockheed Independent Research Program.

1. A.D. Mac Donald, Microwave Breakdown in Gases (John Wiley and Sons, Inc., New York, 1966), pp. 165+ and Appendix.
2. L. Gould and L.W. Roberts, *J. Appl. Phys.*, 27, 1162 (1956).
3. P. Felsenthal, *J. Appl. Phys.*, 37, 4557 (1966).

J5. Interaction of Trichel Pulses from Adjacent Negative Needle Coronas. W.L.LAMA and C.F.GALLO, Xerox Research Laboratories.—Our experiments with a pair of negative needle coronas reveal a competition between the Trichel pulse discharge currents, manifest by locking of the pulse frequencies and the establishment of a fixed phase relationship. In particular, as the needle tips were brought together, the individual frequencies decreased and converged. At the same time, a relative phase was established which approached π . A theoretical model of this phenomena has been developed in which the corona currents are represented by sets of interacting harmonic oscillators. The Fourier component of the corona current from one needle I_1 at frequency ω_n obeys the differential equation $\ddot{I}_{1n} + \omega_n^2 I_{1n} = -\gamma_n^2 I_{2n}$ and similarly for the current from the second needle. Considering the n^{th} harmonic component, the theory shows that for our experiment, the only stable solutions (I_{1n}, I_{2n}) have a relative phase of 0 or π . Energy considerations dictate a phase difference of π where the theoretical frequency modified by the dynamic interaction is decreased to $\omega_n' = \sqrt{\omega_n^2 - \gamma_n^2}$. In addition, the static electric field of the adjacent needle will also decrease ω_n . These theoretical expectations are in agreement with the experimental observation of decreasing ω_n and antiphase establishment.

J6. Systematic Experimental Study of the Electrical Characteristics of the "Trichel" Current Pulses from Negative Needle-to-Plane Coronas. W.L.LAMA and C.F. GALLO, Xerox Research Laboratories.—Systematic variation of the macroscopic experimental parameters has led to the following expression for the Trichel pulse frequency (F) of negative needle-to-plane corona in air at atmospheric pressure, $F \propto [V(V-V_0)/rS^2]$ where V is the applied voltage, V_0 is the threshold voltage, S is the needle-to-plane spacing, and r is the needle tip radius. The threshold voltage V_0 was comparatively independent of r and S. The time averaged corona current (I) was found to have the same dependence on V and S as the frequency, but was comparatively insensitive to the tip radius (r). That is, $I \propto V(V-V_0)/S^2$. Combining these two experimental results leads to $F \propto I/r$, which explains Trichel's correct but misleading conclusion that the frequency is independent of S at constant current. From the current and frequency measurements, we deduce that the charge-per-pulse ($Q = I/F$) is roughly proportional to the needle tip radius, $Q \propto r$, and essentially independent of the voltage and spacing. The similarities between these regularly repetitive Trichel pulses and striations in gas discharges as well as the Gunn effect in solids should be noted.

Theoretical Analysis of Trichel Current Pulses from Negative Needle-to-Plane Coronas. W.L.LAMA and C.F. GALLO, Xerox Research Laboratories.--An analysis of the Trichel pulses from negative needle-to-plane coronas is performed. First, the electrostatic field (E) in this geometry is essentially $E(l) \propto VS[2S(l+r)-l^2]^{-1}$ with l the axial distance from the tip, S the point-to-plane spacing, V the needle voltage, and r the tip radius. Combining our experimental results with theory yields: (a) The time for the negative space charge to travel across the entire gap is $\tau \approx S^2 \ln(2S/r)/3MV$, where M is the negative ion mobility. (b) The number of negative ion charge clouds simultaneously crossing the gap is $N \approx 1 + (C_1/r)(V-V_0)$, where V_0 is the threshold value and all C 's are constants. (c) The total charge in the gap is $Q_T \approx C_2(V-V_0)$. (d) The Trichel pulse period T is given in terms of the clearing length L which is the distance the negative space charge must move before the threshold field at the cathode is restored, $T \approx C_3 L^2/MV$. (e) The clearing length is $L \approx C_4 S [r/(V-V_0)]^{1/2}$. Above threshold, L is much less than S , in agreement with the conclusion that many charge clouds are simultaneously in transit. (f) The voltage dependence of the current derived from first principles is $I \propto V(V-V_0)$. Our observations and calculations are consistent with Loeb's model.

J8. Kinetic Ion-Electron Emission from Clean and Contaminated Metal Surfaces.* †JAMES L. BREUNIG, Univ. of Calif., Berkeley.--This reports comprehensive data of kinetic ion-electron emission from clean metal surfaces. Novel results were obtained for yield vs. ion energy for Mo and W surfaces by subliming metal layers periodically to eliminate entrapped particles. e^- energy spectra were obtained using vacuum deposition of Mg, Al, and Cu layers in uhv. K ions in the range 0.5 to 8 keV were normally incident on the targets. The yield decreased when contaminant layers were eliminated. The resultant thresholds and linear intercepts appear to be in good agreement with the theoretical prediction of Parilis and Kishinevski. High energy cutoffs of the e^- energy spectra were found to be consistent with the hypothesis of Auger neutralization of holes in different energy levels of each target atom. Where there was relatively great separation in the energies of the first two levels, the distribution curves were essentially independent of incident ion energy suggesting that the yield was composed almost exclusively of Auger electrons from the metal.

*Submitted by LEONARD B. LOEB.

†Supported by U. S. Office of Naval Research.

SESSION K

Tuesday Afternoon, 5 October
4:00 p.m.

TRANSPORT PROPERTIES AND DISTRIBUTIONS

Chairman: A. V. Phelps, JILA

K1. Two-Fluid Theory of the Positive Column.
 J. H. INGOLD, General Electric Lighting
Research Laboratory, Cleveland, Ohio.--The
 positive column of a planar gas discharge is
 analyzed from the point of view that the
 electrons and ions in the positive column
 behave as inviscid fluids with different
 temperatures. New boundary conditions con-
 sistent with the fluid equations are imposed
 to validate the formulation for gas pressures
 from the free-fall limit to the continuum
 limit, including the high-field sheaths at the
 walls as well as the almost field-free plasma
 at the center of the discharge. Numerical
 results for the characteristic value, wall
 field, wall potential, and ion energy at the
 wall are given for many different pressures
 and central Debye lengths, and it is shown
 that the results are identical to those of
 Allis and Rose in the continuum limit and very
 close to those of Self in the free-fall limit.

K2. Determination of Cross Sections From Rate Constants
Measured in Drift Tubes* S.B. Woo, J.H. Whealton, C. Russ,
 and S.F. Wong, University of Delaware--Woo and Wong¹ sugge-
 sted using a displaced Maxwellian, whose first two moments
 were matched to experimentally determined values, to help
 unfold the cross section, σ , out of the rate constants,
 K , obtained from the drift experiments. K is related to σ
 by

$$K = \int_{v^*}^{\infty} g(v_r) \sigma(v_r) v_r dv_r \quad (1)$$

where $g(v_r)$ is the joint ion-gas speed distribution and v^*
 is the threshold speed. Two aspects of the suggestion re-
 quire closer examination. First, how closely does such a
 displaced Maxwellian approximate the ion distribution wh-
 ich forms, together with the gas distribution, the $g(v_r)$
 in eq. (1)? Secondly, is the result of the unfolding theo-
 retically unique, and is the numerically unfolding process
 operationally reliable? It will be shown that although the
 displaced Maxwellian is but a very crude approximation to
 the ion velocity distribution, a reliable $g(v_r)$ is gene-
 rated from it. Comparison with the Monte Carlo and the Ki-
 netic Model calculations are made. Examples show that the
 numerical unfolding is operationally reliable.

¹S.B. Woo and S.F. Wong, J. Chem. Phys., Sept. 1, 1971 issue.

*Research supported in part by Ballistic Research Labora-
 tories, Aberdeen, Maryland.

K3. Determination of Electron Transport Coefficients near Thermal Energies in Oxygen. * D. R. NELSON and F. J. DAVIS, Oak Ridge National Laboratory. -- Several modifications of an electron swarm time-of-arrival experiment have led to a resumption of electron transport studies in oxygen. The drift-dwell-drift (DDD) technique¹ is successfully used for determining thermal and low E/P transport coefficients even when significant electron attachment occurs. A thermal (300° K) value of $DP = 1.20 \pm 0.11 \text{ cm}^2 \mu\text{sec}^{-1} \text{ torr}$ has been determined which is ~18% larger than a preliminary value previously reported.²

* Research sponsored by the U.S. Atomic Energy Comm. under contract with Union Carbide Corporation.

¹ D. R. Nelson and F. J. Davis, J. Chem. Phys. 51, 2322 (1969).

² D. R. Nelson and F. J. Davis, Bull. Am. Phys. Soc. 16, 217 (1971).

K4. Momentum Transfer Cross Sections for Electrons in a Weakly Ionized Cesium Plasma. * F. Murray, D.M. Cox, H.H. Brown Jr. and B. Bederson, New York University. -- The electron-cesium momentum-transfer cross section is being investigated by measuring the dc electric conductivity of a weakly ionized, homogeneous cesium plasma in near-thermodynamic equilibrium. The plasma is contained between coaxial tantalum cylinders which are radiatively heated in the range 1000 to 1500°K. The neutral cesium density is determined using a surface ionization detector, and the plasma density is calculated using the Saha equation. A thermally isolated cesium oven independently varies the plasma density; a magnetic field can be applied parallel to the cylinder axis. The dc conductivity as a function of applied magnetic field at several plasma densities is obtained from the current-voltage characteristics of the plasma and geometric factors. Data have been obtained for densities of from 10^{12} - 10^{14} particles/cc with fractional ionization of $\leq 10^{-4}$ and magnetic fields ≤ 180 g. Comparison of the experimental curves with theory based upon assumption of combined electron-neutral, electron-ion and ion-neutral interactions will be presented.

* Supported by the National Science Foundation and ARO

K5. Ionization and Attachment in Boron Trifluoride.

D. KENNETH DAVIES, Westinghouse Research Labs. --
Measurements of steady-state current growth under uniform electric fields have been made in BF_3 over the range $38 < E/p_0 < 500$ V/cm Torr (where E is the electric field in V/cm and p_0 is the gas pressure in Torr corrected to 0°C). The measurements indicate the effects of both electron attachment and ionization in the current growth. Agreement between experiment and theory may be obtained by taking into account ionization and attachment only in the analysis of the data. The analysis yields values of the net ionization coefficient over the entire range of E/p_0 and values of the attachment and ionization coefficients over the range $38 < E/p_0 < 60$ V/cm Torr. The net ionization coefficient is found to be pressure dependent over the accessible range $50 < E/p_0 < 150$ V/cm Torr. However, the deduced values of the attachment coefficient are independent of pressure and consistent with the occurrence of a dissociative attachment process. Thus, the analysis implies a pressure dependent ionization coefficient.

SESSION L

Wednesday Morning, 6 October

8:30 a.m.

CLUSTERING

(PANEL)

Chairman: F. E. Niles, Aberdeen Research and Development Lab

L1. Molecular Clustering about Gaseous Metal Ions.*

A. W. Castleman, Jr. and I. N. Tang, Brookhaven National Laboratory--Clustering of the polar molecules H_2O and SO_2 about sodium and lead ions has been studied in a field-free reaction cell. The measurements were made over the temperature range 20° to 120°C by sampling the ionic species with a quadrupole mass spectrometer. Argon and nitrogen at pressures ranging from 2 to 6 torrs were used to thermalize the primary ion beam, thereby enabling the free energies of the clustering reactions to be measured. Bond energies were evaluated for the clusters $\text{Na}^+(\text{H}_2\text{O})_2$ (SO_2), $\text{Na}^+(\text{H}_2\text{O})(\text{SO}_2)_2$, $\text{Na}^+(\text{SO}_2)_3$; they are 23, 21 and 19, respectively. Likewise, the bond energies for the species $\text{Pb}^+(\text{H}_2\text{O})_m$, $m \leq 6$ are 17, 16, 15, 14, 13.1, and 12.2, respectively. A comparison of these bond energies with those calculated from a hydration model will be discussed.

*This work was performed under the auspices of the U.S. Atomic Energy Commission.

L2. Clustering of N_2 to Li^+ . G. E. KELLER AND L. M. ROMANO, Ballistic Research Laboratories.- A drift tube-mass spectrometer has been used to study the clustering of N_2 to Li^+ for $E/N = 6$ to 24 Td. Li^+ , the cluster ions $\text{Li}^+\cdot\text{N}_2$, $\text{Li}^+\cdot 2\text{N}_2$, and $\text{Li}^+\cdot 3\text{N}_2$, and impurity ions $\text{Li}^+\cdot\text{H}_2\text{O}$ and $\text{Li}^+\cdot\text{CO}_2$ were identified. Rate constants are deduced by comparison of time arrival spectral of the ions with theoretical curves produced by a numerical computer drift tube model, which considers 3 ions, ion drift, diffusion and reactions. Preliminary reduction of the data yields the first cluster formation rate constant at 12 Td of 2×10^{-30} cm^6/sec , with the breakup rate constant of $\text{Li}^+\cdot\text{N}_2$ of about 1×10^{-14} cm^3/sec . The clusters $\text{Li}^+\cdot\text{N}_2$, $\text{Li}^+\cdot 2\text{N}_2$, and $\text{Li}^+\cdot 3\text{N}_2$, always reach chemical equilibrium under the experimental conditions before they are swept from the tube.

L3. Ion Induced Large Cluster Formation. PETER COFFEY and V. A. MOHNEN, State University of New York at Albany - The reaction between $\text{NH}_4^+(\text{H}_2\text{O})_n$ ion cluster and HCl and HNO_3 molecules in air at atmospheric pressure is investigated. A chemical gradient chamber using H_2O and HCl indicates macroscopically that large clusters active at a supersaturation of a few percent are produced. Typically an air stream having ammonia concentration of .02 ppm will, after passing an alpha source ionizer, immediately produce a dense cloud of droplets in the chamber. In the absence of an ionizing agent no cluster growth occurs. This result implies that the $\text{NH}_4^+(\text{H}_2\text{O})_n$ cluster, never observed to have more than a few water molecules, attached rapidly (within msec.) and experienced a dramatic growth to ultra-large clusters. This ion molecule reaction has been further investigated using a drift tube working at atmospheric pressure and interfaced with a quadrupole mass spectrometer. Ion induced large cluster formations play an important role at atmospheric levels up to the mesosphere.

This work is supported by research grant AP-00942-02 from the APC office of EPA and by NSF grant GA22760.

L4. Laboratory Production of Positive Water Cluster Ions.* P. MAHADEVAN, and H. C. CARPENTER, McDonnell Douglas Research Laboratories--Positive ions extracted from a low pressure electron bombardment ion source operating with moist air as the source gas are observed to include several hydrated ion clusters of the type $(\text{XY})^+n\text{H}_2\text{O}$ where $(\text{XY})^+$ represents ions such as $(\text{OH})^+$ and $(\text{NO})^+$ and $n = 0,1,2,3...$ These cluster ions are formed in secondary reactions of primary ions with the source gas in the ion source itself and are relatively long lived (microseconds). The secondary reactions appear to deplete the O_2^+ ions heavily. Conventional beam techniques are adopted for the extraction, focussing and mass analysis of these ions. The higher mass range extends up to 100 amu. The mass spectra observed here have features quite similar to those recorded in rocket flights by Narcissi¹ and his collaborators.

*This research was conducted under the McDonnell Douglas Independent Research and Development Program.

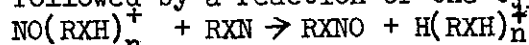
¹R. S. Narcissi and W. Roth, Advances in Electronics and Electron Physics 29, 79 (1970).

L5. Negative Ion Molecule Reactions of Atmospheric Interest. V. A. MOHNEN and PETER COFFEY, State University of New York at Albany - A. Experimental Set-Up: A drift tube working at atmospheric pressure and interfaced with a quadrupole mass spectrometer is used to study near thermal ($E/p \approx 0.1$ eV) ion molecule reactions over a period up to 100 msec. and thus increasing the collision frequency by orders of magnitude. The drift tube is directly coupled with a GC-MS system for neutral gas analysis and a Wilson type particle counter capable of detecting clusters larger than 70A that are, with certain trace gases present, formed by ion molecule reactions. B. Results: We have studied negative ion molecule reactions in air-like mixtures containing known amounts of H_2O , CO_2 and NO_2 . Equilibrium distributions are reported for the resulting $O_2^-(H_2O)_n$, $CO_4^-(H_2O)_j$ and $NO_2^-(H_2O)_k$ ions and other ionic species that have been mass identified as a function of trace gas constituents and concentration.

The concept of ion induced large cluster formation as discussed in an earlier paper (Mohnen, PAGEOPH 84, 1971/I) will be presented and further refined.

This work has been supported by the Office of Naval Research (N00014-69-C-0043) and NSF grant GA22760.

L6. The Reaction of NO^+ with H_2O , H_2S and Methanol. LARRY I. BONE, East Texas State University - A photoionization quadrupole mass spectrometer has been used to study the reactions of NO^+ with H_2O , CH_3OH and H_2S . The nitric oxide is ionized by a krypton resonance lamp with a calcium fluoride window producing a single line at 10.03 eV. The other reactant is not ionized. The general reaction scheme is similar to that known for the NO^+ - water system. NO^+ is sequentially solvated by 3 waters, 2 methanols or one H_2S followed by a reaction of the type:



where R is CH_3 or H and X is S or O. A vacuum ultra violet photolysis experiment confirms the production of CH_3ONO . In the $NO(H_2S)_n^+$ and $H(H_2S)_n^+$ species n is never greater than one. All this information points to the importance of hydrogen bonding in ion clusters.

L7. CO₂ and CO Clustering to NO⁺. J. M. HEIMERL and J. A. VANDERHOFF, Ballistic Research Laboratories, Aberdeen - A stationary afterglow has been used for 300° K studies of the reaction $\text{NO}^+ + \text{X} + \text{M} \leftrightarrow \text{NO}^+ \cdot \text{X} + \text{M}$, X = CO₂ or CO. In neither case was the cluster itself observed. With the addition of trace amounts of water the forward rate constant for cluster formation was determined, viz., 2×10^{-29} cm⁶/sec for X = CO₂ \approx M and 2×10^{-30} cm⁶/sec, for X = CO \approx M. These rate constants lend support to the map proposed by Keller and Niles* for initial positive ion clustering at room temperature.

* G. E. Keller and F. E. Niles, paper to be published in Chem. Phys. Letters, Aug. or Sept. 1971.

L8. Partial Charge-Transfer and Cluster Reactions of Mg⁺⁺, Ca⁺⁺, and Ba⁺⁺. K. G. SPEARS, F. C. FENFELD, M. McFARLAND, AND E. E. FERGUSON, NOAA Environmental Research Labs, Boulder, Colo. 80302.

We have used the NOAA flowing afterglow to measure rate constants for room temperature reactions of Mg⁺⁺, Ca⁺⁺, and Ba⁺⁺. The rate constants for formation of single neutral clusters are reported for many neutrals, including Ar, O₂, N₂, CO, CO₂, N₂O, and H₂O. Attempts are made to explain the three order of magnitude difference in these clustering rates. In addition, partial charge-transfer reaction rate constants are reported for Mg⁺⁺ and Ca⁺⁺ with NO and for Mg⁺⁺ with Xe, O₂, CO₂, N₂O, SO₂, and NH₃. The analysis of these reaction rates gives an approximate electron jumping efficiency from 2.5 to 14.4 Å. In addition, the analysis of the partial charge-transfer cross section with Xe in terms of a pseudo-crossing of reactant and product potential curves yields the potential curve interaction energy in agreement with theoretical expectation.

SESSION M

Wednesday Morning, 6 October

10:30 a.m.

NEUTRAL-NEUTRAL COLLISIONS AND EXCITATION TRANSFER
(PANEL)

Chairman: R. M. St. John, University of Oklahoma

M1. Dynamical Coupling Potential in Simple Exchange Collisions: Two State Coupled Channel Calculations of Atomic Exchange Cross Sections for $H+H_2$, $D+H_2$, and $H+D_2$.* PAUL MCGUIRE and DAVID A. MICHA†, U. of Florida.-Exchange collisions of the type $A+BC \rightarrow AB+C$ are investigated where the exchanged particle B may be an electron, an ion, an atom or a molecule. The total wave function is expressed as a superposition of the electronic states of the initial (A,BC) and final (AB,C) configurations, with coefficients describing the relative and internal (if present) motions. Choosing convenient trial functions having the proper boundary conditions, the Kohn variational principle provides coupled differential (rather than the usual integro-differential) equations for the relative motion wave functions in R_3 (the AC separation). The potential matrix elements are dynamical in that they depend upon the initial k_1 and final k_2 wave vectors. Employing covalent valence bond electronic states, two-state coupled-channel computations of the differential and integral cross sections for $H+H_2$, $D+H_2$ and $H+D_2$ are presented up to 0.8eV.

*Supported by NSF Grant GP-23574 and by the Petroleum Research Fund (ACS).

†Alfred P. Sloan Foundation Fellow.

M2. An Extension of the Uniform Semiclassical Approximation for Differential Elastic Scattering. J.M. MULLEN Univ. of Fla.*-- The uniform semiclassical approximation (USCA) of Berry¹ has been extended to allow direct comparison with differential cross sections computed by exact evaluation of the phase shift sum using JWKB phase shifts. These comparisons show that the USCA cross sections reproduce the complicated oscillatory structure of the "exact" cross sections with remarkable fidelity, so long as the parameter kr_m (which is approximately the number of deBroglie waves contained inside the potential well of the scatterer) is greater than about 15 and the collision energy is sufficiently large to preclude orbiting. The greatly increased speed with which cross sections may be calculated in this approximation has been exploited to produce tables of rainbow extrema for some realistic central potentials. This data should be of interest to workers needing quick rough estimates of potential well depth and range from scattering data.

*Work supported in part by the U.S. Air Force Office of Scientific Research and the U.S. Office of Naval Research.

¹ M.V. Berry, Proc. Phys. Soc. 89, 479 (1966)

M3. Distribution of Excitation Transfer in Helium.*
J. D. JOBE[†] and R. M. ST. JOHN, University of Oklahoma
--The distribution of atom-atom collisional excitation among various levels of the helium atom is determined. The determination is made by analyzing absolute measurements of the optical electron excitation cross sections of 63 levels at 100 eV electron energy and 63 mtorr pressure. A detailed analysis is made on the n=4 level and collisional excitation transfer cross sections are found to be $(4.7 \pm 1.5) \times 10^{-14} \text{ cm}^2$ for 4F to 4D transfer and $(2.3 \pm 0.6) \times 10^{-14} \text{ cm}^2$ for 4¹P to 4F transfer. The pressure dependence of the apparent electron excitation cross sections of 47 levels has been determined at 100 eV electron energy. Our work shows that the apparent cross sections of levels with large principal quantum numbers decrease as the pressure increases, an effect opposite to that observed for levels of low principal quantum number.

*Work supported in part by Air Force Office of Scientific Research.

[†]Present address: Shell Oil Co., Houston Res. Lab., Deer Park, Texas 77536

M4. Excitation Transfer Reactions Involving the He₂(2p³π) Molecule.* C. B. COLLINS, B. W. JOHNSON, and M. J. SHAW, U. of Texas at Dallas--A tuneable, 1 Mw peak power, -4-methylcoumarin laser has been used in the UTD Fast Reaction System to optically pump selected R-branch components of the He₂(2s³Σ_u⁺ → 2p³π_g) system into superradiance. This effect has been investigated as it forms an upper limit to the useable pumping power from the laser. Subject to this constraint the reactions of the He₂(2p³π) molecule with electrons and neutral atoms have been investigated.

*Work supported by NASA Grant NGL44-004-001.

M5. Cross Sections for Vibrational Energy Transfer, $\text{CO}_2\text{-N}_2$. T. A. DILLON and E. W. SMITH, N.B.S., Boulder, Colo. - Vibrational exchange cross sections for $\text{CO}_2\text{-N}_2$ collisions are calculated using classical curved trajectories and retaining all orders in the scattering matrix. The results are compared with an equivalent calculation using the usual straight path trajectory and first Born approximations. It is found that severe discrepancies exist even for the case of a single quantum of vibrational excitation where the first Born approximation is valid. For the degree of vibrational excitation important in a $\text{CO}_2\text{-N}_2$ laser system, the first Born approximation introduces errors in excess of 500% and the complete scattering matrix is required. Short range repulsive terms in the potential are shown to have a great influence on the cross sections even at low temperatures. It is concluded that the straight path trajectory is always unsatisfactory over a broad range of temperatures, the first Born approximation is valid only for vibrational excitations of one or two quanta and that repulsive terms have a profound effect on the cross section even at low temperatures.

SESSION N

Wednesday Evening, 6 October

8:00 p.m.

LASERS I

CO LASERS

Chairman: A. Garscadden, Aerospace Research Laboratory, WPAFB

N1. Electron Density and Temperature Measurement in a CO Laser Plasma*. D. COHN, B. O'BRIEN, W. B. LACINA and M. L. BHAUMIK, Northrop Corporate Laboratories, Hawthorne, Ca. -- The electron density in an electrically excited room temperature carbon monoxide laser has been determined using a double probe as well as a microwave resonance technique to be 3×10^9 per cc. The electron temperature was obtained from the slope of the double probe I-V characteristics to be approximately 2 ev. The electron temperature is observed to be lower by about 20% when lasing takes place, with an output power of 4 watts. The effect of various gas additives on the electron density and temperature has also been studied, and the influence of these effects on the CO laser operation has been determined.

*Work supported in part by the Advanced Research Projects Agency of the Department of Defense and monitored by the Office of Naval Research under Contract N00014-72-C-0042.

N2. Comparison of CW and Pulsed Operation of Carbon Monoxide Laser (CO, N₂, Xe, He Mix). W. J. GRAHAM and J. C. KERSHENSTEIN, Naval Research Laboratory.-- A non-flowing CO laser has been studied at 195°K and 77°K both CW and pulsed. A sliding delay double pulse technique was used to measure lasing threshold recovery times. A mixture of (CO; N₂; Xe; He) = (.55; .63; .60; 7.41) torr gave a CW output of 8 watts (for 2% coupling) at 195°K bath temperature. Spectral output covered numerous lines from 8 → 7 to 17 → 16 band. However, the same mix produced only the 6 → 5 (P₉) transition with pulses up to 60 μsec and 200 mA. The measured post-pulse dead time of 12 msec is substantially longer than that in a (CO; He) mix. At 77°K no dead time occurred, lasing pulse lengths were longer, and a pronounced enhancement occurred on the second pulse. Operation CW at 77°K bath yielded many lines from 4 → 3 to 8 → 7 band. Values of E/N ranged from 1.6×10^{-16} to less than 1×10^{-16} depending on pressure and temperature. These results will be discussed in relation to the role of the additives.

N3. CO-N₂-He Direct Discharge Laser Model*,
Edward R. Fisher, George Abraham and Alexander Glass,
RIES, Wayne State University - A numerical code has been
developed to model the CO-N₂-He Laser both in pulsed and
CW operation. The code models the laser by a set of
coupled quadratically non-linear rate equations in the
concentration of molecular vibrational states. All vi-
bration-translation and vibration-vibration energy trans-
fer processes are included in the single quantum transi-
tion approximation which is expected to be valid at the
low operation temperatures obtained in laser operation.
Multi-quantum electron-diatomic vibrational excitation
is included together with spontaneous emission for the
prediction of sidelight emission. The behavior of a
CO-N₂-He hot electron laser system containing 30 levels
in both CO and N₂ will be presented as a function of
CO/N₂ molecular densities and compared to CW laboratory
data² in which the current and He concentration are kept
constant. In addition, a comparison of the predicted
laser sequencing to available pulsed data will be pre-
sented.

* Work Supported by ARPA through ARO-Durham

N4. Electron Kinetic Processes in CO Lasers. W. L.
NIGHAN, United Aircraft Research Laboratories.--Electron
energy distributions have been obtained for electrically
excited CO laser mixtures by numerically solving the
Boltzmann equation for conditions typical of electric
discharges. The calculated distribution functions were
found to be markedly non-Maxwellian for mixtures composed
of CO, N₂, Xe, and He. Solution of the electron energy
conservation equation using the computed distribution
functions revealed that vibrational and electronic exci-
tation of CO, N₂, and Xe dominates electron energy ex-
change processes for average electron energy in the 1 -
2 eV range characteristic of electric discharge condi-
tions. For typical mixtures, between 20 and 70 percent
of the total electrical power is transferred to CO vi-
brational levels by direct electron excitation, a result
consistent with the high electrical-optical conversion
efficiency of CO laser discharges. Estimates of maximum
available optical power were also found to be consistent
with experimental values.

N5. Rate Coefficients for Processes in CO Lasers. G.HANCOCK, C. MORLEY, B.A.RIDLEY and I.W.M.SMITH, Cambridge U., Eng. -- The relative rates (R_v) at which the reaction, $O + CS \rightarrow CO + S$, produces CO in different vibrational levels have been derived by analysing the CO infrared chemiluminescence and by using a cw CO laser to determine the vibrational distribution when the reaction was initiated by flash photolysis. The results of these quite different experiments are in good agreement and yield: $R_{v \leq 6} \sim 0$, $R_7 = 0.15$, $R_8 = 0.28$, $R_9 = 0.40$, $R_{10} = 0.55$, $R_{11} = 0.70$, $R_{12} = 0.88$, $R_{13} = 1.0$, $R_{14} = 0.8$, $R_{15} = 0.28$. The overall rate constant $\approx 1.4 \times 10^{-11} \text{ cm}^3 \text{ molecule}^{-1} \text{ sec}^{-1}$. The analogous reaction, $O + CSe \rightarrow CO + Se$, chiefly populates $v=14$ to $v=19$ and could also form the basis of a chemical laser. Rate coefficients for de-excitation of $CO(4 \leq v \leq 13)$ by He, CO, NO, N_2 , O_2 , OCS, N_2O and CO_2 were determined by studying the quenching of the ir emission by these gases. $CO(v=0)$ preferentially deactivates the lower levels and the results emphasise the importance of vibration-vibration energy exchange in all CO lasers.

N6. Vibration-to-Vibration Energy Transfer in Collisions Between Diatomic Molecules.* J. DANIEL KELLEY, McDonnell Douglas Research Laboratories--In this treatment of vibrationally inelastic collisions, the molecules are taken to be harmonic oscillators coupled by a time-dependent interaction potential. This interaction potential contains terms which are linear and quadratic in the oscillator coordinates, and therefore produces vibration-vibration (V-V) and vibration-translation (V-T) energy transfer. The unitary time-evolution operator $U(t, t_0)$ for this interaction potential is obtained exactly, as is the transition probability between any initial pair of vibrational states j, k and any final pair j', k' ; i.e., $P(j', k'; j, k) = |\langle j', k' | U(t, t_0) | j, k \rangle|^2$. The results apply to any pair of oscillators with the same or different vibrational frequencies and are not restricted to small transition probabilities or single-quantum transitions. The calculation of V-V transfer probabilities is discussed, and the results compared to those obtained from less exact treatments.

*This research was conducted under the McDonnell Douglas Independent Research and Development Program.

N7. V-V Transfer Processes in CO Lasers.*

W. Q. JEFFERS, and J. DANIEL KELLEY, McDonnell Douglas Research Laboratories--This paper presents detailed calculations of vibration-vibration transfer probabilities in CO-CO collisions including both long-range and short-range interactions. Comparison is made with experimental data, and the results show that the relative contributions of the long- and short-range interactions to the V-V transfer probability depend on energy defect and temperature. Our calculations match the experimental data at 300 K to within 25%; at this temperature the short-range interactions dominate in determining the transition probability for vibrational energy defects greater than 210 cm^{-1} , while the long range interactions dominate for smaller defects. The time evolution of specific initial distributions of CO molecules has been studied using the transition probabilities discussed above in the master equation for vibrational relaxation. Results for initial distributions characteristic of the O/CS₂ CO chemical laser and the pulse-discharge-excited CO laser will be presented.

*This research was conducted under the McDonnell Douglas Independent Research and Development Program.

SESSION O

Wednesday Evening, 6 October

9:50 p.m.

AFTERGLOWS IN MOLECULAR GASES

Chairman: M. A. Biondi, University of Pittsburgh

01. Collisional Deactivation of Metastable Ar($^3P_{0,2}$) Atoms and N $_2$ ($A^3\Sigma_u^+$) Molecules. * R. A. GUTCHECK and E. C. ZIPF, Univ. of Pittsburgh, Penna. -- In a series of afterglow experiments, we measured the rate coefficients for the collisional depopulation of argon atoms in the metastable $^3P_{0,2}$ state by Ar, CO, N $_2$, and O $_2$, and we found that $k(\text{Ar}) = 2.2 \times 10^{-15}$ cm 3 /sec, $k(\text{CO}) = 1.5 \times 10^{-11}$ cm 3 /sec, $k(\text{N}_2) = 2.8 \times 10^{-11}$ cm 3 /sec, and $k(\text{O}_2) = 1.2 \times 10^{-10}$ cm 3 /sec. Inelastic collisions between metastable argon atoms, resulting in the ionization of one collision partner, were also observed and from simultaneous electron density measurements we obtained a tentative value of 5×10^{-10} cm 3 /sec for the corresponding rate coefficient. The excitation of the 2nd Positive System of N $_2$ ($C^3\Pi_u \rightarrow B^3\Pi_g$), produced by the depopulation of metastable argon atoms by N $_2$, was studied in detail and the specific rate coefficient for this important process was found to have a value of 1.2×10^{-13} cm 3 /sec. The collisional deactivation of metastable N $_2$ ($A^3\Sigma_u^+$) molecules by CO, O $_2$, and Ar was also studied, and the following rate coefficients were obtained: $k(\text{CO}) = 1.7 \times 10^{-12}$ cm 3 /sec, $k(\text{O}_2) = 3.0 \times 10^{-12}$ cm 3 /sec, and $k(\text{Ar}) < 8 \times 10^{-17}$ cm 3 /sec.

*Work supported, in part, by NASA and ARPA.

02. Detection of Vibrationally Excited Nitrogen by Raman Spectroscopy. L. Y. NELSON, A. W. SAUNDERS, JR. A. B. HARVEY, Naval Research Laboratory AND G. O. NEELY, Jarrell-Ash Division, Fisher Scientific Co. - Using laser Raman techniques, vibrationally excited nitrogen in a flowing afterglow has been studied. Relative populations of the $V'' = 0, 1, 2$ and 3 states have been determined. The general application of Raman spectroscopy to the study of vibrational excitation in chemical reactions, as well as electrical discharges, will be discussed.

03. Two-Body Recombination of O_2^+ and O_2^- in Low-Pressure Oxygen. M.N.Hirsh and P.N.Eisner, Dewey Electronics.--Time-resolved measurements of positive ion, negative ion, and electron densities have been made in dilute thermal oxygen plasmas at 300°K, at pressures between 0.01 and 1.0 Torr. A spatially uniform flux of 1.5-MeV electrons irradiates the gas intermittently to produce the plasma; measurements are made during irradiation and in the afterglow. At the lowest pressures O_2^+ and O_2^- dominate the ion spectrum; at higher pressures some tri- and tetra-atomic species are seen. The low-pressure data satisfy a simple analytical model for O_2^+ , O_2^- , and n_e which includes: 3-body electron attachment to O_2 , with rate coefficient $k_3 = (2.1 \pm 0.1) \times 10^{-30}$ cm⁶/sec, fundamental-mode diffusion of three spatially congruent species, with free-ion diffusion coefficients $D(O_2^+) = (55 \pm 10)$ cm²/sec, and 2-body recombination of O_2^+ and O_2^- , with coefficient $\alpha(O_2^+, O_2^-) = (1.0 \pm 0.1) \times 10^{-7}$ cm³/sec. The predictions of a more correct numerical analysis of the 3-species diffusion now being made will be presented.

04. Ion-Ion Recombination, Ionic Mobilities, and Ion-Neutral Collision Frequencies in Thermal N₂:O₂ Plasmas at 300°K. P.N.EISNER and M.N.HIRSH, Dewey Electronics.--Mass spectrometer and conductivity probe measurements have been made in the afterglow of dilute thermal plasmas produced by megavolt-electron bombardment of airlike N₂:O₂ mixtures at 300°K and pressures between 2 and 22 Torr. The ion spectra resemble those in the ionosphere: NO₂⁻ and NO₃⁻ dominate the negative ions, and either NO⁺ or the hydronium ions H₃O⁺·nH₂O control the positive ions, according to the water concentration. Effective values of ion-neutral collision frequency (ν), reduced mobility (μ_0), and ion-ion recombination coefficient (α) for the ambient ion mixture over this pressure range are shown below; the data vary smoothly from the 2 Torr values to the pressure-independent results at 10 Torr and above.

p(Torr)	2	10 - 22
α (cm ³ /sec)	4×10^{-8}	2×10^{-7}
ν (sec ⁻¹)	7.5×10^6	2.3×10^6
μ_0 (cm ² /volt sec)	3.0	10

05. Calculated Densities in Ionized Air at Pressures of 2, 5, and 10 Torr. F. E. NILES AND E. L. LORTIE, US Army Aberdeen Research and Development Center - The number densities of the constituents in 4:1 gaseous mixtures of N_2 and O_2 containing either 6 ppm or 0.6 ppm water vapor have been calculated using the AIRCHEM code for the time following the onset of continuous irradiation by 1.5 MeV electrons. Particular emphasis is placed on the densities around 10^3 sec. By this time the densities are changing slowly and comparison can be made with measurements at the Dewey Electronics Corporation. The calculations show that the major negative ions for the gaseous mixture containing 6 ppm water vapor are the pernitrite form of NO_3^- which we denote $OONO^-$, $NO_3^- \cdot H_2O$, NO_2^- , O_3^- , $NO_2^- \cdot H_2O$, and $O_2^- \cdot H_2O$. The major positive ions are $H_3O^+ \cdot 2H_2O$, NO^+ , and $NO^+ \cdot H_2O$.

06. Time-Resolved Spectroscopy of Plasma Instabilities. W.G. BRAUN, R.F. PAULSON and R.D. FRANKLIN, Aerospace Research Laboratories, Wright-Patterson AFB, Ohio.- The time-resolved coefficients of emission and absorption in a striated argon - mercury discharge have been determined by the Double Path method using a photon counting technique with a multichannel analyzer. With the Double Path method, the problems resulting from time-dependent line shapes are simplified; digital storage requires the least experimental time to achieve the necessary statistical accuracy of the intensity measurements. As has been observed previously ¹, several lines in the visible range exhibit self-absorption. Phase diagrams produced by plotting the time-dependent line absorption versus the line emission obtained from the intensity measurements with the assumption of a uniform discharge cross section and low self-absorption exhibit hysteresis, explicable by the life times of metastable states.

1) A. GARSCADDEN, Bull. Am. Phys., 12, 223, (1967)

SESSION P

Wednesday Evening, 6 October

8:00 p.m.

IONIZATION

Chairman: C. B. Opal, JILA

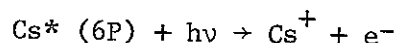
P1. Simultaneous Photoionization-Excitation of Helium: Optical Measurements.* D. H. TRACY and F. L. ROESLER, U. of Wisconsin.--Helium gas at 77K and pressures as low as 25 millitorr was irradiated with intense undispersed XUV synchrotron radiation from the U. W. Physical Sciences Laboratory 240 MeV electron storage ring. The resulting weak 4686\AA $4s,p,d,f \rightarrow 3s,p,d$ He^+ radiation was recorded using a 150mm aperture scanning Fabry-Perot spectrometer at sufficient resolution to obtain the photoionization-excitation cross sections for the $4s,p,d,f$ states of He^+ . The total cross section for exciting $n=4 \rightarrow 3$ radiation, averaged over incident photon energies from threshold (75.6 eV) to about 300 eV, is $4 \times 10^{-22} \text{ cm}^2 \pm 50\%$. Marked pressure dependence of the relative intensities of the fine structure components was observed and will be discussed.

*Work supported in part by the National Science Foundation.

P2. Alkali Atom Photoionization Cross Sections: Spin-Orbit and Core Polarization Effects.* J.C. WEISHEIT, Harvard College Observatory and Smithsonian Astrophysical Observatory -- Cross sections have been computed for the photoionization of sodium, potassium, rubidium, and cesium. The spin-orbit perturbation of continuum p-electron wavefunctions and the core polarization correction to the dipole transition moment are included in the calculation. For each atom, the behavior of the cross section from threshold through the region of its minimum and the degree of polarization of photo-electrons (Fano effect) are in agreement with recent measurements.

*Supported in part by National Aeronautics and Space Administration Grant NGL 22-007-136.

P3. Photoionization of Photoexcited Cesium*
ROBERT E. HEBNER, JR. and KAARE J. NYGAARD, Univ. of
Missouri, Rolla -- The cross section for the process



has been determined in a triple crossed beam experiment. A beam of cesium atoms was excited by a light beam containing the 6S-6P transition wavelengths, 8521 Å and 8944 Å. The excited atoms were subsequently ionized by a second beam of light. The ions thus produced were counted with a Channeltron. The excitation radiation was modulated to allow discrimination against background effects. The relative cross section will be presented and techniques for the absolute calibration of the apparatus will be discussed.

* Supported in part by the Office of Naval Research and the National Science Foundation.

P4. Production of Excited Ions by Electron Collisions with Cesium Atoms *, YU BONG HAHN and KAARE J. NYGAARD, Univ. of Missouri-Rolla -- Excited states of CsII have been studied in a crossed beam apparatus. A neutral beam of Cs atoms is intersected at 90 degrees by a well collimated beam of electrons with an energy spread of about 0.2 eV. The vacuum uv photons emitted from the excited ions are counted by a Channeltron. With the Channeltron located in a magnetic field of 200 Gauss it was necessary to increase the applied voltage to 4000 volts to maintain a sufficiently high gain. Data were taken from 0 to 100 eV. A well-defined onset around 17 eV is in agreement with the 5P⁵6s, 6d levels between 17 and 19 eV.

* Supported in part by the National Science Foundation and the Office of Naval Research.

P5. Electron Impact on Argon.* L. R. PETERSON and J. E. ALLEN, JR., University of Florida.--A reasonably complete set of phenomenological electron-impact cross sections is given for Argon using a combination of data and theoretically meaningful extrapolations of the generalized oscillator strengths. The members of the set include the important allowed and forbidden discrete states, the differential energy loss continuum states and estimates of the inner shell cross sections. The cross sections are used to compute the effects of electron degradation in Ar for electrons up to a few keV. Final populations for each excited and continuum state are given as a function of incident energy. When applied to ionization, the resulting value for eV per ion pair is very close to 26.4. Inner shells in our work appear to contribute mainly by adding on the order of 10% to the loss function at energies above a few hundred eV.

*Work supported by the National Aeronautics & Space Administration.

P6, Secondary Electron Distributions.* A. E. S. GREEN, T. SAWADA and A. J. YEZZI, University of Florida.--The importance of secondary electrons following primary bombardment by various ionizing radiations has been established in many recent studies on charged particle energy deposition. Here we first develop an improved analytical characterization of the differential cross section leading to secondary electrons following primary electron bombardment at fixed energies. This form permits us to describe phenomenologically the fall off in the production of secondary electrons at low and at high secondary electron energies more accurately. With a small modification this same characterization can be used to describe the number of secondary electrons arising from the complete deposition of a primary particle from its initial energy to the ionization threshold. Parameters for the differential ionization cross section and for the number of secondary electrons following primary energy deposition are given for important atomic and molecular species. The results are intended for application to various charged particle energy deposition studies.

Work support by the United States Atomic Energy Commission

P7. Ionization of Rare Gases in the Born Approximation.* R. A. BERG and A. E. S. GREEN, University of Florida.--Utilizing the first Born approximation and Bethe's generalized oscillator strength formalism, expressions are developed for the total generalized oscillator strength (GOS) and the various partial wave contributions to it. Using an analytical potential with parameters which have been established in previous work on excitation GOS, these equations are solved numerically to obtain the ionization GOS and its partial wave contributions for Ne, Ar, Kr, and Xe. We find that there is continuity across the ionization threshold between a partial wave contribution to the ionization GOS and the properly energy normalized excitation GOS that has the same final state angular momentum. Our GOS are compared with the results of other theoretical calculations. The secondary electron distributions and various associated quantities are compared with recent experimental data.

Work supported by the Air Force Office of Scientific Research.

SESSION Q

Wednesday Evening, 6 October

9:45 p.m.

EXCITATION BY ELECTRONS
(PANEL)

Chairman: C. C. Lin, University of Wisconsin

Q1. Electron Excitation of Potassium and Cesium.*
 JERRY E. SOLOMON, DALE F. KORFF, AND CHUN C. LIN,
 University of Wisconsin-- Electron excitation cross
 sections of some twenty-two states of the ns, np, nd,
 and nf series of potassium have been measured from
 threshold to 100 eV by the optical method. The excitation
 functions of the p states show a broad peak,
 those of the f states have intermediate breadth, and
 the s and d states give narrow excitation functions.
 Theoretical calculations of the cross sections have
 been performed by the Born approximation and by the
 method of close coupling, and the results are compared
 with the experimental data.

*Work supported in part by the U. S. Air Force Office
 of Scientific Research and by the Air Force Cambridge
 Research Laboratories, Office of Aerospace Research.

Q2. Electron Impact Excitation of Atomic Nitrogen.*
 E. C. ZIPF and E. J. STONE, Univ. of Pittsburgh, Penna.
 -- The absolute cross sections for the excitation of
 five NI vacuum-ultraviolet multiplets by electron
 impact on atomic nitrogen were measured from threshold
 to 350 eV. The following results were obtained:

Multiplets	λ (Å)	Q(max; cm ²)	E(max; eV)
NI(3s ² p → 2p ³ 2p)	1743	1.8 × 10 ⁽⁻¹⁷⁾	17
NI(3s ² d → 2p ³ 2D)	1243	1.7 × 10 ⁽⁻¹⁷⁾	17
NI(3s ⁴ p → 2p ³ 4S)	1200	5.5 × 10 ⁽⁻¹⁶⁾	25
NI(3d ² d → 2p ³ 2D)	1164	4.0 × 10 ⁽⁻¹⁷⁾	18
NI(2p ⁴ 4p → 2p ³ 4S)	1134	4.8 × 10 ⁽⁻¹⁶⁾	22

The use of VUV absorption techniques to measure the
 absolute nitrogen density provided an opportunity to
 measure the oscillator strength of the NI(2p⁴ 4p -
 2p³ 4S) transition. The branching ratio for the
 NI(λ1164Å/λ1311Å) multiplets was also determined.
 These results will be discussed in detail.

*Work supported, in part, by NASA and ARPA.

Q3. Electron Impact Excitation of the Werner Bands of H₂. * E. J. STONE and E. C. ZIPF, University of Pittsburgh, Penna. -- The Werner band system of molecular hydrogen ($C^1\Pi_u \rightarrow X^1\Sigma_g^+$) was excited by electron impact on H₂ and studied in the wavelength region 1100Å - 1250Å with sufficient instrumental resolution to resolve much of the rotational structure of the bands. The absolute cross section for the excitation of the Q1 line of each of the prominent bands in this wavelength region was determined. The absolute spectral sensitivity of the apparatus was determined by observing the dissociative excitation of Lyman Alpha in H₂ and Lyman-band fluorescence in HD. It was found that the Werner bands are a satisfactory basis for a spectral sensitivity determination only if the intensity measurements are made with sufficient resolution (FWHM < 0.44Å). The perturbation interaction between the B and C states of the hydrogen molecule was clearly observed in the rotational intensity distribution in one set of bands; these results will be discussed in detail.

* Work supported, in part, by NASA and ARPA.

Q4. Excitation of the Metastable A³Σ_u⁺ State of N₂ by Electron Impact. WALTER L. BORST, University of Pittsburgh and Southern Illinois University. -- The total metastable excitation function of N₂ was decomposed into individual contributions from the various metastable states using previous time-of-flight measurements. The sensitivity of the Auger surface detector was determined as a function of metastable excitation energy. Absolute metastable excitation cross sections were obtained by using the known detector sensitivity and "Franck-Condon weighting" the secondary electron yields for individual vibrational levels. The method discriminated strongly against the lower vibrational levels of the A³Σ_u⁺ state. This effect was utilized to determine the cross section for direct excitation of the A³Σ_u⁺ state for which the upper vibrational levels are preferentially populated. Cascade effects were of minor importance in the present case because they lead to population of lower levels of the A³Σ_u⁺ state. The cross section for direct excitation of the A³Σ_u⁺ state was determined from threshold to 40 eV and had a peak value of $(5.3 \pm 2.0) \times 10^{-17} \text{cm}^2$ near 10.7 eV. The total apparent cross section of the A³Σ_u⁺ state including cascade was estimated to have peak values of about $1.2 \times 10^{-16} \text{cm}^2$ at 10.7 and 14.5 eV.

Q5. Translational Spectroscopy of Fast Metastables Produced by Electron Impact Dissociation of Atmospheric Gases.* W. C. WELLS, W. L. BORST[†] and E. C. ZIPF, Univ. of Pittsburgh, Penna. -- Our early studies of low energy electron impact dissociation of atmospheric gases - O₂, N₂, CO, and CO₂ - have been expanded to include incident electron energies of up to 300 eV. Time of flight spectra taken at these higher electron impact energies revealed faster metastable fragments than had heretofore been observed. At low electron impact energies (< 50 eV) where dissociative excitation was the dominant process, mean fragment energies for the fastest fragments were about 2.5 eV. At higher electron impact energies simultaneous dissociative ionization and excitation became the dominant process and the mean fragment energy rose to about 6 eV. Excitation functions for these fast metastable fragments exhibited characteristic maxima around 100 eV. The production of O(⁵S⁰) atoms by electron impact on CO and CO₂ will be discussed in detail. Implications of these results concerning repulsive molecular states and applications to the upper atmosphere will be mentioned.

*Work supported, in part, by NASA and ARPA.

[†]Present address: Dept. of Physics, Southern Illinois University, Carbondale, Illinois 62901.

Q6. Hydrogen Balmer Cross-Sections from Electron-Molecule Collisions.* R. A. MICKISH and R. M. ST. JOHN, University of Oklahoma--An experimental investigation of H_α, H_β, H_γ, and H_δ Balmer radiation has been carried out in order to determine when atom-molecule, atom-ion, and multi-electron collisions perturb the radiation from hydrogen atoms due to hydrogen molecule excitation and dissociation by single electron impact. The experiment was carried out using a conventional electron gun and radiation measuring system. The results indicate that atom-molecule collisions become significant above approximately 5.25μ, 4μ, 1.1μ, 0.35μ for H_α, H_β, H_γ, and H_δ respectively and is independent of the electron beam current. Atom-ion and multi-electron collisions are a function of the beam current and occur at much higher pressures. The excitation functions and cross-sections of H_α and H_β were obtained at 5.25μ and 4μ respectively and compared to those of other investigators.

*Work supported in part by Air Force Office of Scientific Research.

SESSION R

Thursday Morning, 7 October

8:30 a.m.

LASERS II

COLLISIONAL PROCESSES IN LASERS

Chairman: D. R. Keefer, University of Florida

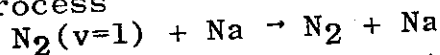
R1. Operating Parameters of Sealed-off CO₂ and CO₂-He Lasers. W. T. WHITNEY, NRL - The output power of the sealed-off CO₂ laser was investigated as a function of the initial fill pressures of CO₂ and He, the discharge current, and the tube diameter. The optimum fill pressure of pure CO₂ for maximum power output and efficiency is $(5/d)$ Torr, where d is the tube diameter expressed in cm. The optimum current for maximum power output is $7d$ mA. With addition of He, the optimum current is increased to $18d$ mA, and the output power is increased five-fold, indicating the importance of the increased thermal conductivity of the gas. The results suggest that the maximum laser output is obtained at the same value of electron mean energy. The optimum value of E/N is about 5×10^{-16} V cm², which according to the analysis of Nighan¹, indicates the importance of collisional transfer of energy from vibrationally excited carbon monoxide.

¹William L. Nighan, Phys. Rev. A 2, 1989 (1970)

R2. The Influence of Plasma-Generated Impurities on Molecular Gas Discharges.* W. J. Wiegand, United Aircraft Research Laboratories.-- Plasma induced chemical reactions occurring in molecular gas discharges result in the formation of impurity species which significantly influence discharge properties by modifying the dominant charged particle production and loss processes. In order to investigate the effects of discharge plasma chemistry, an experiment featuring two flowing gas discharges connected in series was developed. Experiments indicated that minority species produced in quantities on the order of parts per million can substantially alter discharge characteristics through the formation of stable negative ions. A kinetic analysis of neutral and charged particle plasma chemistry supported this conclusion and revealed that negative ion concentrations exceeding the electron density are produced on a time scale of approximately 10^{-2} seconds.

R3. Influence of Contaminants on the CO₂ Laser
 P. BLETZINGER, M. HUGHES, P. D. TANNEN and A. GARSCADDEN,
 A. R. L., Wright-Patterson A. F. B., --The history of the gas
 composition in a CO₂-N₂-He laser has been studied by
 subjecting discharged samples to high resolution mass
 spectrometry. Compounds found include CO, NO, N₂O, H₂O, O₂
 and CN. Also, correlations between these gases, the plasma
 properties, discharge stability, and laser output and
 efficiency were determined by adding calibrated amounts
 of contaminant. The plasma properties were monitored by
 Langmuir probe and spectroscopic methods. It was found
 that the electron energy distribution is especially
 sensitive to the additives, then the discharge stability
 and homogeneity (less than 1% for most of these gases),
 and then the laser output (approx 1%). Nitrous oxide was
 found especially effective. It perturbs the plasma by
 forming negative ions, and the laser by modifying the
 electron energy distribution at low energy and by di-
 verting vibrational energy from the upper laser level.
 These effects were higher at higher flow-rates, indica-
 ting that they were due to N₂O and not one of its
 dissociated products. Constriction was not synonymous
 with severe degradation of laser output for all of the
 contaminants.

R4. Experimental Studies on Effects of Na Vapor
 mixed with Active N₂^{*}. R. E. Walker and J. C.
 Pirkle, Johns Hopkins University, Applied Phys-
 ics Laboratory. Photometric measurements have
 been made of resonant (D-line) and non-resonant
 radiation that occurs when Na vapor is mixed
 with electrically-discharged N₂. The experi-
 ments were conducted in a low-pressure fast-
 flow reactor using a photomultiplier which
 tracked along the tubular reactor. Vibrational
 temperatures and vibrational distributions (non-
 Boltzmann) are inferred from absolute intensity
 measurements and relative intensity decay data
 have been used to evaluate the rate constant
 for the V-T process



which is found to be fast ($k=25000 \text{ torr}^{-1} \text{ sec}^{-1}$)
 and in accord with theoretical predictions by
 Fisher and Smith. The effects of foreign gases
 (CO₂ and CO) have also been examined.

*Work conducted under Task A170 of Contract
 N00017-72-C-4401 with NOSC, U. S. Navy.

R5. Measurement of the Vibrational Population Distribution in Discharged N₂. S. J. YOUNG and K. P. HORN, The Aerospace Corp. --A gas mixing flow system is being used in a comparative study of the vibrational population distribution in discharged N₂ as measured by (1) the Penning ionization reaction of metastable He(³S) with N₂ and analysis of the N₂⁺(1-) band system emissions and (2) the addition of CO to the N₂ as an IR-emitting tracer. The CO tracer technique requires knowledge of the V-V interaction between N₂ and CO and analysis of the CO IR radiation at 2.3 μm. The Penning ionization technique requires knowledge of the radiative transition probabilities for the (1-) system of N₂⁺ and the collisional loss rates for N₂⁺ ions in He - N₂ gas mixtures. These loss rates have been measured in an experiment with undischarged N₂, and an inference has been drawn as to which of several published and derivable transition probability sets is most correct. The ratio of the rate constants K(1)/K(0) = 5. With these data and available Penning ionization F-C factors, the N₂⁺ spectral data for He reactions with discharged N₂ has been reduced. Preliminary results indicate that the Penning technique gives consistently higher values (by as much as 1000°K in some cases) for the effective vibrational temperature of the v = 1 level of N₂ than does the CO tracer technique.

R6. Laser Excited Vibrational Energy Transfer Studies of Hydrogen Fluoride. W. H. GREEN and J. K. HANCOCK, U.S. Naval Research Laboratory - An electrically initiated, pulsed HF (hydrogen fluoride) chemical laser has been used to excite infrared fluorescence from HF and mixtures of HF with AR, H₂, D₂, DF, NO, CO and CO₂. Cross-sections for vibrational deactivation of room temperature HF have been obtained. These data have both theoretical and practical implications for understanding energy transfer processes which are important in existing chemical lasers.

SESSION 5

Thursday Morning, 7 October

10:20 a.m.

LASERS III

LASERS – GENERAL

Chairman: D. R. Keefer, University of Florida

S1. Gas Pumping by Striations in dc Discharges. C. C. Leiby, Jr., AFCRL - The simple steady-state approximation to the Leiby-Oskam theory of electrophoresis in plasmas¹ consistently underestimates observed gas flow velocities when striations are present. A more sophisticated approximation is developed which takes into account temporal variation of plasma parameters. In the presence of sinusoidal ionization waves where plasma electric fields, electron temperatures and densities are strongly modulated, this time-dependent approximation predicts gas flows 2 to $2\frac{1}{2}$ times greater than those predicted by the steady-state approximation. These greater predicted gas flows are consistent with observed gas flows in striated dc discharges in Ar, Kr and Xe.

A comparison of electron momentum transfer rates (as inferred from measured electron mobilities) with those calculated using published cross-sections and measured electron temperatures shows them to be in good agreement when striations are absent. In the presence of striations, however, observed momentum transfer rates are up to 20 times larger than the calculated rates. It is suggested that this excess electron momentum transfer rate may constitute the force driving the observed striations.

¹ Phys. Fluids 10 1992 (1967).

S2. Laser Emission from the Werner Band of Hydrogen

Ronald W. Waynant, Naval Research Laboratory

Although theory^{1,2} predicted vacuum ultraviolet laser emission from both the Werner and Lyman bands of hydrogen, it was the Lyman band that was first discovered experimentally. Werner band lines believed to be lasing have now been found. Two lines at 1231 and 1162 Å corresponding to Q(2) rotational lines between the vibrational levels $v' = 3 - v'' = 7$ and $y' = 1 - v'' = 4$ of the electronic transitions $C^1\Pi_u - X^1\Sigma_g$ appear to be lasing, but with less than one hundredth (i.e. 10 kW) that of the Lyman band lasing lines. Observations of Werner band lasing lines were made with the same system used to produce Lyman band lines^{3,4} except that the system's optical losses in the Werner band spectral region were reduced by modifications of the optical path. Other Werner band lines are expected to be observed at further reduced power levels.

¹ P. A. Bazhulin, I. N. Knyazev, and G. G. Petrash, Soviet Phys. JETP 21, 649 (1965).

² A. W. Ali and A. C. Kolb, Appl. Phys. Letters 13, 259 (1968).

³ R. W. Waynant, J. D. Shipman, Jr., R. C. Elton, and A. W. Ali, Appl. Phys. Letters 17, 383 (1970).

⁴ R. W. Waynant, J. D. Shipman, Jr., R. C. Elton, and A. W. Ali, Proc. IEEE 59, 679 (1971).

S3. Excitation and Heating Processes in a Pulsed Argon Ion Laser Plasma. B. G. BRICKS, JOHN D. LITKE, DONALD E. KERR, Johns Hopkins University
--A study of the excitation and heating processes in a pulsed A^+ laser is described. The plasma is maintained below threshold by a steady weak background current and then pulsed into oscillation by nearly square current pulses of typically 40 μ sec duration at a 50 Hz rate. Measurements of intensity and Doppler broadening of atomic and ionic spectral lines reveal the excitation and apparent temperature before the pulse and as a function of time during the pulse. Saturation of T_{\perp}^i and T_{\parallel}^i with pulse-current amplitude is observed. For all conditions T_{\parallel}^i rises rapidly to a constant value during the pulse. Background current and pulse repetition rate affect dramatically occurrence of negative laser gain but not temperatures during the pulse. The results demonstrate the importance of wall effects as well as radiation trapping on laser gain.

SESSION T

Thursday Afternoon, 7 October

2:30 p.m.

LASERS IV

CO₂ LASERS

Chairman: W. J. Graham, Naval Research Laboratory

T1. A Stable, Scalable, High Pressure Gas Discharge As Applied to the CO₂ Laser. J. D. DAUGHERTY, E. R. PUGH, D. H. DOUGLAS-HAMILTON, Avco Everett Research Laboratory - High pressure, large volume gas discharges suffer from ionization instabilities. A high energy electron beam can produce the ionizations necessary to the discharge. The resulting discharge is stable and scalable and has produced lasing in CO₂ at 1 atm.

T2. Characteristics of an Electron Beam Controlled Plasma Discharge* CHARLES A. FENSTERMACHER, MURLIN J. NUTTER, WALLACE T. LELAND, and KEITH BOYER, Los Alamos Scientific Lab.--Electrical and optical measurements on the previously reported¹ electron beam controlled plasma discharge have been extended to encompass longer times (to 10 μsec) and higher pressures (to several atmospheres) in mixtures ranging from pure CO₂ to mixtures rich in He and N₂. Voltage-current relationships, small signal optical gain at 10.6 μ wavelength have been determined, and some information on the electron-ion recombination rate as a function of electron energy has been obtained. For the experimental conditions here, resistivities of ~ 500 ohm-cm and small signal gain of 5% cm⁻¹ were observed at field strengths up to 8 kV/cm corresponding to E/N values of 2 x 10⁻¹⁶ volts-cm².

*Work supported by the U. S. Atomic Energy Commission.
¹C. A. Fenstermacher, M. J. Nutter, J. P. Rink, and K. Boyer, Bull. Am. Phys. Soc. 16, Series 11, No. 1, 42 (1971).

T3 A Cold Glow Discharge Laser Energy Source.*
CARROLL B. MILLS, LASL.--Upper limits of molecular vibration energy are being investigated using recent developments on vibrational excitation rates by Phelps. The reference experiments use a high current but cold and uniform plasma for collisional excitation of vibrations being studied by Fenstermacher. The steps to lasing action are: (a) s.t.p. gas mixture ionization by an electron beam with a rate $R_{ion} \approx 10^{19}$ ions/cc-sec; (b) current flow with $2 < E < 6$ KV/cm and $1 < I < 10$ amp/cm² for 10 μ sec; and (c) concurrent equilibration of molecular vibrational levels in the gas. A parametric study of excitation rates for lower CO₂ levels as a function of potential gradient per molecule showed that for a constant ionization rate in a He/N₂/CO₂ gas mixture of 3/1/1 mol ratio and a potential gradient of 2 to 3.5 KV/cm, the electron density values were 5.2 to 8.6×10^{12} /cc and the experimental gain (%/cm) was 2.8 to 4.8. Computed values ranged from 3.7 to 4.2. The ion recombination rate had a simple (characteristic energy)⁻¹ dependence.

*Work performed under the auspices of the U.S. Atomic Energy Commission.

T4. Current in the Cold Laser Plasma.* CARROLL B. MILLS and JAY TODD, JR., LASL.--The cold glow discharge of interest for vibrational excitation of a gaseous laser is ignited by a high energy electron beam and maintained for 0-10 μ sec by 2-6 KV/cm. This plasma provides a test bed for gaseous electronics studies of several kinds. The solution of the current continuity equation for high space charge density ($\sim 10^{13}$ /cc) provides numbers for excitation rate integrals. The integration was done for $n_e(x,t)$ by numerical means using the donor cell approximation for continuity and Poisson eq's, solving the space mesh with a tridiagonal matrix, and solving the time development in the form $d^2E/dxdt = A d/dx (I_e + I_{ion})$, where E is electric gradient and I is current density. The result showed that the sheath was the current source, and that for a uniform ion density there may be a uniform electric gradient.

*Work was performed under the auspices of the United States Atomic Energy Commission.

T5. The Kinetics of Electron Beam Controlled CO₂ Laser Systems. * ANDREW M. LOCKETT III, LASL--The prediction of the behavior of electron beam controlled gas lasers is at present hampered by the rather sizable experimental and theoretical uncertainties in the relevant cross sections and rate constants for electronic and molecular collisions. The limits of uncertainty in these parameters have been narrowed by a comparison of theoretical calculations with the detailed time history of the current and small signal optical gain obtained experimentally by Fenstermacher et al.¹ over a substantial range of gas mixtures, pressures, voltage, gradients, and electron beam intensities in the CO₂/N₂/He system. Predictive calculations have then been performed over a wider spectrum of experimental condition directed toward optimizing either the optical gain or, alternatively, the corresponding absolute population inversion density.

*Work performed under the auspices of the U.S. Atomic Energy Commission.

¹C. Fenstermacher, M. Nutter, W. Leland and K. Boyer, Abstract at this meeting.

T6. The Transient Glow Discharge in a Pulsed Atmospheric CO₂ Laser. JEAN ROCCA SERRA, Laboratoires de Marcoussis, France. Experiments have been made to obtain a uniform transient glow discharge ($\approx 2 \mu\text{s}$) in a typical CO₂/N₂/He (1,1,3) mixture at atmospheric pressure. The effective discharge volume was 350 cm³ with (33 x 3.5 x 3 cm) a 35 mm gas discharge. A uniform preionization supplied by an auxiliary discharge at the cathode level has been used along with some restrictions upon the applied voltage rise time ($\approx 2 \mu\text{s}$, 50 kV), the electric field configuration, and the low value inductance of the external discharge circuit. Time resolved measurements of discharge current and voltage have been made ($j \approx$ several A/cm²), from which electron density inside the volume has been deduced⁽¹⁾. Using⁽²⁾ the numerical computation of Nighan⁽³⁾ the electron energy distribution has been obtained for our particular gas mixture and reduced field. Pictures of the discharge have been taken.

- (1) BROWN Basic Data on Plasma Physics MIT 1967
(2) VON ENGEL Ionized Gases OXFORD
(3) NIGHAN Physical Review A 2 1969-1970

SESSION U

Thursday Afternoon, 7 October

4:30 p.m.

LASERS V

CO₂ LASERS

Chairman: W. L. Nighan, United Aircraft Research Laboratories

U1. Abstract Withdrawn

U2. Afterglow Gain Characteristics of Uniform Glow, High Pressure Discharges in CO₂-N₂-He Mixtures. L.J. DENES, Westinghouse Research Laboratories--A wavelength selectable, CW CO₂ laser has been used to measure the temporal and spatial small signal gain of pulsed high-pressure CO₂ discharges in continuous, planar electrode configurations. These electrode configurations produce longitudinally extended diffuse-glow discharges with cross sections of low aspect ratio by means of a midgap auxiliary electrode or corona source. Energy is supplied by a fast switched (<10 nsec), capacitor-dumped, low-inductance supply. The temporal behavior of the small-signal gain is measured as a function of spatial position, capacitor voltage (energy), capacitance, mixture composition, mixture pressure and CO₂ rotational transition using several methods of discharge initiation. These single pass gain studies show that nearly uniform volumetric glow discharges are obtained. Typically, the small signal gain pulse rises to a peak value in one usec and decays subsequently with a 20-30 usec time constant. A peak gain of 3% cm⁻¹ has been achieved for a CO₂:N₂:He mixture of 1:3:1 at 300 Torr.

U3. The Generation of Infrared Radiation and the Transition from Glow to Arc in Discharges Through CO₂:N₂ Near Atmospheric Pressure. T. V. GEORGE and E. W. SUCOV, Westinghouse Research Labs.--Pulsed discharges through CO₂:N₂ mixtures near atmospheric pressure were studied to determine the relation between infrared emission and properties of the discharge. Time variation of visible radiation was obtained from streak and framing photographs. The discharge was found to progress through three stages. (1) Excitation: duration about 100 nsec, 90% of total power transferred from capacitor bank, strong luminosity. (2) Glow: duration from 500 to 1500 nsec, luminosity extinguished except in front of cathode, infrared radiation emitted with time constant about 850 nsec. (3) Arc: formed in 50 nsec, infrared radiation absent, strong luminosity. The luminous cathode spot was stationary through the glow phase but luminosity of lower intensity propagated with velocity of 8×10^5 cm/sec from both anode and cathode to form the arc when they met.

U4. Excitation and Ionization of a CO₂ Laser Plasma by Nuclear Reaction Products. H. S. Rhoads, and R. T. Schneider, University of Florida - The output of a CO₂ laser is significantly increased by products of the nuclear reaction He³ (n,p)T. Helium-3 replaces the natural helium normally present in the CO₂ laser gas mixture. The laser was irradiated in a thermal reactor with a neutron flux of about 10^9 neutrons cm⁻² sec⁻¹. Power output of the laser doubled while the electrical power input decreased; electrical efficiency was more than doubled. Nuclear power input is negligible compared to electrical power input. The effect is possibly caused by the charged particles altering the electron energy distribution and density.

U5. Combined RF and DC Excitation of a CO₂ Laser
J. C. SWINGLE and D. R. KEEFER, University of Florida,
Gainesville, Florida--The performance of a flowing gas
CO₂ electric discharge laser using RF excitation has
been measured and correlated with flow velocity and elec-
trical power input. Further experiments were performed
in which the electrical power input to the discharge was
supplied simultaneously by the segmented solenoid of an
RF resonant circuit and a conventional DC circuit. The
total electrical power input was maintained constant
while the percentage of RF power was increased and the
current in the DC circuit was decreased. The maximum
laser power of 2.5 watts was obtained with 30% RF power,
representing a 25% increase in laser power over the all
DC case. This maximum was shown to be accompanied by a
minimum gas temperature as determined by spectroscopic
analysis of the discharge.

U6. Fast Pulse Rate Electrical Discharges in a
Supersonic CO₂-N₂-He Gas. W. M. Brandenburg, Boeing
Scientific Research Labs. - Fast pulse rate electrical
discharge techniques in high pressure CO₂-N₂-He gas
mixtures flowing at supersonic velocity are being in-
vestigated. To date, spatially diffuse electrical dis-
charges at repetition rates of 17kHz and Mach 3 flow have
been achieved using either pin electrode arrays or paral-
lel plate electrodes with rf preionization near the cathode.
Optical gains of 1.6 m⁻¹ at 10.6 μ and average laser out-
put power of 340 watts from 10 cm³ discharge volume have
been measured at static pressures of 160 Torr. Results
on voltage/current characteristics in supersonic flows,
discharge stability and laser performance will be dis-
cussed.

SESSION V

Thursday Morning, 7 October

8:30 a.m.

ION-MOLECULE REACTIONS AND CHARGE TRANSFER

Chairman: R. C. Isler, University of Florida

V1. Ion-Molecule Experiments Involving Negative Ions of Tungsten and Rhenium Oxides. * R. E.

CENTER, Avco Everett Research Laboratory-- Rate constants for the reactions of ReO_3^- and $(\text{WO}_3)^-_{n=1,2,3}$ with Cl_2 and NO_2 have been measured in a drift tube mass-spectrometer apparatus from thermal energies (295°K) to $\sim .07$ eV in the center of mass system. The rate constants for these reactions involving atom exchange agreed to within a factor of 2 with the theoretical orbiting rate constant of approximately 7×10^{-10} cm^3/sec for both reactants. ReO_4^- did not react with either NO_2 or Cl_2 . Ordinary charge transfer was not observed implying electron affinities in excess of 2.4 eV for these metal oxides. The mass identified zero-field mobilities of these ions in Ar were measured at 295°K and were found to be 1.94, 1.67, 1.95, 1.50 and $1.20 \text{ cm}^2 \text{ volt}^{-1} \text{ sec}^{-1}$ for ReO_3^- , ReO_4^- , WO_3^- , $(\text{WO}_3)_2^-$ and $(\text{WO}_3)_3^-$, respectively.

* This research was supported by the Advanced Research Projects Agency of the Department of Defense and Space and Missile Systems Organization.

V2. Reactions of H^- and D^- with D_2 , H_2 , and HD .

JOHN F. PAULSON, Air Force Cambridge Research Labs. -- Cross sections have been measured in the range of interaction energies from 0.5 to 10 eV for the reactions (1) $\text{H}^- + \text{D}_2 = \text{D}^- + \text{HD}$, (2) $\text{D}^- + \text{H}_2 = \text{H}^- + \text{HD}$ and for the analogous reactions with HD . In all cases the cross sections increase rapidly with increasing energy and show clear maxima at about 2 eV. Relative ion collection efficiencies of the double mass spectrometer used in these experiments are about 0.4 for low energy product ions isotropically distributed in the laboratory system and about unity near the thresholds of endothermic reactions. Subject to these uncertainties, the cross section maxima are 1.3 \AA^2 for reaction (1) and 4 \AA^2 for reaction (2). Cross sections for the analogous reactions with HD are roughly half these values. Retarding potential analyses for reaction (2) near the cross section maximum show that the energy transferred from translational to internal modes corresponds to the production of vibrationally excited HD , mostly $v = 2$.

V3. Charge Transfer and Ionization in Collisions between Atomic Ions and Rare Gas Atoms for Primary Ion Energies below 100 eV. WILLIAM B. MAIER II, Los Alamos Scientific Lab.-- Cross sections for production of Kr^+ , Kr^{++} , Xe^+ , and Xe^{++} in collisions of H^+ , He^+ , and Ne^+ with Kr and Xe have been measured for primary ion energies E between 0.5 and 100 eV. As E is increased, the cross sections rise sharply, reach a maximum (0.1 to 40 \AA^2), and then decrease slowly. Production of doubly charged ions corresponds to production of free electrons, and these cross sections are not adequately represented by the theoretical expressions with which the data were compared. Cross sections for production of singly charged positive ions are larger for the more complex target atoms and lighter primary ions and are well represented by the theory of Rapp and Francis¹ whenever the theory is expected to apply. The present data agree fairly well with previous experimental results.

¹D. Rapp and W. E. Francis, J. Chem. Phys. 37, 2631 (1962).

V4. Electron Transfer in Collisions of Doubly Charged Rare Gas Ions and Rare Gas Atoms for Primary Ion Energies Below 100 eV.* WILLIAM B. MAIER II and BRUCE STEWART, Los Alamos Scientific Lab.-- Cross sections for production of Ne^+ , Kr^+ , and Kr^{++} in collisions of Ne^{++} with Kr and of Kr^{++} with Ne have been measured for primary ion energies E between 0.5 and 100 eV. Cross sections for pickup of a single electron are 5 - 30 \AA^2 and increase steeply with decreasing E for $E \lesssim 5$ eV. The experimental cross section for $Ne^{++} + Kr \rightarrow Kr^{++} + \dots$ is about 1.2 \AA^2 for $10 \lesssim E \lesssim 97$ eV; the cross section rises as E is decreased and is $\approx 4.5 \text{\AA}^2$ at $E = 0.5$ eV. Comparison of the cross sections for the production of Ne^+ and Kr^+ in each of $Ne^{++} + Kr$ and $Kr^{++} + Ne$ yields information about the efficiency with which secondary ions are collected in this experiment.

*Work supported by the Atomic Energy Commission.

V5. Drift Tube Measurements of the Reactions $U^+ + O_2$ and $U^+ + N_2$ from Thermal Energy to ~ 11 eV.* R. JOHNSEN and MANFRED A. BIONDI, Univ. of Pittsburgh, Penna. ---
 A drift tube-mass spectrometer apparatus is used to determine the rate constants for the reactions of uranium ions with oxygen and nitrogen. Uranium ions produced by an evaporative source drift through helium buffer gas containing the reactant gas oxygen or nitrogen. The reaction $U^+ + O_2 \rightarrow UO^+ + O$ is exothermic by ~ 2.9 eV and is observed to occur with a large rate constant of $(8.5 \pm 1.5) \times 10^{-10}$ cm³/sec at thermal energy (300°K), decreasing very slightly with increasing ion energy. (The Wannier formula and the measured $\mu_0 = 24.4$ cm²/V sec at 300°K and $E/p \approx 3$ are used to calculate the mean energy.) Due to the large mass of U^+ the time required to reach the terminal drift velocity is not always negligible compared with the reaction time, indicating that the actual mean ion energy may have been $\sim 30\%$ less than the calculated energy at the highest energies. No reaction (exceeding $\sim 10^{-11}$ cm³/sec) is observed for $U^+ + N_2$ (which may reasonably be expected to be endothermic) up to U^+ energies of ~ 11 eV.

*Research supported in part by ARPA, DA-31-124-ARO-D-40.

V6. Total Collision Cross Sections for Ion-Polar Molecule Collisions. J. V. DUGAN, JR., NASA-Lewis R. C. and J. L. MAGEE, Univ. of Notre Dame---
 Previous work on ion-dipole collisions consisted of capture cross section calculations and studies of ion-molecule complex formation via computer-plotter techniques¹. This paper reports on numerical calculations of momentum transfer cross sections and differential scattering cross sections for rotational energy transfer. The analytical momentum transfer cross section σ_T is large but finite ($\sim 10^3 - 10^4$ Å²) at thermal energy for linear targets but infinite for symmetric top polar molecules. Thus σ_T values for tops are obtained using uncertainty relations to calculate a meaningful maximum impact parameter b_m . Differential scattering cross sections are calculated for various b values; significant scatterings are obtained for $b=50$ Å at thermal velocity for highly polar targets. The diffusion coefficients for ions in polar gases are quite small and strongly temperature dependent at low temperature.

¹ "Dynamics of Ion-Molecule Collisions" by J. V. Dugan, Jr., and J. L. Magee in "Chemical Dynamics, Vol. 21, Advances in Chemical Physics, John Wiley and Sons, 1971.

SESSION W

Thursday Morning, 7 October

10:10 a.m.

ELECTRON SCATTERING

Chairman: P. D. Burrow, Yale University

W1. Crossed Beam Experiments on Low Energy e-O₂ Collision Processes. F. Linder* and H. Schmidt, Fachbereich Physik der Universitat Trier-Kaiserslautern, 675 Kaiserslautern, W. Germany.

Elastic scattering, vibrational excitation to $v = 1, 2, 3, 4$ of the electronic ground state, and electronic excitation to the states $a^1\Delta_g$ and $b^1\Sigma_g^+$ of O₂ have been measured in a crossed beam apparatus for collision energies from nearly 0 eV to 4 eV. Differential and integral cross sections have been determined and calibrated on an absolute scale. From 15 vibrational levels of O₂⁻, which could be observed as resonances in the cross sections, the spectroscopic constants for the vibrational structure of O₂⁻ have been derived: $\hbar\omega_e = 135$ meV and $\hbar\omega_{exe} = 1$ meV. The cross sections for vibrational excitation have the order of 10^{-18} cm² eV. The half width of the resonance can be estimated to $\Gamma \approx 0.5$ meV, which corresponds to a lifetime of 10^{-12} sec for the O₂⁻ states.

*Present address: NOAA Environmental Research Laboratories, Boulder, Colorado 80302

W2. Electron Transmission Spectra of NO and O₂.[†] L. SANCHE and G. J. SCHULZ, Yale U.--A transmission experiment which measures the derivative of the current transmitted through a gas-filled chamber is used to observe structures in the total electron impact cross section.¹ Four distinct series of resonances in NO start at 5.04, 5.41, 5.46 and $6.44 \pm .06$ eV respectively and exhibit vibrational structure whose spacing (285 meV) and Franck-Condon factors agree well with those of the $X^1\Sigma^+$ ground state of NO⁺. The NO⁻ states seem to be formed by the addition of 2 Rydberg electrons to a NO⁺ core, which remains unperturbed. Thus we confirm for NO (and O₂) the theoretical considerations of Weiss and Krauss² who point out that Rydberg states, but not valence states, are expected to have sharp resonances associated with them. In O₂, two sharp structures¹ occurring at 8.02 and 8.25 ± 0.03 eV, as well as a new series in the 12-13 eV region, can also be interpreted as temporary negative ion states having Rydberg states of O₂ as their parents.

[†] This work was supported by DASA through AROD.

¹L. Sanche and G.J.Schulz, Phys.Rev.Letters 26,943,(1971).

²A. W. Weiss and M.Krauss, J. Chem.Phys.52,4363,(1970).

W3. Low Energy Electron Scattering by Polar Molecules.*

W. R. GARRETT, Oak Ridge Nat'l. Lab. --A systematic theoretical study has been made of elastic, inelastic, total, and momentum transfer cross sections for thermal energy electrons incident on dipolar target systems. Results are given for pure dipole fields and for model molecular potentials which include monopole, dipole, and induced dipole terms in the electron-molecule interactions. The effect of critical dipole moments on low energy momentum transfer cross sections is carefully examined and conclusions contrary to those of Itikawa¹ are reached; namely, there is no particular value of dipole magnitude which leads to a resonance effect in momentum transfer cross sections for thermal energy electrons on polar molecules.

*Research sponsored by the U. S. Atomic Energy Commission under contract with Union Carbide Corporation.

¹Y. Itikawa, J. Phys. Soc. Japan 27, 444 (1969).

W4. Measurements of Large Angle Inelastic Scattering Cross Sections in Helium.* C. B. OPAL and E. C. BEATY, Joint Institute for Laboratory Astrophysics. --The inelastic electron scattering cross sections for the $n=2$ levels of helium have been measured in a crossed beam apparatus over the 30° to 150° range for incident energies of 82 and 200eV. In both cases, at angles greater than 40° the total inelastic cross section was a constant fraction of the elastic scattering cross section, in qualitative agreement with a similar experiment in atomic hydrogen. The four $n=2$ states were observed to have markedly different angular dependencies at 82eV incident energies. Only the $1S$ and $1P$ states were important at 200eV; the ratio $1S/1P$ was very nearly 2 at all angles larger than 60° . Over the range of variables studied, the only cross sections predicted correctly by the first Born approximation were those for $1P$ at angles less than 45° at 82eV incident energy, and for $1S$ and $1P$ at 30° and 200eV incident energy; it appears that methods other than the usual first Born approximation should be employed in order to compute cross sections at large scattering angles.

*This work was supported in part by the Advanced Research Projects Agency.

SESSION X

Thursday Afternoon, 7 October

2:30 p.m.

CHEMI-IONIZATION
(PANEL)

Chairman: C. B. Collins, University of Texas at Dallas

X1. Excitation Transfer Between Helium Metastables and CO.* W. B. HURT and W. C. GRABLE, U. of Texas at Dallas--The Penning ionization and dissociative excitation channels of the excitation transfer reaction between He(2^3S) and CO have been examined in a flowing afterglow experiment. Absolute intensity measurements of the reaction flame combined with absorption determinations of the He(2^3S) and CO densities in the flame permit calculation of the Penning ionization rate into excited states of CO⁺ and the dissociative excitation rate into excited states of C. The measured rate constants for these two processes are 1.7×10^{-11} and 2.9×10^{-12} cm³/sec, respectively. The production of excited CO⁺ is thus seen to be one-fifth of the total Penning ionization probability and the probability for dissociative excitation is comparable to the He(2^3S) + Ne interaction where the ionization channel is energetically unavailable.

*Work supported in part by NASA Grant NGL44-004-026.

X2. Penning Ionization of Atomic Hydrogen.* J. S. COHEN[†] and NEAL F. LANE, Rice U.--A theoretical study of Penning ionization cross sections for H by 2^3S and 2^1S helium atoms has been carried out, using available adiabatic He*-H potential curves.¹ For the triplet case, the cross section at 0.027eV resulting from a full quantum mechanical calculation is 40.8×10^{-16} cm² and in the JWKB approximation, 43.8×10^{-16} cm², about twice the observed thermal-energy result.² The recently-determined triplet width of Miller³ gives improved results. For the singlet case the width² is much less certain and our calculated cross section of 8×10^{-16} cm² at 0.027eV is clearly too small.

*Supported in part by the U. S. Atomic Energy Commission.

[†]National Science Predoctoral Fellow.

¹W.H. Miller and H.F. Schaeffer III, J. Chem. Phys. 53, 1421 (1970); H. Fujii, H. Nakamura and M. Mori, J. Phys. Soc. Japan 29, 1030 (1970).

²M.J. Shaw, P.C. Bolden, R.S. Hemsworth, and N.D. Twiddy, Chem. Phys. Lett. 8, 148 (1971).

³W.H. Miller (private communication).

X3. Rotational Excitation in Penning Excitation of Molecules*, W. K. MCGREGOR and J. M. LENTS**, ARO, Inc.,—A controversy centers around whether the angular momentum of rotating molecules is conserved during Penning excitations. Fishburne¹ and Stedman and Setser² have observed "enhanced" rotational excitation of several molecules at low gas temperatures ($\sim 300^\circ\text{K}$) due to collisions with metastable atoms of the noble gases, and claim that the rotational angular momentum selection rules are violated. In several experiments described in this paper it is shown that an analysis based upon equating rates of excitation to rates of radiation and incorporating dipole selection rules and Maxwell-Boltzmann statistics leads to quite satisfactory descriptions of the observed spectra. In these experiments the gas temperature was on the order of 1500°K and could be varied. Collisions studied were between argon and helium metastable atoms with nitrogen and argon metastables with ammonia.

*Sponsored by Arnold Engineering Development Center, (AFSC), Arnold Air Force Station, Tennessee.
**Now with Chattanooga Pollution Control Bureau, Chattanooga, Tenn.

¹E. S. Fishburne, J. Chem. Phys. 54, 1363 (1971)
²Stedman and Setser, J. Chem. Phys. 52, 3957 (1970)

X4. Coherent Excitations of Ions by Penning Collisions
L. D. SCHEARER - University of Missouri-Rolla

We have demonstrated experimentally that Penning collision results in a coherent excitation of the ions. The coherence appears as a modulation of the intensity of the light emitted by the excited ions. In the experiment coherence is induced between the eigenstates of helium metastable (2^3S_1) atoms by a rf magnetic field at their Zeeman resonance frequency. Following an ionizing collision between the metastable atoms and impurity atoms such as Sr, Ba, and Ca, the excited ions decay radiatively and the emission is modulated at the metastable resonance frequency. Thus, the coherence has been transferred to the excited ions; it persists until the phase difference between the precession frequencies of the metastable atoms and the excited ions becomes appreciable. Demonstration of the coherent excitation of ions by Penning collisions suggests that level-crossing techniques can be successfully applied to the excited states of Penning ions which are inaccessible by optical excitation. Similar experiments have been performed for collisions of the second kind between metastable helium and neon atoms.

X5. Measurement of Reaction Times in the Nano-second Range.* C. B. COLLINS, B. W. JOHNSON, and M. J. SHAW, U. of Texas at Dallas--A system has been developed for the measurement of the reactions of excited states with lifetimes in the nanosecond range. A flowing afterglow produces large populations of chemically unstable species and a frequency-doubled, tuneable dye laser optically pumps this population into the reacting state. A photon logging computer monitors the evolution of the reacting populations. Illustrative measurements made on this system of the associative ionization rate of He (5^3P) give a rate coefficient of $8 \times 10^{-11} \text{ cm}^3 \text{ sec}^{-1}$.

*Work supported by NASA Grant NGL44-004-001.

SESSION Y

Thursday Afternoon, 7 October

4:30 p.m.

ELECTRON-ION RECOMBINATION

Chairman: D. E. Kerr, The Johns Hopkins University

Y1. Recombination of Electrons with Positive Ions of the $H_3O^+ \cdot (H_2O)_n$ Series.* M. T. LEU, M. A. BIONDI and R. JOHNSEN, University of Pittsburgh, Penna. --- A microwave afterglow/mass spectrometer apparatus has been used to determine the recombination coefficients of electrons with ions belonging to the hydrated hydronium ion series $H_3O^+ \cdot (H_2O)_n$, where $n = 0, 1, 2, 3, 4, 5$. This process is important in determining ionization levels in the D region of the ionosphere. Measurements of electron density decays in helium-water vapor mixture afterglows are correlated with the decay of mass-identified ion currents to the wall of the microwave cavity. By varying the temperature of the gas and the partial pressure of the water vapor in the mixture, different groups of hydronium series ions are made to dominate the afterglow. The recombination coefficients range from $\alpha(19^+) = (1.1 \pm 0.2) \times 10^{-6}$ cm³/sec at 540°K to $\alpha(109^+) = (10 \pm 2) \times 10^{-6}$ at 205°K.

*This research has been supported, in part, by the Army Research Office (Durham), (DA-ARO-D-31-12470-G34).

Y2. Recombination of Electrons with Molecular Helium Ions.* A. WAYNE JOHNSON and J. B. GERARDO, Sandia Labs. --The decay of electrons in a molecular helium ion afterglow (300°K) was found to be strongly influenced by metastable-metastable ionizing collisions. Over a wide range of conditions, both theory and experiment yielded the result that $1/Ne$ decays linearly with time, thus yielding (if so analyzed) an effective electronic recombination coefficient which is less than the actual recombination coefficient. The recombination coefficient was measured by temporarily increasing the ratio of the electron density to the metastable density. The electronic recombination coefficient (α) in a molecular helium afterglow was found to be about a factor of 5 larger than previously accepted. Over the pressure range from 15 to 55 Torr, the measured α ranged from 1.7 to 3.3×10^{-8} cm³sec⁻¹.

*Work supported by the U. S. Atomic Energy Commission.

Y3. Measurements of the Spectral Light Emission from Decaying High Pressure Helium Plasmas. J. STEVEFELT and J. JOHANSSON, AB Atomenergi, Sweden and F. ROBBEN, Univ. of Calif., Berkeley.—Measurements of the absolute intensity of the light emission and the electrical conductivity in the early afterglow of a helium pulsed discharge at pressures from 100 to 600 Torr are reported. The electron density decays typically from 10^{13} to 10^{11} cm^{-3} . The effective recombination rate coefficient increased faster than linearly with gas pressure, and the total photon emission rate was significantly lower than the effective recombination rate. Below 400 Torr the afterglow intensity was dominated by molecular helium bands; however, at higher pressures these bands became weaker while atomic lines originating from the $n=3$ and 2^3P states begin to dominate the afterglow. Absorption measurements give evidence for recombination directly into the 2^3S state as well. The light emission had a T_e^{-x} dependence on electron temperature, with $0 < x < 0.4$ for the atomic line and $0.8 < x < 1.1$ for the molecular bands. The phenomena observed are perhaps related to the formation of He_3^+ and He_4^+ ions at higher pressures.

Y4. The Effect of Rotational States on the Collisionally Stabilized Recombination of Molecular Ions with Electrons.* C. B. COLLINS, U. of Texas at Dallas
—The collisional-radiative recombination of light molecular ions with electrons has been considered theoretically. A stabilization channel has been introduced in which excess population resulting from inverse autoionization of high rotational states is relaxed by collisions with neutral particles. This channel is shown to result in three-body rate coefficients of $10^{-26} \text{ cm}^6 \text{ sec}^{-1}$ for molecules having large rotational energy spacings.

*Work supported by NASA Grant NGL44-004-001.

Y5. Direct Measurement of the Rate Coefficient for the Recombination of He⁺ with Electrons in a High Pressure Afterglow.* C. B. COLLINS, H. S. HICKS, and W. E. WELLS, U. of Texas at Dallas--A computer linked spectroscopic system has been used to directly measure the rate of recombination of He⁺ with electrons at 44.6 Torr without the need of a priori assumptions about the particular functional dependence on experimental parameters. In contradiction to theory the rate coefficient for He⁺ was found to have little similarity to the rate for He₂⁺ measured under the same conditions. Over the 10¹¹ to 10¹² cm⁻³ range of electron densities the best fit to data is obtained with a three-body recombination rate coefficient with electrons of
$$K_e = 1.8 \times 10^{21} \text{ cm}^6 \text{ sec}^{-1}.$$

*Work supported by NASA Grant NGL44-004-001.

Y6. Direct Measurement of the Rate Coefficients for Recombination of He⁺ and He₂⁺ with Electrons at an Asymptotically Low Neutral Gas Pressure.* R. BURTON, C. B. COLLINS, and H. S. Hicks, U. of Texas at Dallas--A computer linked spectroscopic system has been used together with a 35G Hz Fabry-Perot resonator to directly measure the rates of recombination of He⁺ and He₂⁺ in a low pressure, 1.86 Torr, pulsed helium afterglow. At this pressure theory indicates that stabilization of the recombination by collision with neutral atoms is negligible. Measurements span the 10¹⁰ to 10¹¹ cm⁻³ decades of electron densities.

*Work supported by NASA Grant NGL44-004-001.

SESSION Z

Friday Morning, 8 October

8:30 a.m.

EXCITATIONS BY IONS
(PANEL)

Chairman: L. D. Doverspike, College of William and Mary

21. Study of Light Produced by Collisions of Low-Energy He⁺ with N₂.* REDUS F. HOLLAND and WILLIAM B. MAIER II, Los Alamos Scientific Lab. Spectra of the light produced by collisions of N₂ with He⁺ having kinetic energy E below 500 eV are obtained between 1200 and 3200 Å. NI, N₂⁺ second negative (2N), and strong, unresolved emissions are found. The cross section σ for the total emission between 1200 and 3200 Å is $\sim 10^{-16}$ cm² and is smaller than σ for He⁺ + N₂ → N₂⁺ + He. For E \lesssim 40 eV, the unresolved emissions are stronger than the 2N emissions and increase with decreasing E. Apparent populations of different vibrational levels of N₂⁺ (C ²Σ_u⁺) depend differently on E. The electronic transition moment of C ²Σ_u⁺ → X ²Σ_g⁺ is found to vary considerably with the wavelength of the emitted light.

*Work supported by the Atomic Energy Commission and the Defense Nuclear Agency.

22. Polarization of the H_α Line Produced in He⁺ + H₂ Collisions. R. C. ISLER and R. D. NATHAN, Univ. of Florida - The polarization of the H_α line produced by dissociative charge transfer in He⁺ + H₂ collisions has been measured from 45 to 700 eV.¹ This polarization is strongly dependent upon the energy of the He⁺ beam below 100 eV and indicates both that the excitation cross section is angular dependent and that the magnetic sublevels of the n = 3 states of hydrogen are being populated unequally. A zero-field level-crossing experiment (Hanle effect) has also been performed, and the results indicate that at low energies the polarization arises from the preferential population of the 3²D_{5/2}^{1/2} and 3²D_{3/2}^{-1/2} states. The relationship between the polarization measurements and the angular distribution of the excitation cross sections will be discussed.

1. R. D. Nathan and R. C. Isler, Phys. Rev. Letters 26, 1091 (1971).

23. Cross Sections for Excitation of Pure Vibrational Transitions in H₂ by Proton Impact. F. A. HERRERO and J. P. DOERING, The Johns Hopkins University.

--The cross sections for excitation of the first four vibrational levels of H₂X¹Σ_g⁺ by proton impact have been measured from 2.5 eV to 750 eV relative kinetic energy. The apparatus, except for some modifications required for this study, has been described elsewhere.⁽¹⁾ The cross section measurements were made directly from observed energy loss spectra (proton beam energy spread = 80 millivolts FWHM). In the energy interval from 2.5 eV to 60 eV, the cross sections increase roughly by a factor of ten reaching values of $\sigma(v:0 \rightarrow 1) = 1.20 \pm .01$, $\sigma(v:0 \rightarrow 2) = .298 \pm .007$, $\sigma(v:0 \rightarrow 3) = .110 \pm .005$ and $\sigma(v:0 \rightarrow 4) = .020 \pm .005$ in units of 10⁻¹⁶ cm². The observed cross sections reach maximum values in the range from 60 to 100 eV and then decrease slowly. In collisions of this type it is expected that the probability of excitation will reach a maximum whenever the collision time is approximately equal to the vibrational period of the excited level. On the basis of this assumption, reasonable values are obtained for collision distances: 6.5, 3.2, 1.9, and 1.4 Å for v = 1, 2, 3, 4 respectively.

(1) J. H. Moore, Jr. and J. P. Doering, *Jour. Chem. Phys.* 52, 1692 (1970).

24. Adiabatic Potential Curves for Li⁺ + Li Collisions.*

H. H. MICHELS, United Aircraft Res. Lab. -- Calculations have been performed for the ground and excited state Li₂⁺ potential curves. The symmetries considered are ²Σ_g⁺, ²Σ_u⁺, 2π_g, 2π_u and 2Δ_g. Complete VCI wavefunctions (up to 264 terms) were employed since the Hartree-Fock model cannot properly describe united atom (C⁺) limiting behavior. We find a maximum in the potential difference between the lowest ²Σ_g⁺ and ²Σ_u⁺ states near R = 4.0 a.u. in agreement with our earlier studies.¹ However, these curves cross at a much smaller separation (R ≈ 0.3 a.u.) than previously reported using less accurate wavefunctions.¹ Our present results are in agreement with the more recent study of Bardsley.² These calculations verify the 2π_u-²Σ_u⁺ crossing at R ≈ 5.5 a.u. and indicate a second 2π_u-²Σ_u⁺ crossing between R ≈ 0.25 and 0.5 a.u. No avoided crossings or low-lying ²Σ_g⁺ or ²Σ_u⁺ excited states are indicated but a ²Δ_g-X ²Σ_g⁺ crossing occurs between 0.1 and 0.25 a.u.

*Supported in part by AFOSR, Contract F44620-71-C-0066

¹J. M. Peek, et. al. *Phys. Rev. Lett.* 20, 1419 (1968)

²J. N. Bardsley, *Phys. Rev. A* 3, 1317 (1971)

25. Curve Crossing in the Ne-He⁺ System. S.M. BOBBIO, L.D. DOVERSPIKE, W.A. RICH, and R.L. CHAMPION, College of William and Mary.--The perturbation seen in the experimental differential elastic scattering cross section for the 40eV He⁺+Ne system can be attributed to a single crossing of the intermolecular potential energy curves. This particular crossing has received much attention in the literature. New theoretical methods of dealing with the curve crossing problem have been devised which are far more complete than the standard Landau-Zener-Stuckleberg method which has been used heretofore. One of these new methods, namely the treatment of Delos¹, has been employed to obtain the crossing probabilities and phases. These parameters, together with the theoretically predicted value by Sidis² for the interaction term ($H_{12}=.26\text{eV}$) have been utilized in a partial wave calculation of the cross section which is in quantitative agreement with our experiment. For intuitive reasons the observed cross section is discussed in semiclassical terms and a possible parameterization of the problem in this context is pointed out.

¹J. Delos, Doctoral Dissertation, M.I.T.

²V. Sidis and H. Lefebvre-Brion, to be published, J. Phys. B

26. Absolute Differential Cross Sections for Excitation of the He(1s2s) + Ne⁺(2p⁵) State in He⁺-Ne Collisions. PREBEN LOFTAGER, DONALD C. LORENTS, and JAMES R. PETERSON, Stanford Res. Inst. --The angular distribution of metastable He(1s2s) atoms produced in He⁺ + Ne collisions has been measured in a new scattering apparatus. Kinetic energies range from 40 to 150 eV, and scattering angles range from 3° to 50°(c.m.). The reduced cross sections $\rho = \theta \sin \theta \cdot \sigma(\theta)$ as a function of $\tau = \theta \cdot E$ show an oscillatory structure characteristic of a curve crossing. The measurements are compared to theoretical cross sections¹ for the reaction He⁺ + Ne → He(1s2s) + Ne⁺(2p⁵). There is good agreement both in the order of magnitude of the cross sections and in the spacing between the peaks. The structure in these experimental data is closely correlated to the structure in the cross sections for the He⁺ + Ne → He⁺ + Ne(2p⁵3s) reaction measured previously in this laboratory.²

¹R.E. Olson, private communication.

²D. Coffey, Jr., D.C. Lorents, and F.T. Smith, Phys. Rev. 187, 201(1969).

SESSION AA

Friday Morning, 8 October

10:15 a.m.

RADIATIVE LIFETIMES

Chairman: D. A. Micha, University of Florida

AA1. Excited State Lifetime Measurements in Atomic Helium. R. G. FOWLER and R. T. THOMPSON, University of Oklahoma--Measurement of the lifetimes of excited states in helium up to 9^1S , 10^1P , 9^1D , 4^1F , 9^3S , 9^3P , 11^3D , and 4^3F will be reported. Overall agreement with theory is relatively good. The results clearly display the $n^1P \rightarrow n(1^1F+3^1F)$ transfer mechanism. It is found that blockading of the n^1P states plays the important role expected of it both in this process and in the population of the 1^1S states. The combination of transfer and blockading is most apparent with the 4^1F and 4^3F states where it plays the dominant role in excitation of the 3^3D state. Higher F states become progressively less active in populating the D states.

The technique of photon coincidence counting applied to the Holzberlein invertron was used to obtain the data.

AA2. Radiative Lifetime of the $A^2 \Sigma^+$ State of OH
R. ANDERSON and R. SUTHERLAND - University of Missouri-Rolla

The radiative lifetime of the $v'=0, 1, 2$ and 3 levels of the $A^2 \Sigma^+$ state of OH have been measured. The lifetimes are pressure dependent and complex with a short lifetime component. When the data is extrapolated to zero pressure with the short lifetime component removed, there is excellent agreement between our measurements and Smith¹ and others ^{2,3,4,5}. The lifetime was shortened due to predissociation with increasing vibrational quantum numbers.

1. W. H. Smith, J. Chem. Phys. 53, 792 (1970)
2. K. R. German and R. N. Zare, Phys. Rev. 186, 9 (1969)
3. K. R. German and R. N. Zare, Phys. Rev. Letters 23, 1207 (1969)
4. A. Marshall, R. L. de Zafra, and H. Metcalf, Phys. Rev. Letters 22, 445 (1969)
5. R. L. de Zafra, A. Marshall and H. Metcalf, Phys. Rev. A3, 1557 (1971)

AA3. Radiative Lifetime of the $v = 1$ Level of the $A^1\Pi$ State of Carbon Monoxide. R. L. BURNHAM AND R. C. ISLER, Univ. of Florida - Zero-field level-crossing measurements have been made on several resolved rotational features in the $v = 1$ level of the $A^1\Pi$ state of CO. These measurements yield values of $g_J\tau_J$, the product of the Landé g factor and the lifetime of states which have rotational quantum numbers from $J = 19$ to $J = 26$. The lifetime of the $v = 1$ level is obtained by assuming that g_J can be calculated from a case (a) coupling scheme for the states which have $J = 19, 20, 21, 26$ and the average value is $\tau(v = 1) = 10.0 \pm 0.9$ ns. Interaction with the $a'^3\Sigma^+$ state causes a perturbation which has a maximum at $J = 23$ in the $v = 1$ level of the $A^1\Pi$ state. The effects of these perturbations upon the g factors are seen in the $J = 22$ to $J = 25$ states and provide a measurement of the coupling constant between the two states.

AA4. Emission from Long-Lived States of NO^+ .* REDUS F. HOLLAND and WILLIAM B. MAIER II, Los Alamos Scientific Lab.--The spectrum of emission from long-lived states of NO^+ is studied for 1250-3400 Å. Over 32 distinguishable spectral features are found between 1250 and 2200 Å, but no spectral features are found between 2200 and 3400 Å. Spectral features attributable to $b^3\Pi \rightarrow X^1\Sigma^+$, (0,0) - (0,5) and (1,1) - (1,6), have been found. The energies of the zeroth and first vibrational levels of $b^3\Pi$ are 7.301 ± 0.006 and 7.511 ± 0.01 eV above the ground state of NO^+ . The apparent lifetime of $b^3\Pi$ is 135 ± 35 μ sec. The other emissions have apparent lifetimes of 10.8 ± 2 μ sec and 160 ± 50 μ sec; the spectral features corresponding to these other emissions are compared with the energy levels inferred from photoelectron spectroscopy.

*Work supported by the Atomic Energy Commission and the Defense Nuclear Agency.

AA5. Study of the A \rightarrow X Transitions in CO⁺ and N₂⁺.* WILLIAM B. MAIER II and REDUS F. HOLLAND, Los Alamos Scientific Lab.--CO⁺ and N₂⁺ are formed in an ion source by electron impact on CO and N₂ and are removed to an observation region where emissions from their long-lived states are studied. The electron-energy dependences of the emissions are examined. Emission spectra from CO⁺ and N₂⁺ are obtained for 3200 - 5200 Å and 6000 - 8300 Å, respectively. CO⁺ comet-tail bands and N₂⁺ Meinel bands are prominent in these spectra. Light output in selected bands is measured as a function of transit time from the ion source to the observation region; the data are interpreted in terms of apparent lifetimes τ of the emissions. For the CO⁺ (A \rightarrow X) (3,0) and (4,0) bands, $\tau \approx 2 - 2.5$ μ sec.

*Work supported by the Atomic Energy Commission and the Advanced Research Projects Agency.

SESSION BB

Friday Morning, 8 October

8:30 a.m.

ATTACHMENT

Chairman: R. Celotta, NBS, Washington

BB1. Final-State Effects in the Dissociative Attachment of Electrons to H_2 , HD and D_2 . GEORGE V. NAZAROFF, Mich. State Univ. -- Analytic expressions have been derived for the structures occurring in the dissociative attachment cross sections for H_2 , HD and D_2 . The large sharp peak at 13.6 eV arises from a large scattering length in the final-state $H-H^-$ wavefunction. The enhancement of the scattering length occurs as a result of weakly-bound states (the higher vibronic levels of the 13 eV H_2^- resonance). The 10.1 eV peak arises from a large scattering length in the final state $e^- - H_2^-$ wavefunction which is brought about by the existence of a bound state of the electron in the field of the lowest repulsive triplet state of H_2 . The sharp 3.75 eV peak results from an enhanced scattering length which is caused by the attractive H_2^- ground state which is bound for internuclear separations greater than 1.8 \AA . The various observed isotope effects are directly predicted by the formulas. The sudden onsets in the 13.6 and 3.75 eV peaks are also given directly by the expressions.

BB2. Electron Attachment in SF_4 . C. L. CHEN and P. J. CHANTRY, Westinghouse Research Labs, -- The attachment of low energy electrons (0-3 eV) in SF_4 has been studied in the temperature range $300^\circ - 1000^\circ K$, with a monoenergetic electron beam and mass analysis. At room temperature it is found that (1) SF_4^-/SF_4 has a resonance peak at zero electron energy similar to SF_6^-/SF_6 ; (2) SF_3^-/SF_4 has a small peak at zero energy and a broad peak at 1.3 eV resembling the case of SF_5^-/SF_6 reported previously;¹ (3) F^- and F_2^-/SF_4 are produced at zero energy. As the temperature of the gas is increased, (2) SF_4^- and F_2^- decrease monotonically, whereas (b) F^- and SF_3^- peaks increase. The measured temperature variations of the F^- and SF_3^- zero energy peaks are analyzed assuming that the activation energy is D-A, where D is the strength of the broken bond and A the affinity of the fragment ion. Using the known value of $A(F) = 3.40 \text{ eV}$, one obtains $D(SF_3-F) = 3.57 \text{ eV}$, in reasonable agreement with Bott², and $A(SF_3) = 3.34 \text{ eV}$.

1. C.L. Chen and P.J. Chantry, Bull. Am. Phys. Soc. 15, 418 (1970).
2. J. F. Bott, J. Chem. Phys. 54, 181 (1971).

BB3. Dissociative Attachment in Ozone.* P.J. CHANTRY
 Westinghouse Research Laboratories--The total dissociative attachment cross-section and the cross-sections for O^- and O_2^- production from O_3 have been measured by electron beam techniques^{1, 3}. Total ion current measurements, and mass-spectrometric measurements of O^- were made as a function of absolute pressure and were calibrated by similar measurements on other gases whose cross-sections are known. The total cross-section has a peak value of $(3.0^{+0.7}_{-0.4}) \times 10^{-17} \text{ cm}^2$ at 1.07 eV. $Q(O^-)$ is finite at zero energy and peaks at 1.25 eV. The shape of $Q(O_2^-)$ was measured mass-spectrometrically and its magnitude adjusted to give $Q(O_2^-) + Q(O^-) = Q(\text{total})$ over as wide an energy range as possible. The resulting O_2^- cross-section has an onset, determined by linear extrapolation, at 0.40 $^{+0.15}_{-0.05}$ eV, and peaks at 0.95 eV. The ratios of the cross-sections $Q(\text{total}): Q(O^-): Q(O_2^-)$, at their peaks, are 1.6:1:0.75. No temperature dependence of the onsets or cross-sections could be detected in the range 112-360°K, justifying the deduction, from the measured O_2^- onset, of $A(O_2) \geq 0.60^{+0.05}_{-0.15}$ eV for the electron affinity of O_2 .

*Supported in part by ARPA, Contract DAHCO4-69-C-0094.
¹P. J. Chantry, J. Chem. Phys. 51, 3369 (1969).

BB4. Dissociative Attachment* from the $a^1\Delta_g$ State of O_2 . P. D. BURROW, Yale U.--The production of O^- by electron impact on O_2 molecules in the electronically excited $a^1\Delta_g$ state has been observed. The energy dependence of the cross section suggests that the process takes place through the same repulsive state of O_2^- ($^2\Pi_u$) which is responsible for dissociative attachment from the ground state of O_2 . The magnitude of the cross section at its peak is approximately five times that for production of O^- from the ground state. The data also yield information on the electron excitation of the $a^1\Delta_g$ state which proceeds through the intermediate formation of O_2^- ($^2\Pi_u$). The contribution of this process to the total excitation cross section will be discussed.

*Work supported by ARPA through ONR.

BB5. Three-body Attachment in O₂ using Electron Beams.^{*}
D. SPENCE and G. J. SCHULZ, Yale U.--Three-body attachment in pure O₂, $e + 2 O_2 \rightarrow O_2^- + O_2$, is studied by using electron beams. The energy dependence of the rate constant is found to contain structure with a spacing of about 120 meV. The peaks of this structure are found to coincide energetically with the vibrational levels of the O₂⁻ system.¹ The energy dependence of the rate constant determined here is in excellent agreement with the theoretical calculations of Chapman and Herzenberg. The largest peak in the rate constant occurs at about 0.1 eV incident electron energy and the magnitude is found to agree with previous values.² The rate constant is shown to decrease with increasing gas temperature and the temperature dependence becomes weaker at higher incident electron energy in qualitative agreement with the theory of Herzenberg.³

^{*}This work was supported by ARPA through ONR and by DASA through AROD.

¹D. Spence and G. J. Schulz, Phys. Rev., A2, 1802, (1970).

²L. M. Chanin, A.V. Phelps and M. A. Biondi, Phys. Rev., 128, 219, (1962).

³A. Herzenberg, J. Chem. Phys., 51, 4943, (1969).

BB6. Low Temperature Thermal Electron Attachment in O₂.^{*} F. K. TRUBY, Sandia Laboratories -- The three-body process $e + 2O_2 \rightarrow O_2^- + O_2$ has been studied at 113°K, 200°K, and 300°K using microwave cavity techniques and mass analysis. Initial electron densities were produced by photoionization of trace amounts of NO in the O₂. The electron density decay rates were determined after a single photoionization pulse and for a given O₂ pressure were independent of the NO trace concentration used. The value for the oxygen three-body electron attachment coefficient obtained by varying the O₂ pressure was found to be 2.1×10^{-30} cm⁶/sec at 300°K, 1.5×10^{-30} cm⁶/sec at 200°K, and 7.2×10^{-31} cm⁶/sec at 113°K. The decay of O₂⁻ increases with increasing O₂ pressure at a given temperature and increases with decreasing temperature for a given O₂ number density. The O₂⁻ decay relates to the formation of O₄⁻.

^{*}This work was supported by the U. S. Atomic Energy Commission.

SESSION CC

Friday Morning, 8 October

10:15 a.m.

DETACHMENT

Chairman: C. L. Chen, Westinghouse Research Laboratories

CC1. Electron Avalanches in Oxygen: A Fast Electron Detachment Process.* D. Goodson, L. Frommhold, and R. Corbin, U. of Texas at Austin -- Electron current pulses of electron avalanches in oxygen were studied at room temperature over a pressure range of 1 to 32 torr in O₂. The ratio of electric field to pressure was from about 30 to 200 V/cm · torr. The transients consisted of electrons produced by both direct ionization and detachment from negative ions. By a curve fitting method, electron attachment and detachment frequencies were obtained that are improved and extended values of those previously published¹ and ascribed to the atomic ion O⁻. In the course of the work evidence was obtained that, under certain conditions, at least one slower electron detachment process was occurring; this lead to the work described in the following abstract.

- *) Supported by N.S.F. grant GP 2848926 and Joint Services Electronics Program, AF.
1) L. Frommhold, Fortschritte der Physik 12 (1964) 592.

CC2. Electron Avalanches in Oxygen: A Slow Electron Detachment Process.* L. Frommhold, D. Goodson, and R. Corbin, U. of Texas at Austin -- Ion current transients of avalanches in oxygen were studied at room temperature over a pressure range from 1 to 16 torr. The ratio of electric field to pressure ranged from about 40 to over 100 V/cm · torr. Each pulse was found to consist of detached electrons, negative ions, and positive ions. Electron attachment and detachment rates were obtained by a curve fitting method. The attachment rates seemed to indicate a modified Schultz-Curran two body process (O₂⁻ from O⁻) which is strongly favored at low pressures. The detachment frequencies are roughly one to two orders of magnitude smaller than those published previously¹ for O⁻ and indicate an electron affinity of about 0.44 eV. We thus suspect the negative ion to be O₂⁻ and expect to have mass-spectrometer identification of the negative ion involved in the near future.

- *) Supported by N.S.F. grant GP 2848926 and Joint Services Electronics Program, AF.
1) L. Frommhold, Fortschritte der Physik 12 (1964) 592.

CC3. Physics of Associative Detachment.* J. L. MAUER and G. J. SCHULZ, Yale U.--The associative detachment reaction, $O^- + CO \rightarrow CO_2(v) + e$, is studied experimentally using a negative ion beam (0 - 3 eV) impinging on a gas-filled collision chamber. The detached electrons are energy analyzed by retarding potentials and are counted on a channeltron multiplier. The total detachment cross section follows a $1/v$ dependence at low ion energies¹ (< 0.3 eV, center of mass) corresponding to autoionization of the attractive ($^2\Pi_u$) state of CO_2^- . At higher energies, a broad peak is observed which indicates that detachment proceeds via repulsive states² of CO_2^- . The energy distributions for the detached electrons are peaked at low electron energy (70 meV) corresponding to the excitation of high vibrational and rotational states of CO_2 .

*This work supported by DASA through AROD.

¹F. C. Fehsenfeld, E. E. Ferguson, A. L. Schmeltekopf, J. Chem. Phys., 45, 1844, (1966).

²C. R. Claydon, G. A. Segal, H. S. Taylor, J. Chem. Phys., 52, 3387, (1970).

CC4. Collisional Detachment Studies of NO^- . M. McFarland, D. B. Dunkin, F. C. Fehsenfeld, A. L. Schmeltekopf, and E. E. Ferguson, NOAA Environmental Research Labs., Boulder, Colo. 80302.

Rate constants for the reaction $NO^- + X \rightarrow NO + e + M$ have been measured from 193 to 506°K for $X = He, Ne, H_2, N_2, CO, NO, CO_2, N_2O, NH_3, CH_4,$ and CF_4 . The data fit Arrhenius plots, $k_d = Ae^{-E/kT}$, with activation energies E ranging from 0.05 to 0.12 electron volts and pre-exponential factors A ranging from 1.6×10^{-12} to $4.4 \times 10^{-10} \text{ cm}^{-3} \text{ molecule}^{-1} \text{ sec}^{-1}$. The activation energy in every case substantially exceeds the electron affinity of NO . This implies a positive temperature dependence for electron attachment to NO , $NO + e + M \rightarrow NO^- + M$, in the thermal range. Using statistical mechanics, rate constants for the inverse three-body attachment to NO have been computed. At 300°K this leads to a value $6.6 \times 10^{-31} \text{ cm}^6 \text{ sec}^{-1}$ for attachment in pure NO .

INDEX TO AUTHORS OF CONTRIBUTED PAPERS

Abraham, G.	59	Devoto, R. S.	5*
Allen, J. E.	69	Dillon, T. A.	56*
Anderson, R.	110	Doering, J. P.	107
Aubel, J. L.	36	Dougal, A. A.	40
Augis, J. A.	20	Douglas-Hamilton, D. H.	83
Bacon, F. M.	26*	Doverspike, L. D.	108
Bandel, H. W.	41	Drop, P. C.	36*
Barthelheimer, D.	5*	Dugan, J. V., Jr.	93*
Bauder, U. H.	5	Dunkin, D. B.	119
Beaty, E. C.	96	Ecker, G. H.	27*
Bederson, B.	46	Eckert, H. U.	31*
Benenson, D. M.	13	Eisner, P. N.	64*, 64
Benedetto, K. R.	30	Fehsenfeld, F. C.	52, 119
Berg, R. A.	70*	Fenstermacher, C. A.	83*
Bhaumik, M. L.	58	Ferguson, E. E.	52, 119
Biondi, M. A.	93, 102	Fieffe-Prevost, P.	8
Bletzinger, P.	77*	Fisher, E. R.	59*
Bloch, S. C.	36*	Fitts, C. M.	15*
Bobbio, S. M.	108*	Fowler, R. G.	110*
Bone, L. I.	51*	Franklin, R. D.	65
Borst, W. L.	73*, 74	Fredrich, O. M.	40
Boyer, K.	83	Frommhold, L.	118*, 118
Brandenberg, W. M.	89*	Gallo, C. F.	37, 42, 42, 43
Braun, W. G.	65*	Garrett, W. R.	96*
Breunig, J. L.	43	Garscadden, A.	77
Bricks, B. G.	81*	George, T. V.	88*
Brown, H. H., Jr.	46	Gerardo, J. B.	102
Burnham, R. L.	111*	Glass, A.	59
Burrow, P. D.	115*	Goldie, H.	23
Burton, R.	104*	Goodson, D.	118, 118*
Campbell, H. D.	4, 4	Grable, W. C.	98
Carpenter, H. C.	50	Graham, W. J.	58*
Castleman, A. W., Jr.	49*	Green, W. H.	78*
Center, R. E.	91*	Green, A. E. S.	69*, 70
Champion, R. L.	108	Grissom, J. T.	25*, 26
Chantry, P. J.	114, 115*	Gross, P. J.	31
Chen, C. L.	114*	Guenther, A. H.	40
Chou, T. S.	28	Gutcheck, R. A.	63*
Coffey, P.	50*, 51	Hahn, Y. B.	68*
Cohen, J. S.	98*	Hammond, T. J.	37*
Cohn, D.	58*	Hancock, G.	60*
Collins, C. B.	55*, 100*, 103*, 104, 104*	Hancock, J. K.	78
Corbin, R.	118, 118	Harvey, A. B.	63
Cox, D. M.	46	Haynes, G. W.	40*
Cremers, C. J.	12	Hebner, R. E., Jr.	68*
Daugherty, J. D.	83*	Hefferlin, R. A.	30
Davies, D. K.	47*	Heimerl, J. M.	52*
Davis, F. J.	46	Herrero, F. A.	107*
Denes, L. J.	87*	Hicks, H. S.	104, 104

* - Denotes "senior" author

Hirsch, M. N.	64*, 64	Meyer, T.	12*
Holland, R. F.	106*, 111*, 112	Micha, D. A.	54
Horn, K. P.	78	Michels, C. J.	17*
Hughes, M.	77	Michels, H. H.	107*
Hunter, A. M.	30	Mickish, R. A.	74*
Hurt, W. B.	98*	Mills, C. B.	84*, 84*
Ingold, J. H.	45*	Mohnen, V. A.	50, 51*
Isler, R. C.	106*, 111	Morley, C.	60
Jasby, D. L.	15*	Morris, J. C.	9*, 10*
Jeffers, W. Q.	61*	Mukherjee, D.	5
Jobe, J. D.	55*	Mullen, J. M.	54*
Johansson, J.	103	Murray, F.	46*
Johnsen, R.	93*, 102	Nathan, R. D.	106
Johnson, A. W.	102*	Nazaroff, G. V.	114*
Johnson, B. W.	55, 100	Neely, G. O.	63
Judd, O.	87*	Nelson, D. R.	46*
Keefer, D. R.	31*, 89	Nelson, L. Y.	63*
Keller, G. E.	49*	Newton, J. C.	26*
Kelley, J. D.	60*, 61	Nielsen, C. E.	15
Kerr, D. E.	81	Nighan, W. L.	59*
Kershenstein, J. C.	58	Niles, F. E.	65*
Korff, D. F.	72	Novak, J. M.	17*
Lacina, W. B.	58	Nutter, M. J.	83
Lama, W. L.	42*, 42*, 43*	Nygaard, K. J.	37, 68, 68
Lancaster, B. M., Jr.	37*	O'Brien, B.	58
Lane, N. F.	98	Opal, C. B.	96*
Leiby, C. C.	80*	Ott, W. R.	8*
Leigh, G. H.	16*	Patterson, P. L.	10, 19*
Leland, W. T.	83	Paulson, J. F.	91*
Lents, J. M.	99	Paulson, R. F.	28*, 65
Leu, M. T.	102*	Pendleton, W. K.	40*
Levy, S.	20*	Peterson, J. R.	108
Lieberman, R. W.	6*	Peterson, L. R.	69*
Lin, C. C.	72	Pfender, E.	12, 28*, 28
Linder, F.	95*	Philips, R. L.	17
Litke, J. D.	81	Pirkle, J. C.	77
Lockett, A. M.	85*	Polman, J.	36
Loftager, P.	108*	Popenoe, C. H.	9
Lohnert, G. H.	38	Pugh, E. R.	83
Lorents, D. C.	108	Regan, D. R.	15
Lortie, E. L.	65	Rich, W. A.	108
Lowke, R. E.	22*	Rhoads, H. S.	88*
Ludwig, H. C.	22*, 22	Ridley, B. A.	60
MacDonald, A. D.	41	Robben, F.	103
Mack, J. M., Jr.	4*	Rocca Serra, J.	85*
Magee, J. L.	93	Roesler, R. L.	67
Mahadevan, P.	50*	Rogoff, G. L.	23*
Mahan, J. R.	12*	Romano, L. M.	49
Maier, W. B., II	92*, 92*, 106, 111, 112*	Russ, C.	45
Malghan, V. R.	13*	Sanche, L.	95*
Marhic, M.	15	Saunders, A. W., Jr.	63
Mauer, J. L.	119*	Sawada, T.	69
McClure, G. W.	25*	Schearer, L. D.	99*
McFarland, M.	52, 119*	Schikorr, W. M.	38*
McGregor, W. K.	99*	Schmeltekopf, A. L.	119
McGuire, P.	54*	Schmidt, H.	95
Medgyesi-Mitschang, L. N.	30*	Schmitz, G.	16

* - Denotes "senior" author

Schneider, R. T.	4, 38, 88
Schrade, H. O.	13*
Schreiber, P. W.	30*
Schubert, D. C.	23*
Schulz, G. J.	95, 116, 119
Schulz-Gulde, E.	19*
Shaw, M. J.	55, 100
Shih, K. T.	27*
Shumaker, J. B.	9*
Slade, P. G.	19
Smith, E. W.	56
Smith, I. W. M.	60
Solomon, J. E.	72*
Spears, K. G.	52*
Spence, D.	116*
Srivastava, S. K.	8
Stevelfelt, J.	103
Stewart, B.	92
St. John, R. M.	55, 74
Stone, E. J.	72, 73*
Sucov, E. W.	88
Sutherland, R.	110
Swingle, J. C.	89*
Tang, I. N.	49
Tannen, P. D.	77
Taylor, P.	30
Tetenbaum, S. J.	41*
Thompson, R. T.	110
Todd, J., Jr.	84
Tracy, D. H.	67*
Truby, F. K.	116*
Usher, J. L.	4, 4*
Vanderhoff, J. A.	52
Voshall, R. E.	22
Walker, R. E.	77*
Watson, A.	41*
Waynant, R. W.	80*
Whealton, J. H.	45
Weisheit, J. C.	67*
Weissler, G. L.	8*
Wells, W. C.	74*
Wells, W. E.	104
Whitney, W. T.	76*
Wiegand, W. J.	76*
Wiese, L. L.	8, 20*
Wong, S. F.	45
Woo, S. B.	45*
Wynands, A.	16*
Yezzi, A. J.	69
York, T. M.	17
Young, S. J.	78*
Zipf, E. C.	63, 73, 72*, 74

* – Denotes "senior" author